HYDROGEOLOGY AND SIMULATION OF FLOW AND THE EFFECTS OF DEVELOPMENT ALTERNATIVES ON THE BASALT AQUIFERS OF THE HORSE HEAVEN HILLS, SOUTH-CENTRAL WASHINGTON

By F.A. Packard, A.J. Hansen, Jr., and H.H. Bauer

U.S. GEOLOGICAL SURVEY
Water-Resources Investigations Report 94-4068

Prepared in cooperation with the
WASHINGTON STATE DEPARTMENT OF ECOLOGY

Tacoma, Washington
1996

U.S. DEPARTMENT OF THE INTERIOR
BRUCE BABBITT, Secretary
U.S. GEOLOGICAL SURVEY
GORDON P. EATON, Director

For additional information
write to:

District Chief
U.S. Geological Survey
1201 Pacific Avenue, Suite 600
Tacoma, Washington 98402

Copies of this report can be
purchased from:

U.S. Geological Survey
Branch of Information Services
Box 25286, Denver Federal Center
Denver, Colorado 80225

CONTENTS

PLATES

[Plates are in pocket]

FIGURES

TABLES

CONVERSION FACTORS AND VERTICAL DATUM

To convert from	To	Multiply by
inch (in)	millimeter (mm)	25.40
foot (ft)	meter (m)	0.3048
cubic foot (ft^3)	cubic meters (m^3)	0.02832
mile (mi)	kilometer (km)	1.609
acre	square meter (m^2)	4,047.
square mile (mi^2)	square kilometer (km^2)	2.590
acre-foot (acre-ft)	cubic meter (m^2)	1,233.
square feet per second (ft^2/s)	square meters per second (m^2/s)	0.0929
foot per second (ft/s)	meter per second (m/s)	0.3048
cubic foot per second (ft^3/s)	cubic meter per second (m^3/s)	0.02832
degree Fahrenheit (°F)	degree Celsius (°C)	F = 9/5 °C + 32

Sea level: In this report "sea level" refers to the National Geodetic Vertical Datum of 1929--a geodetic datum derived from a general adjustment of the first-order level nets of both the United States and Canada, formerly called Sea Level Datum of 1929.

Well Numbers and Well Records

Well numbers in Washington are based on the township-range land net. In Horse Heaven Hills, all townships are north of the Willamette Base Line and east of the Willamette Meridian. Each square mile section of land net is subdivided into 16 40-acre squares, labeled as shown with letters; a sequential number after the letter designates each successive well drilled in a 40-acre square. The well numbered 6N/23E-24B1 is the first well to be drilled in Township 6 North, Range 23 East, section 24, square B.

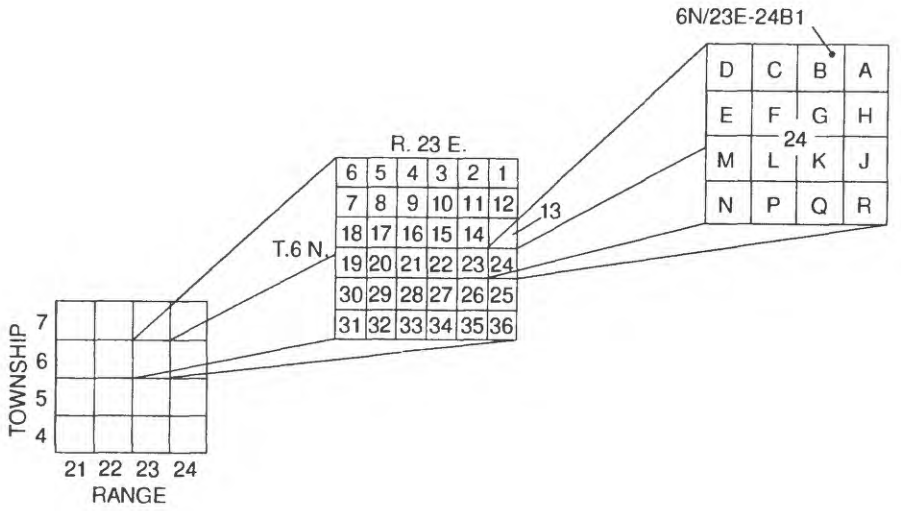

HYDROGEOLOGY AND SIMULATION OF FLOW AND THE EFFECTS OF DEVELOPMENT ALTERNATIVES ON THE BASALT AQUIFERS OF THE HORSE HEAVEN HILLS, SOUTH-CENTRAL WASHINGTON

--

By F.A. Packard, A.J. Hansen, Jr., and H.H. Bauer

--

ABSTRACT

Model simulations of large water-level declines and partial aquifer dewatering were used to help define limitations of ground water available for irrigation in parts of the Horse Heaven Hills area of southern Washington. Three formational units within the Columbia River Basalt--the Saddle Mountains, Wanapum, and Grande Ronde--make up the aquifer system in the area, supplying irrigation and domestic-use water from a flow system with a ground-water ridge coincident with the Horse Heaven anticlinal axis. Flow from this ridge to the north and south toward two major drains, the Yakima and Columbia Rivers, is characterized by several broad areas of gentle hydraulic gradient separated by narrow linear areas of steep gradients. These steep gradients lie along barriers of small horizontal hydraulic conductivity coincident with major faults and tightly folded anticlines. The flow system is also controlled by low values of vertical hydraulic conductivity along the Horse Heaven anticline as compared with that found in adjacent synclinal areas.

Recharge values, as calculated using daily weather data with a modified Blaney-Criddle formula, were tested in two areas against core-hole measurements of steady-state flux, and were found to be close to flux along ephemeral stream channels, but were larger than flux along adjacent ridge crests. Model calibration indicated the calculated recharge to be realistic.

After model calibration, three pumpage alternatives were simulated with recharge from imported water of 16 cubic feet per second and pumpage from the main aquifer of 41, 62, and 104 cubic feet per second. Results indicate that in each case, a number of pumping nodes are dewatered and that, within 50 to 100 years, the system would nearly reach equilibrium with the remaining pumpage. About 80 percent of the pumped water is supplied by capture of ground-water discharge to the Columbia River and most of the rest is supplied by downward leakage of imported irrigation water.

INTRODUCTION

Ground-water-level declines in the basalt aquifers of the Columbia Plateau can be large outside of areas where surface water is used for irrigation. In places of extensive and intensive pumpage, such as the greater Odessa area of east-central Washington (Cline, 1984), these declines exceed 10 feet per year and, in places, total more than 100 feet between 1968 and 1978. Declines in excess of 350 feet since 1965 (Oberlander and Miller, 1981) have been recorded in the Umatilla area of north-central Oregon. Concerns about the effects of these water-level declines on such things as stream capture and lift costs have prompted the Washington State Department of Ecology (WDOE) to fund studies in areas outside of large pumping centers where large amounts of dryland farming exist and where rapid ground-water development has been taking place--areas such as the Horse Heaven Hills (fig. 1). A preliminary water-resource study was completed in the Horse Heaven Hills area by Molenaar (1982), in which available data were collected on the geology, well distribution, and surface- and ground-water use in the area.

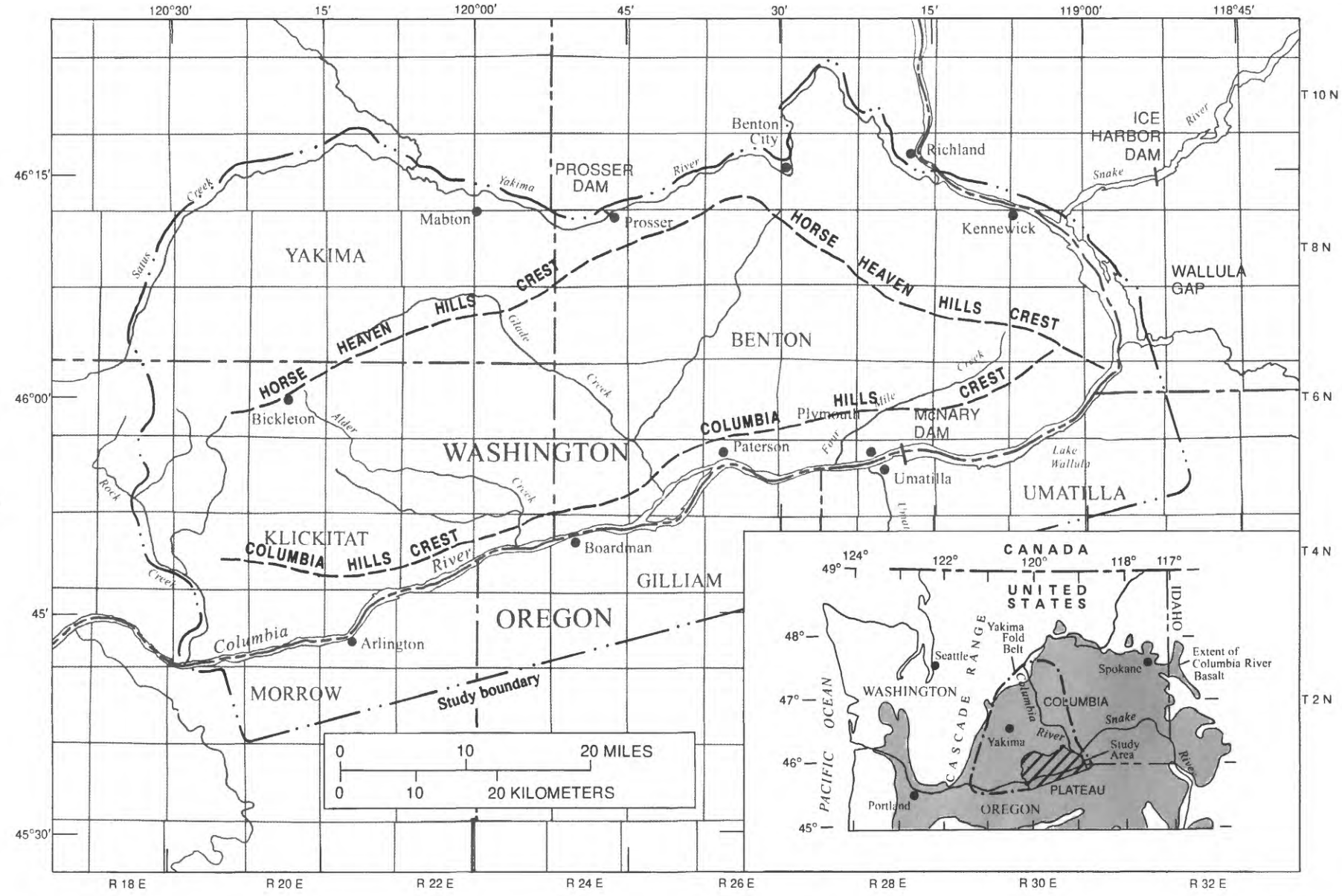

Figure 1. Location of the study area, Yakima fold belt, and extent of the Columbia River Basalt.

To provide the data and information needed (Molenaar, 1982) to manage present and pending water-rights issues, the U.S. Geological Survey (USGS), in cooperation with the WDOE, began a quantitative study of ground-water availability in the Horse Heaven Hills.

Location and Boundaries of Study Area

The area of study (approximately 2,300 mi^2 [square miles]), includes the Horse Heaven Hills, westward to a point near Satus Pass and from this point southward along the deeply entrenched Rock Creek, a significant hydrologic boundary for the area (fig. 1). Although the deepest aquifer continues to the west beneath Rock Creek, a large part of the Horse Heaven Hills aquifer system is truncated in this canyon, and significant quantities of water are discharged from seepage faces along canyon walls and to Rock Creek. North of the Horse Heaven Hills crest, the southeast part of the Satus Creek basin and the north and northeast flanks of the Horse Heaven Hills structure were included for the same reason; that is, Satus Creek, the Yakima River, and the Columbia River were judged to be major discharge points for ground-water flow from the Horse Heaven Hills aquifers. Model boundaries are essentially the same as boundaries of the study area.

Purpose and Approach

The purposes of this report are to: (1) to describe and quantify ground-water movement in the Horse Heaven Hills study area; and (2) to estimate the the effects of alternative development schemes on the hydrologic system in terms of ground-water levels and discharges.

Available data were used to develop a preliminary three-dimensional, finite difference ground-water flow model during the first several months of the study. Sensitivity "runs" of this model indicated that the most important controls of the flow system were low hydraulic conductivity features along linear "flow-barrier" elements coincident with major faults and tightly folded anticlines. Simulation results were also sensitive to the distribution of low vertical-hydraulic conductivities in the study area. Furthermore, a preliminary assessment of methods for calculating recharge through the use of either area-wide discharge measurements or monthly precipitation in water-balance schemes showed that more accurate procedures would have to be developed. At the beginning of this study, no information was available to comprehensively describe the hydraulic characteristics, thickness, or extent of aquifers in the area, or to define water levels or water-level changes through time for these units. Additionally, no data were available to describe the distribution and rates of ground-water pumpage or of water importation from the Columbia River through time. These information and data needs dictated the scope of this study.

The geometry (used in the report to mean the three-dimensional configuration and areal extent of the various bedded units; that is, geologic structure and layering) was defined through the use of geophysical logs, drillers' logs, and some additional field work devoted to better define interbed lithology. Structure and thickness maps (Brown, 1980) were produced for major member units in the upper two of the three major basalt formations (Saddle Mountains and Wanapum; fig. 2) and saturated thickness maps of the Saddle Mountains and Wanapum aquifers were subsequently made. Only three wells in the study area completely penetrate the Wanapum and extend into the

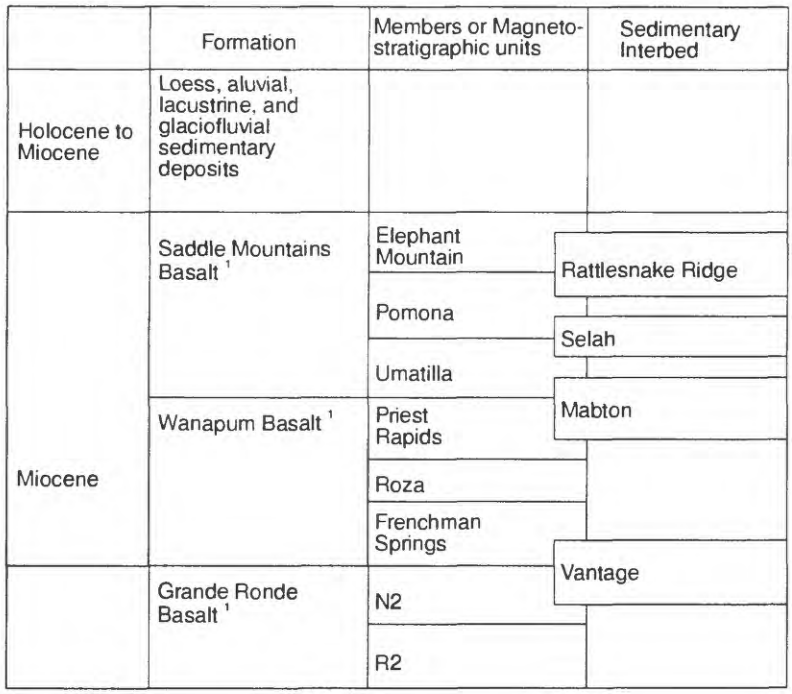

[1] The Saddle Mountains, Wanapum, and Grande Ronde Basalts are included in the Yakima Basalt Subgroup.

Figure 2. Time-stratigraphic relations between formations and members of the Columbia River Basalt Group and major intercalated sedimentary units of the Ellensburg Formation within the Horse Heaven Hills study area.

Grande Ronde formation, and then only into the top 100 to 200 feet. For this reason, construction of geometry and flow-system maps of this thick lower unit (aquifer) was not possible.

The Saddle Mountains and Wanapum aquifers were defined as hydrogeologic units coinciding with the geologic formational units, and water-level maps were made using data from four mass water-level measurements (1980 to 1983). The density of well control within each formation, and the casing practices of well owners in the area, does not justify any further subdivision of these basalts into aquifer subdivisions.

Hydraulic characteristics of the three aquifers were defined using available specific-capacity test data. One multi-well aquifer test was made by WDOE in the central part of the Horse Heaven Hills area, but no additional testing was done during this study. Initial vertical hydraulic conductance values (leakance) for the three-dimensional model were derived from a contouring of data from five cross-section flow models and these values were only slightly modified during calibration.

Yearly pumpage from major irrigation wells was calculated using electric power-consumption data plus a number of pump efficiency and total-head measurements made during the study. Distributed values of recharge were calculated from daily precipitation data and a modified version of the Blaney-Criddle method (1950). An attempt was made to measure a steady-state recharge

flux within the loess deposits that cover the basalts in order to evaluate these recharge calculations. Baseflow discharge to the larger streams was estimated from gaging-station data and seepage measurements. No spring flow was measured. Samples for water-quality analysis and carbon-14 age dating were collected from selected wells near the end of the study when the flow system was better understood.

The main unknowns determined by model calibration were the distribution of horizontal hydraulic conductivity, river node and drain conductances, and storage coefficients. Part of the Horse Heaven Hills, from its crest southward to the Columbia River, was more intensively studied and more carefully modeled than the rest of the area; that is, those parts of the model in Oregon and north and northeast of the Horse Heaven Hills crest were included mainly to extend the model far enough from pumping centers to eliminate boundary effects during transient simulations.

Physiography

The topographic feature known as the Horse Heaven Hills is an anticlinal basalt ridge which trends east-northeast from the westernmost boundary of the study area, gradually descending from elevations of 4,400 to a low of 2,000 feet at a point 10 miles east of Prosser. From there, it turns southeastward and slopes gently to an 1,800-feet elevation above Wallula Gap along the Columbia River. Slopes are steep north and northeastward from the Horse Heaven Hills into the alluviated synclinal Yakima and Columbia Valleys. South and southwest-facing slopes, descending to the synclinal valley along the Columbia River, are gentle. South of the Horse Heaven Hills, and parallel to and near the Columbia River, a single, narrow anticlinal ridge (Columbia Hills anticlinal ridge) interrupts the otherwise smooth, south-facing slope. Tributary streams flow from the Horse Heaven Hills axis northward into the Yakima River and southward into the Columbia River. These drainages cut deeply into basalt aquifers in the western one-half of the study area (up to 1,800 feet of relief along Rock Creek), but are much shallower in the eastern half. This reflects higher rainfall/runoff (and thus eroding power) and larger relief from crest to major river in the western one-half of the area. In general, there is perennial flow in the larger western tributary canyons and a number of small springs exist in this area. Eastern streams are ephemeral and springs are scarce or absent. The Columbia River, deeply entrenched at Wallula Gap in the eastern end of the study area, flows westward through an area of relatively gentle relief between Plymouth and Paterson, and then cuts an increasingly deep trough through the western one-third of the area.

Climate and Farming

Weather in the study area is characteristically colder and wetter along the higher altitude of the Horse Heaven Hills axis than along adjacent parts of the Yakima and Columbia Valleys to the north and south. Weather stations at Bickleton and MacNary Dam were used along with several stations in Oregon (Boardman, Arlington, Umatilla) and in the Yakima and Columbia River Valleys north of the Horse Heaven Hills (Kennewick, Prosser) for developing the precipitation map (fig. 3). Lines of equal precipitation were drawn with the assumption that distribution is influenced by topography, nearness to the Cascade Range, and the prevailing northeast wind direction. A map showing lines of equal temperature is not presented in this report, but it was assumed

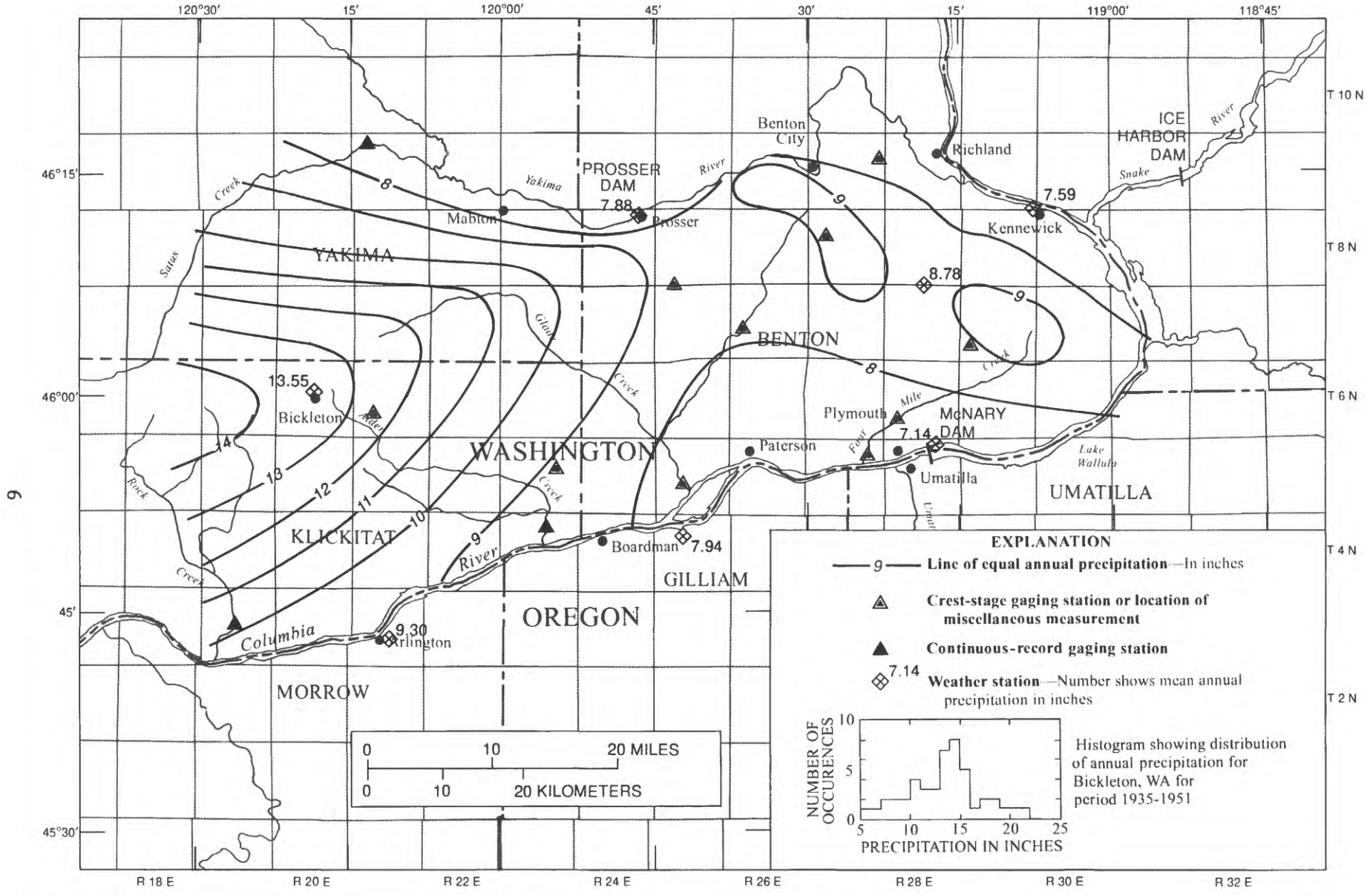

Figure 3. Estimated distribution of mean annual precipitation, histogram of annual precipitation at Bickleton, and location of stream-gaging stations.

for purposes of calculating evapotranspiration that the 6°F (degrees Fahrenheit) difference in temperature (annual average) between MacNary and Bickleton is distributed along lines of equal temperature which, like lines of equal precipitation, are parallel to topographic contours. At the Bickleton and MacNary Dam stations, about one-half of the precipitation falls from November through January, much as snow, and less than 10 percent falls during the period from July through September. Some indication of the variability of precipitation at Bickleton is shown in figure 3.

Generalized areas of irrigated farming (1982 acreage) for the Washington part of the study area are shown in figure 4. Ground-water and surface-water irrigation in the area south of the Horse Heaven Hills crest totaled approximately 8,000 acres and 70,000 acres, respectively, in 1982. Major irrigation with Columbia River water began in 1967, and ground-water irrigation began in 1968, although the amount pumped was not significant until 1972. Most of the area, surrounding and north of the irrigated areas to the crest of the Horse Heaven Hills and westward into the Bickleton area, is used to grow dryland wheat. In the western one-third of the study area, soils become thinner, and in many cases, soil has been completely stripped from basalt ridges in areas of high relief so that no farming can be done. The patterns of soil type and their water-holding capacity almost parallel the patterns of precipitation.

Trees are abundant in the 20 to 30 mi^2 area through the higher westernmost parts of the Horse Heaven Hills, where precipitation exceeds 15 inches per year. Trees are sparse along both shallow and deep canyons in the western half of the region, and are rare in the eastern half. Sage and cheatgrass are the typical natural vegetation over the lower elevations of the western part, and over the entire eastern part of the study area. Cactus grows in the sandy, lower elevations.

Water Use

The current importation of surface water from the Columbia River into the Horse Heaven Hills area began in 1967 (fig. 5) and grew at an average-annual rate of 45 percent per year from 1972 to 1977. From a peak of 178,000 acre-feet in 1977, it has declined and leveled off at 160,000 acre-feet per year. Ground-water pumpage began in 1969 and expanded slowly through 1976 (fig. 5). In the next 3 years, pumpage increased tenfold to a 1979 peak of 26,000 acre-feet per year, and since that time it has decreased to about 21,000 acre-feet per year. On the average, ground-water irrigators apply about 3.0 feet of water per acre per year and surface-water irrigators apply about 2.5 feet of water per acre per year. Quantities for both sources of water were calculated by using electric-power records for each point of water withdrawal. Pumping rates for each well were measured with a sonic transient-time current meter and these measurements were related to observed electric usage to derive pump efficiency. These efficiencies were then used with total head measurements and yearly power-consumption records for each well to calculate amounts of water pumped per year from the ground-water system.

Acknowledgments

Special thanks are due to the many landowners and tenants in the Horse Heaven Hills area who allowed U.S. Geological Survey personnel to make water-level, aquifer test, and water-quality measurements during the 3 years of

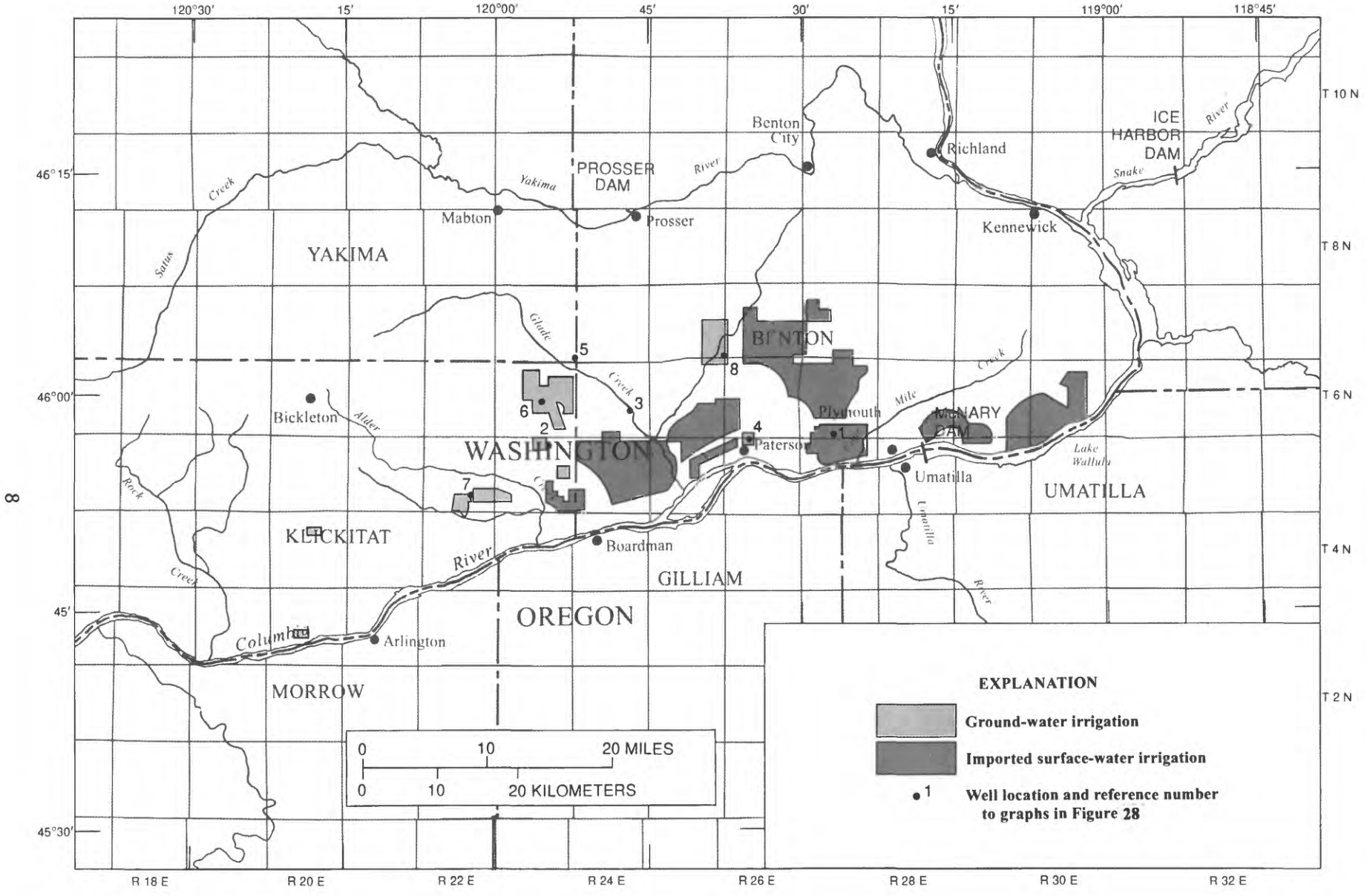

Figure 4. Distribution of irrigated acreage and location of selected wells with long-term records of water levels and pumpage.

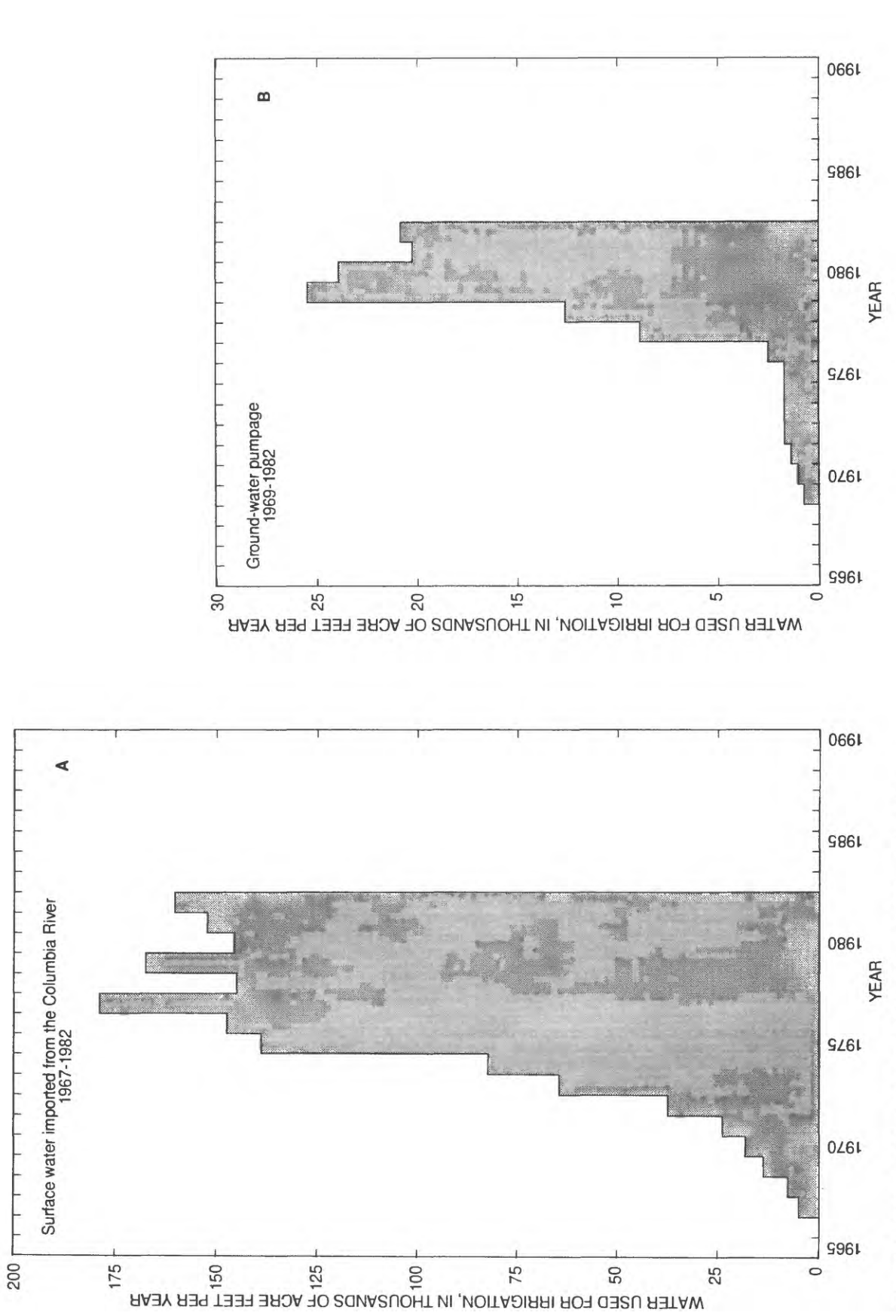

Figure 5. Irrigation sources in the Horse Heaven Hills study area.

field work. Jeffrey Brown (Washington State University) defined the geometry (structural and stratigraphic geology) of the system. Department of Ecology personnel in Yakima and Olympia, Howard Powell, Douglas Clausing, Michael Wilson, William Myers, and Alan Wald, all assisted the USGS in obtaining information about the Horse Heaven Hills area.

HYDROLOGIC SETTING

The description of geology, flow system, hydraulic characteristics, recharge, and discharge, are in effect, a conceptual model of the Horse Heaven Hills natural flow system; that is, a qualitative description of its geometry, its boundaries, and the approximate pattern of ground-water flow in it. This conceptual model was used as a pattern to construct the preliminary numerical model; the numerical model was then used to modify the initial concepts and eventually to quantify the flow system.

Geohydrology

The Horse Heaven Hills study area is underlain by 5,000 feet or more of Miocene basaltic flows which have been classified into formational units (fig. 2; Swanson and others, 1977). From 10 to 200 feet of Pleistocene and Holocene sediment overlie these flows, mostly along topographically and structurally low areas. The nature of rock that underlies the basalts is unknown, but probably is composed of sediment and metasediment of late Mesozoic and early Cenozoic age (Campbell, 1985). Folding, which was contemporaneous with extrusion of at least the younger basalts, has resulted in a large anticlinal fold coincident with the Horse Heaven Hills ridge, and major synclinal valleys to the north and south along the Yakima and Columbia Rivers. The basalt-flow rocks, which constitute the major aquifers in the area, are moderately porous and their permeability is, to some extent, related to the major structures.

Structural Geometry

Structures in the area, mapped by Swanson and others (1979), were studied in detail in this investigation. Structure contours on top of the Mabton, a sedimentary interbed between the Saddle Mountains and Wanapum Basalt Formations are shown in figure 6, and contours on top of the Grande Ronde Basalt are shown in figure 7. Major structural features as listed on figure 6, A-I, include the following:

(A and B) The Horse Heaven Hills anticlinal ridge, east-northeast in orientation, 45-miles long, generally plunging to the east from the Satus-Rock Creek area to Benton City with at least two local closures. It is one of a number of generally east-west oriented anticlinal basalt ridges known as the Yakima Fold Belt, which is located in south-central Washington, along the east flank of the Cascade Range. In this report, this part of the Horse Heaven Hills anticline is informally named the western segment. At Benton City, the axis swings abruptly to a southeast orientation and extends 30 miles in that direction to Wallula Gap, the deep notch cut through the Horse Heaven Hills by the Columbia River. This part of the Horse Heaven Hills axis is informally named the eastern segment and has been mapped as a structural closure. The Horse Heaven Hills axis

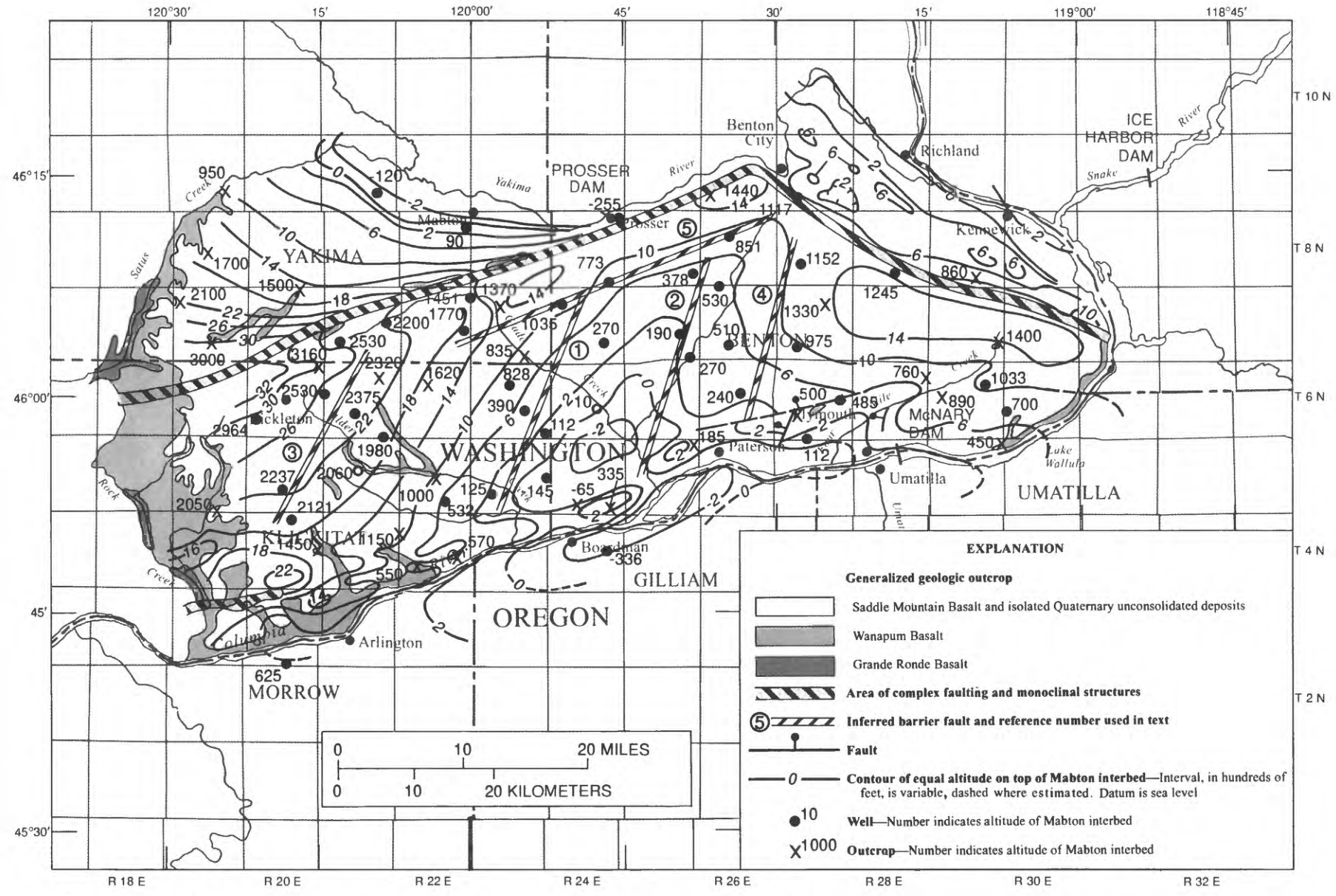

Figure 6a. Altitude of the top of the Mabton interbed and generalized geology of the study area.

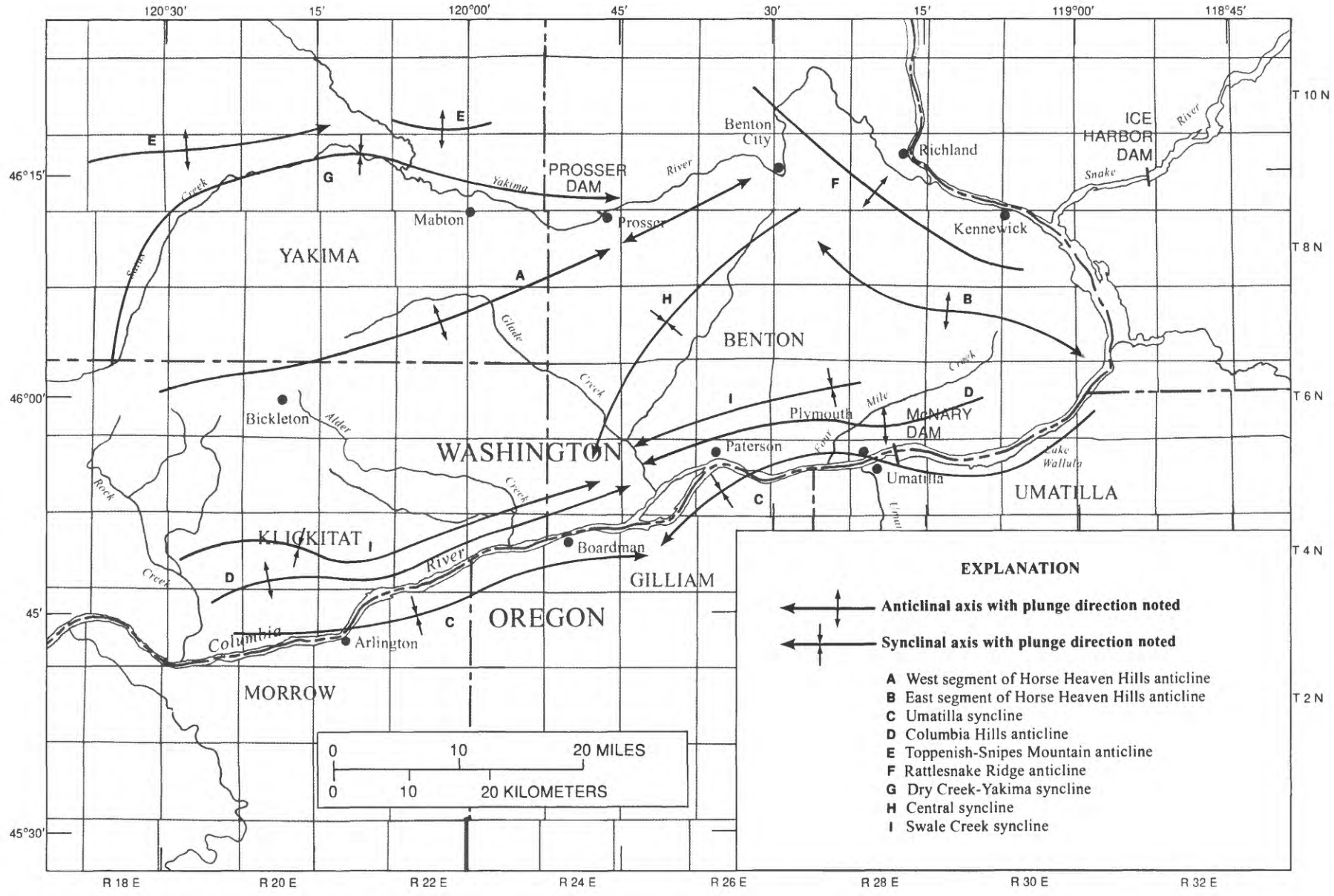

Figure 6b. Index of major structures in the Horse Heaven Hills area.

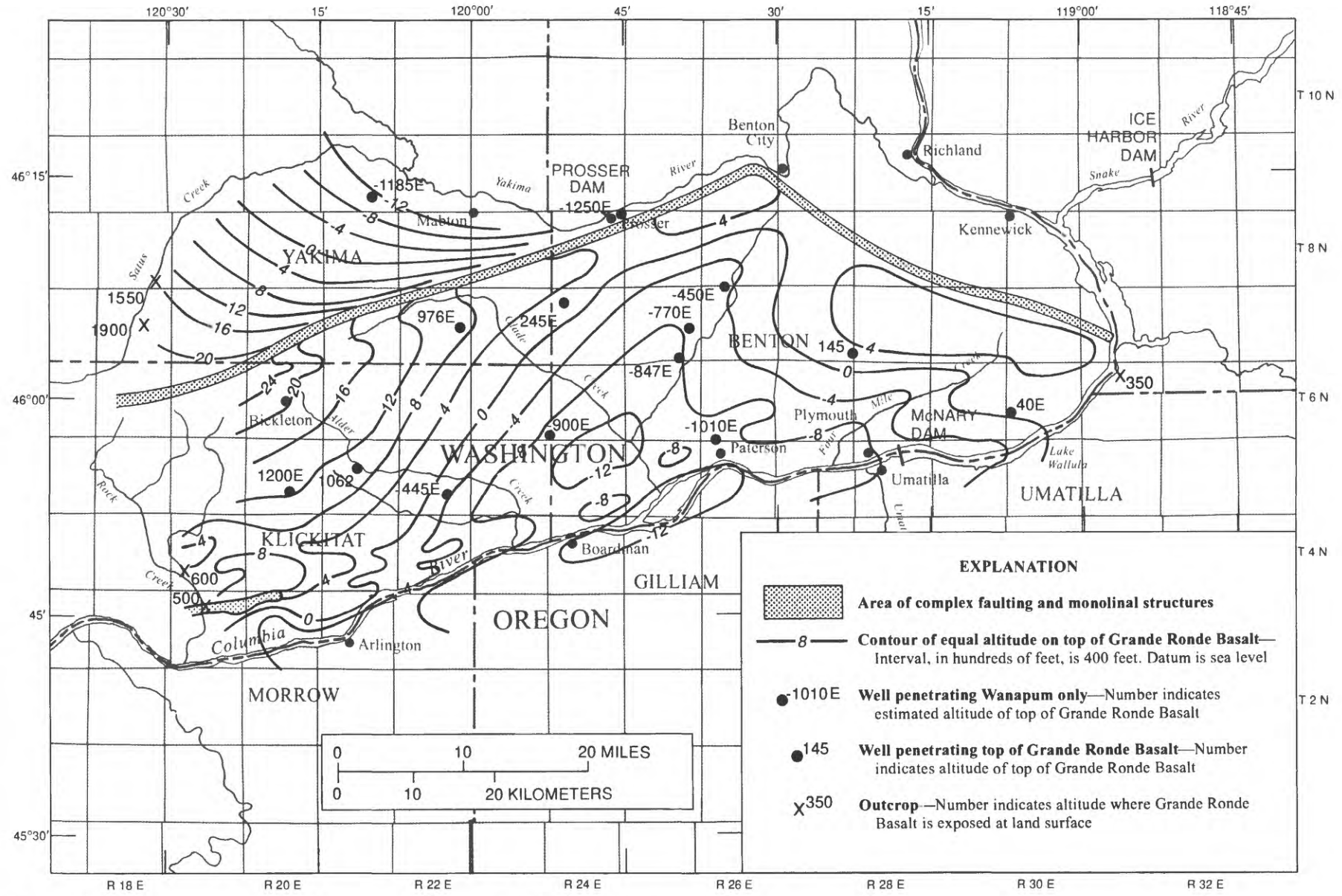

Figure 7. Approximate structural configuration of the top of the Grande Ronde basalt.

continues southeastward into Oregon. Overall, the structure is asymmetric, with a wide, gentle dip slope along its southern flank, and with a short, steeply sloping north flank which is faulted along most of its length (landslide debris covers much of this zone and faulting is in places inferred). This zone of complex faulting, shown without detail in figure 6, includes thrusting as well as high angle reverse faulting and monoclinal flexuring. It is assumed that the thrusting and monoclinal flexuring pass at depth into near vertical faults, but no proof exists of this. In places, a steep, south-dipping monoclinal flexure also is present along the south edge of the central parts of the western segment (4 miles south of Prosser).

(C) The Umatilla syncline lies 20 or more miles south of the Horse Heaven Hills axis, immediately along, and adjacent to, the course of the Columbia River; it has an east-northeast orientation, parallel to the western segment of the Horse Heaven Hills anticline. This syncline is doubly plunging with the lowest structural point in the center of the study area just southwest of Paterson.

(D) The Columbia Hills anticline is a narrow, sharply folded structure oriented east-northeast, parallel to the two major structures described above. It lies immediately north of the Umatilla syncline axis along the southern dip slope of the Horse Heaven Hills anticline. It is structurally much lower than the Horse Heaven Hills axis, is offset in a left-lateral sense 6 miles southwest of Paterson, and is again offset in a right-lateral sense at Plymouth. It is cut by northeast-oriented crossfaults at Plymouth and cut again 7 miles to the west. It is cut by northwest-oriented crossfaults and by thrusting along its western end (thrust shown as zone of complex faulting in fig. 6). There may be a fault along the north edge of the anticline between Plymouth and Paterson. The Columbia Hills anticline is doubly plunging and, like the adjacent Umatilla syncline, has its lowest structural point southwest of Paterson. There is a narrow, sharply defined syncline (Swale Creek Syncline) parallel to, and immediately north of, the Columbia Hills anticline, which also is doubly plunging toward a closed structural low near Paterson.

(E and G) The synclinal axis, along the lower Yakima River and lower Satus Creek, lies north of the western segment of the Horse Heaven Hills axis, and between it and the Toppenish-Snipes Mountain structural high. The nature of the synclinal area (Drost and Whiteman, 1985) is only partly known because of a cover of alluvial fill (in places greater than 200 feet) present along much of its length.

(H) A north-northeast-oriented syncline in the center of the study area lies along the southern dip-slope of the Horse Heaven Hills anticline. This syncline (referred to here informally as the central syncline) plunges to the south-southwest and merges with the Swale Creek syncline along the north side of the

Columbia Hills into a closed low just north of Paterson. Near the Horse Heaven Hills ridge, the syncline turns to the east-northeast and is interpreted in figure 6 to separate and pass between the western and eastern segments of the Horse Heaven Hills anticline.

North-northeast and northwest-oriented faults (possibly shear-couple faults) cross the area, some of which are shown in figure 6a. Numerous northwest-oriented faults (not shown in fig. 6) are mapped over the western quarter of the study area (Swanson and others, 1979). Two of the north-northeast fault sets can be mapped from surface exposures along the eastern one-half of the Columbia Hills anticline, but have not been mapped elsewhere. However, subtle northeast oriented flexuring can be seen in the contouring on either side of the central syncline (see four numbered zones highlighted in figure 6a. These four (faults-flexures) are inferred from a combination of geologic and hydrologic evidence (see section on ground-water flow system) and, because of their orientation, are classed as shear-fault zones.

Stratigraphic Geometry

Swanson and others (1979) have discussed the general stratigraphy of the Yakima Basalt subgroup, and the regional distribution of the various members of the Saddle Mountains, Wanapum, and Grande Ronde formations. Outcrops of these three formations are shown in general form on the structure map (fig. 6) and are generalized from Swanson and others (1979). Most of the study area is immediately underlain by the Saddle Mountains formation. The Wanapum Formation crops out as small inliers along structurally high parts of the eastern segment of the Horse Heaven Hills axis and along Wallula Gap. On the western edge of the study area, extensive Wanapum outcrops are found along Rock Creek, Satus Creek, and along the Columbia River for 20 miles upstream of Rock Creek. Several Wanapum outcrops are found along incised streams crossing the western parts of the Columbia Hills anticline and also along the fault zone bounding the western segment of the Horse Heaven Hills anticline. The Grande Ronde Basalt crops out along the bottom of the deeply incised Rock and Satus Creeks in the west and also at one place in Wallula Gap on the eastern edge of the study are (Sec.4, T.6 N., R.31 E.).

The typical basalt flow has been adequately characterized elsewhere (Swanson and others, 1975) as having porous flow tops and bases, and dense fractured interiors of the colonnade and entablature zones. The flow tops, in combination with superposed permeable flow-base sections, are called interflow zones, and are the more permeable zones in the stratigraphic section. Permeability within each of the flow top or interflow zones is connected with other such zones, above and below, by way of permeability generated by vertical cooling fractures that occur within flow centers, and by structurally generated fractures.

Although flow tops and bases of the individual basalt members can be mapped reasonably well throughout the area with the aid of geophysical and drillers' logs, water levels representative of each basalt member (for example, the Priest Rapids member) are rarely available because many wells are open to several member units. However, WDOE often has required that irrigators case through the Saddle Mountains formation when the main target of those wells is the basalt aquifers in the Wanapum; thus, it is common to find water levels for the formational units (for example, the Wanapum formation).

For this reason, the three basalt formations were chosen as the smallest stratigraphic units usable as aquifers and map units. Members of the sedimentary Ellensburg Formation occur as interbeds within the upper two basalt formations and also between the Grande Ronde and Wanapum formation. For convenience, the Rattlesnake Hills, Selah, and Mabton interbeds have been combined with the Saddle Mountains aquifer, and the Vantage interbed, with the Wanapum aquifer.

Outcrops of thin Quaternary and upper Tertiary sedimentary deposits exist in the lower Satus Creek area, in the area north of the Columbia Hills anticline between Paterson and Plymouth, and along the Columbia River around Paterson. Deposits along the Columbia River are thin (less than 50 feet thick), discontinuous, of small areal extent, and unsaturated in the area just north of Columbia Hills; therefore, these deposits were excluded as a separate aquifer system.

Over most of the study area, 10 to 40 feet of loess covers the basalt. The soil formed on this unsaturated unit supports the dry-land and irrigated agriculture of the area. Soils developed on coarse clastics just north of the Columbia River are sandy and gravelly (Washington State University, 1970). In the low topography north of the Columbia Hills Ridge (fig. 1), the soils are loamy sands, whereas the midslope areas, just to their north, are covered by deep loamy soils with very fine sand, silt, and seams of caliche. Upslope, in the higher one-half to one-third of the area, soils are developed on loess silts and become more compact and higher in organic and clay content with higher rainfall. In the highest areas of the western Horse Heaven Hills, severe erosion has stripped extensive loess and soil cover and has left dendritic patterns of scabland topography with intervening islands of thin soil cover.

Using available geophysical logs plus several lithologic logs obtained from wells drilled during the study, a series of cross sections for correlation were developed for the Horse Heaven Hills study area to trace the continuity of formation and member unit tops (Brown, 1980). Some of these correlated tops have been verified with the small amount of rock-chemistry analysis made by WDOE, U.S. Geological Survey, Washington State University, and Rockwell Corporation. Using these correlated wells as control, other wells were correlated with, and added to the data base before thickness and structure maps were constructed for those units where sufficient control existed. Thickness maps of formational units were used in conjunction with water-level maps and structure maps to generate saturated thickness maps for the Saddle Mountains and Wanapum aquifers (fig. 8). Several generalizations can be made from these maps and from maps constructed by Brown (1980).

(1) The Saddle Mountains aquifer is completely truncated along Rock and Satus Creeks and does not extend beyond the western limits of the study area except in lower Satus Creek. It does continue beyond the study area boundaries in all other directions. Though the Wanapum aquifer is truncated along discontinuous reaches of Rock and Satus Creeks, this aquifer does extend west of the study boundaries in some areas, and beyond all other study boundaries. The Grande Ronde aquifer extends beyond all study boundaries.

(2) Thicknesses of Saddle Mountains Basalt and Wanapum Basalt Formations, and some of their members, are related to major structure with the thickest sections that are located along synclinal axes and indicate

that structural movement was contemporaneous with basalt extrusion. Saturated thicknesses of the Saddle Mountains aquifer range from zero along the Horse Heaven Hills axis to more than 600 feet in the central syncline. Thicknesses of 1,000 feet are present in the lower Satus area where clastic rocks overlying the Saddle Mountains Basalt Formation are included in the Saddle Mountains aquifer. Saturated thicknesses of the Wanapum aquifer range from less than 300 feet to about 1,000 feet. Thickness of the Grande Ronde aquifer is unmeasured, but is assumed to be about 3,500 feet.

(3) The largest percentage changes in total thickness occur in the sedimentary units, for example, the Selah and Mabton interbeds. Some of this thickness variation may be due to errors in interpreting the top of interbed units in areas where overlying basalts have invaded (intruded) the sediment, but mapping of such features in the subsurface could not be done. It was assumed that the regional patterns of thickness were not affected by such features. Some thickness variation probably is due to reworking and accumulation of tufaceous deposits and erosional products from basalt flows into the topographically low synclinal areas, resulting in increased thickness of the sediment. One result of this reworking is increased occurrence of porous and permeable sand and gravel in these synclinal areas (for example, central syncline, Mabton member). The only method to evaluate much of this facies change is by drillers' generalized descriptions which indicate that more sand is found in synclinal than in structurally higher areas (fig. 8c). Some gravel has been reported in the narrow, sharply folded synclinal area northeast of Bickleton along the Horse Heaven Hills crest, and also northeast of Paterson in the Swale Creek synclinal area north of the Columbia Hills anticline. The major importance to ground-water flow in the Horse Heaven Hills study area is the interpreted presence of sandy fluvial deposits in the central syncline, along the Swale Creek syncline immediately north of the Columbia Hills anticline, and along the Umatilla Syncline axis (fig. 6). Cores collected by the U.S. Army Corps of Engineers (COE) from the Mabton interbed at the foot of MacNary Dam along the Umatilla synclinal axis show that sand and gravel make up 50 to 60 percent of the basal Mabton thickness for most of the locations. Overall, these facies patterns are important in estimating the distribution of vertical and horizontal hydraulic conductivities across the Horse Heaven Hills study area.

Selah and Mabton interbeds seem to show similar patterns of thickness and facies, and these patterns are related to major structures in the same way. The inferred facies shown with the Selah interbed thickness map (fig. 8c) is similar to that displayed in the Mabton interbed.

(4) The Selah and Mabton interbeds, and to a lesser extent, the individual basalt flows, show a regional thinning over the shear complex bordering the central syncline on the west (shear 1 on fig. 6). Log correlations and thickness maps indicate that some parts of the Roza Basalt Member may be thin or absent over the west side of this shear complex and, in addition, rock chemistry from a well in this area indicates the possibility of a thin Mabton interbed and the Priest Rapids Member in the same place. One inference is that, during the basalt extrusion, a high topography may have existed along the west side of this shear complex, and at times, this shear may

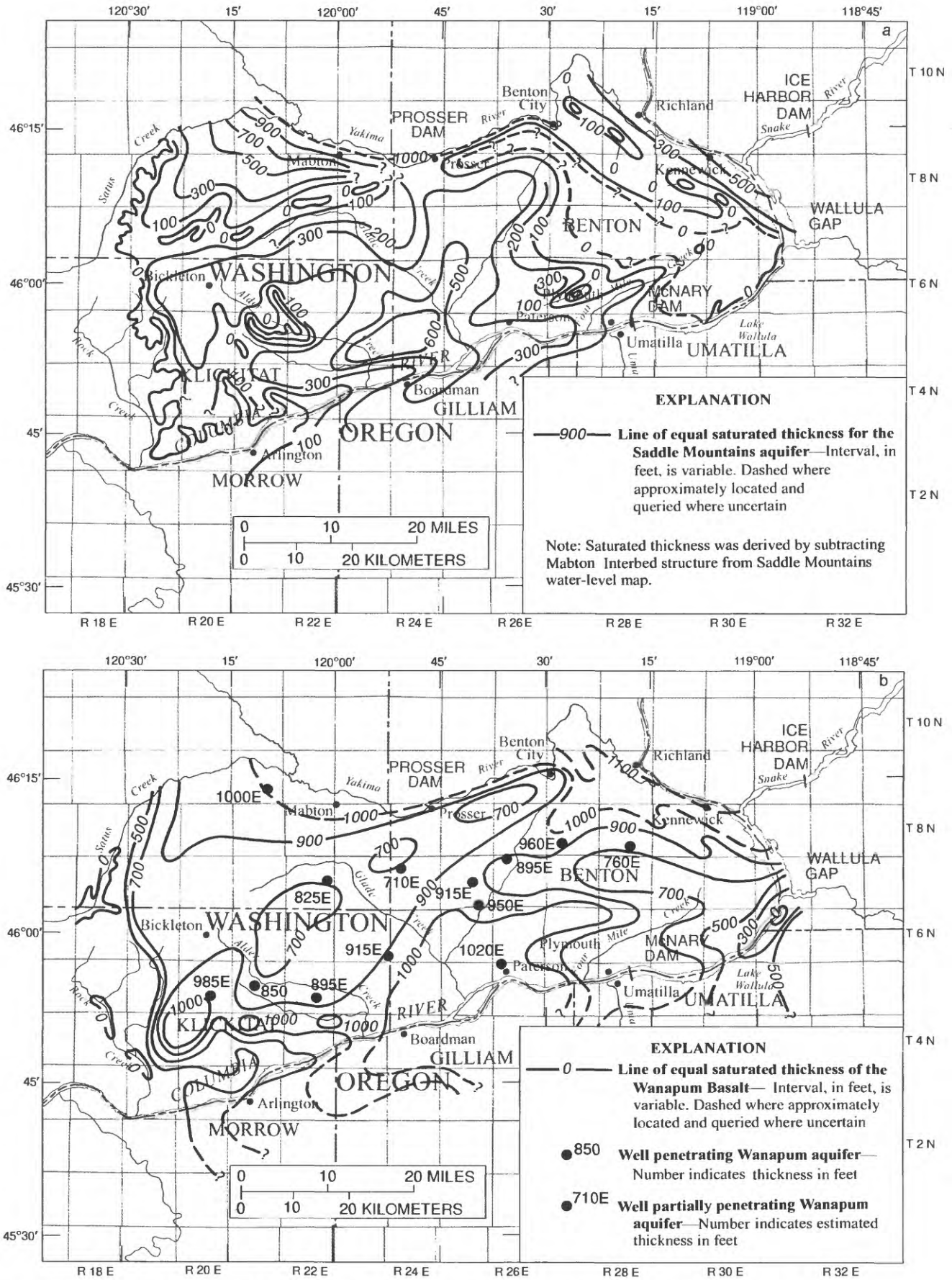

Figure 8. Saturated thickness of (a) the Saddle Mountains aquifer and (b) the Wanapum aquifer.

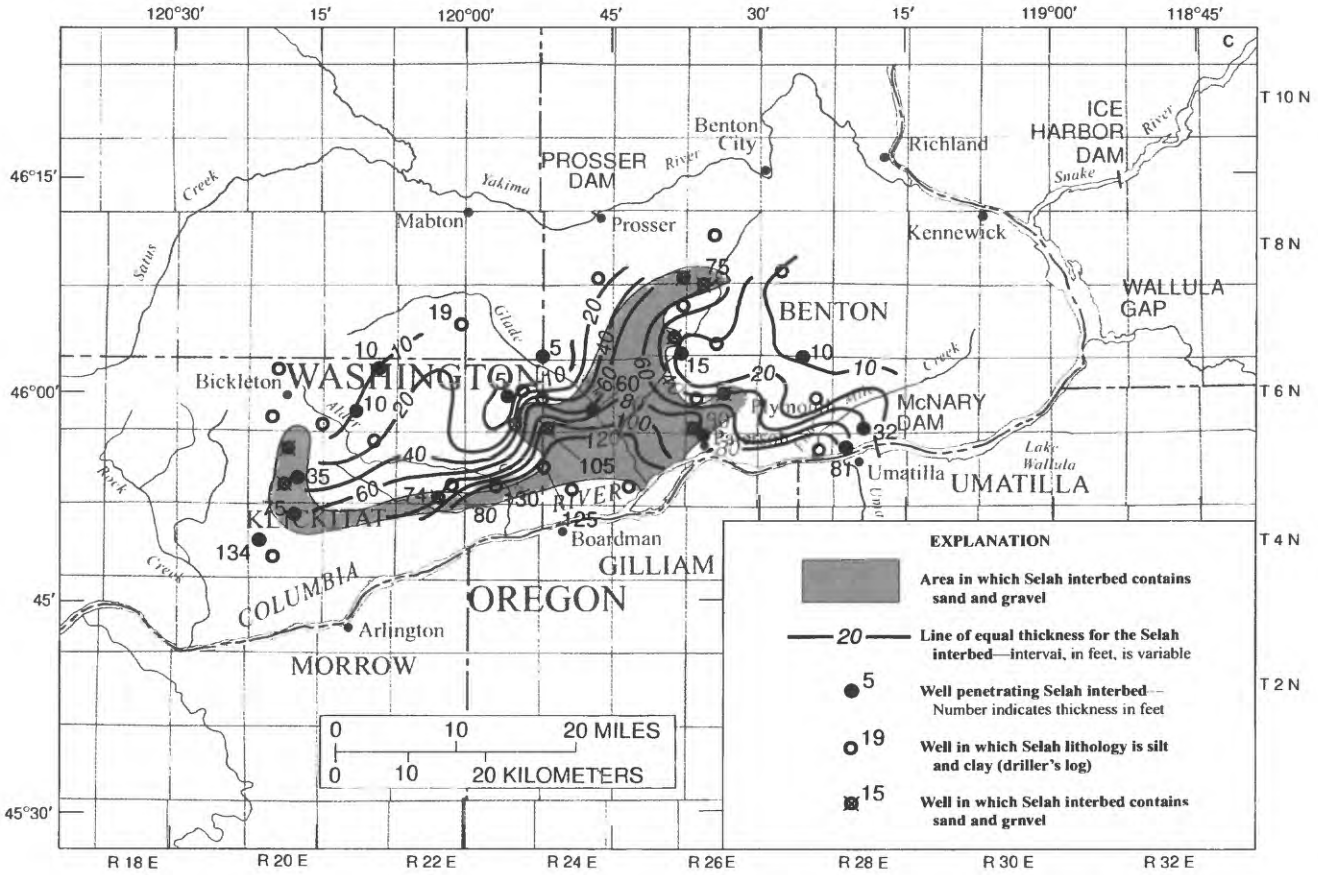

Figure 8c. Thickness and generalized distribution of facies types in the Selah Interbed Member. (Wells without numbers do not fully penetrate the Selah unit.)

have been the locus of significant change in basalt and sedimentary unit thicknesses and rock properties. The other zones of implied shear in the Horse Heaven Hills (fig. 6) are less well identified and controlled (for example, the zone on the east side of the central syncline), but they also may have similar changes in rock properties associated with them.

Only a small amount of information is available for the Grande Ronde Basalt Formation in the Horse Heaven Hills area. Three wells have been drilled into the top of this formation. In two of these wells (5/21-16G and 7/27-36B), penetration of the Grande Ronde Basalt Formation has been verified by chemical analysis of the rock. The third well (in the Wallula Gap area, 6/29-11N) probably penetrated into the top of the Grande Ronde Basalt Formation, but no proof of this exists from rock analyses. To the south of the Horse Heaven Hills, in the Blue Mountains of Oregon, 3,000 to 4,000 feet of Grande Ronde Basalt Formation are exposed. To the north, magnetotelluric data indicate up to 10,000 feet of Grande Ronde basalts, or pre-Wanapum basalts in the Pasco Basin, and drilling indicates 5,000 to 6,000 feet in the Umtanum Ridge area north of Yakima. For this study, it has been assumed that an average of 3,500 feet of Grande Ronde basalts exists beneath the Horse

Heaven Hills study area, and that the patterns of lithologic variation in the Grande Ronde Basalt Formation are similar to those of the Wanapum Basalt Formation.

Ground-Water Flow System

Collectively, the flow system consists of multiple aquifers (flow tops or interflow zones in the basalts, and sometimes, interbeds) hydraulically connected across intervening basalt flow centers by fractures. At places where interbeds are fine-grained, they represent less-permeable units between the more permeable interflow zones. In places where sedimentary interbeds are coarse grained, as in the major synclines, these units may be permeable enough to contribute significant amounts of water to wells.

The major features of the Horse Heaven Hills flow system are listed below. These features constitute the conceptual model of this system on which the numerical model is based.

(1) Topography exerts a major control on the flow system. A ground-water divide was interpreted in all three aquifers along the crest of the Horse Heaven Hills, with flow from this divide to discharge points along the Columbia and Yakima Rivers, to springs along upper and middle slopes, to secondary streams in the western half of the study area, and to seepage faces along canyon walls above them (for example: Satus, Rock, Wood, Pine, and Alder Creeks). Very low gradients exist within the central syncline.

(2) Downward flow from the Saddle Mountains aquifer to the Wanapum aquifer takes place over most of the area except adjacent to the Yakima and Columbia Rivers. Historic records, and data collected during this study, document the presence of upward flow along the Yakima River with data points at the towns of Satus (9/29-28D2) and Prosser (8/24-2J1), and upward flow along the Columbia River with data points at Paterson (5/26-8G1), at Artesian Coulee (T.4 N., R.24 E.), and near Artesian Coulee (5/24-35R1). In general, the head loss with depth is large along the axis of the Horse Heaven Hills and the head gain with depth is small along the major rivers. There is one midslope area where downward flow from the Saddle Mountains aquifer does not occur; specifically, the area of upward flow just west of the central syncline and of shear zone 1 (fig. 6).

Vertical gradients of 0.14 ft/ft (feet per feet) within the Wanapum aquifer along the axis of the Horse Heaven Hills anticline were estimated by using adjacent wells which were completed at different depths in the aquifer. This vertical gradient is close to the 0.18 ft/ft calculated by Strait (1978) for the Saddle Mountains aquifer in this same area. Vertical gradients near the Columbia River were estimated by comparing several surveyed measurements of water levels in the river, made during a 1-week period in the summer of 1982, with water levels in nearby wells. These comparisons show that water levels in wells as deep as 300 feet are higher than, but within several tenths of a foot, of adjacent water levels in the river. In one well near the river (5/24-35R1), water levels measured over several years were compared with a hydrograph of river levels, and showed close, correlated movement, indicating good vertical connection between the basalt aquifers and the river (fig. 9).

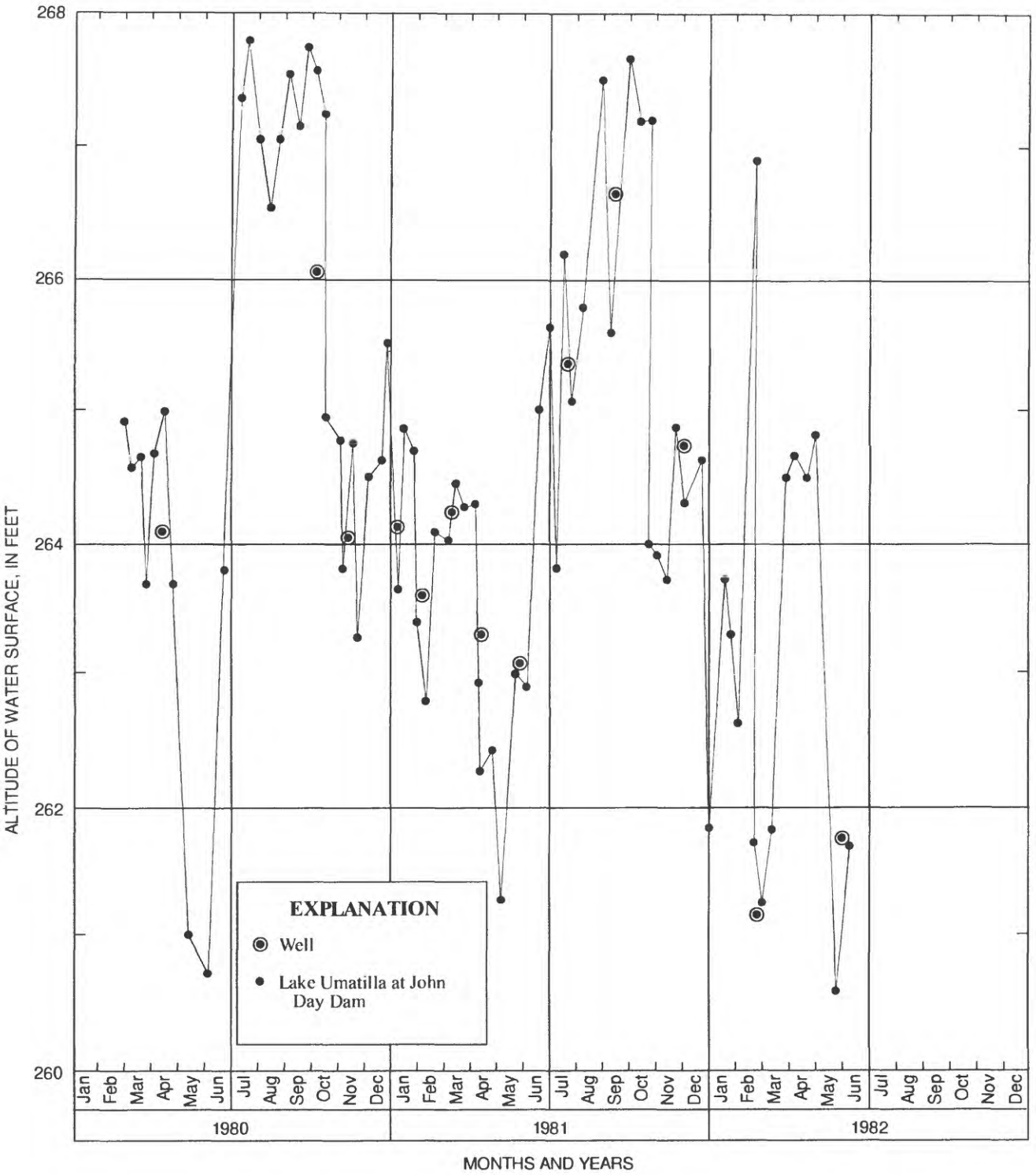

Figure 9. Water-level altitudes in well 5/24-35R1 and in Lake Umatilla, 1980-82.

The head change with depth is not uniform in those wells where data exist. Vertical gradients are documented by two sets of piezometers, one at 7/25-36N and the other at 6/23-15H. In the Paterson test well, 7/25-36N, piezometers show a large head loss across the boundary between the Saddle Mountains and Wanapum aquifers (Brown, 1978) and no head loss in the Wanapum aquifer itself (fig. 10). Data from two other wells that are geographically near one another and monitor separate aquifers also support the concept that there is a greater head change across the Saddle Mountains-Wanapum aquifer boundary than within each aquifer (fig. 10).

Data from piezometer 5/21-16G (not shown on fig. 10), emplaced in the later stages of this study, indicate a large head loss between the lower part and the middle part of the Wanapum aquifer, but did not indicate head difference between the Grande Ronde aquifer and the lower part of the Wanapum aquifer. Abrupt head change within the lower Wanapum aquifer, as indicated by 5/21-16G, is a phenomenon which is not well documented because few wells were completed that deep.

(3) Linear zones of steep hydraulic gradient are found in the Wanapum aquifer and; in some locations, there are similar but lower, gradients within the overlying Saddle Mountains aquifer. Examples of these zones of steep gradient are associated with the major fault zones immediately north of the eastern and western segments of the Horse Heaven Hills axis, with both shear faults 1 and 2 (fig. 6) bordering the central syncline, with the monoclinal flexure at the south edge of the western segment of the Horse Heaven Hills axis, and with the western parts of the tightly folded Columbia Hills anticline. Steep gradients also are inferred to exist along the edges of the deeply entrenched Rock and Satus Creek areas, where seepage faces of undetermined thicknesses exist.

(4) Extensive areas of unsaturated Saddle Mountains aquifer occur along the crestal parts of the eastern segment of the Horse Heaven Hills anticline from Wallula Gap north. Partially saturated or unsaturated areas within the Saddle Mountains aquifer are inferred to also exist adjacent to Wanapum Basalt Formation outcrops within the fault zone along the north edge of the Horse Heaven Hills crest. Unsaturated or partially saturated material also is assumed to exist adjacent to Saddle Mountains Basalt Formation pinchouts along deep canyons tributary to the Columbia River in the western one-third of the area. Partial saturation of the Wanapum aquifer is interpreted to occur along the westernmost parts of the Columbia Hills anticline, along Alder, Rock, and Satus Creeks, where streams cut deeply into the Wanapum aquifer, and along crestal parts of the eastern segment of the Horse Heaven Hills axis. The thickest area of saturated Saddle Mountains aquifer occurs along the central and Umatilla synclines and along the Swale Creek syncline just north of the Columbia Hills anticline.

Hydraulic Characteristics

On the basis of specific capacity test data, basalt and interbed horizontal-hydraulic conductivities generally are related to large structures in the Horse Heaven Hills, with lower values along the anticlines than along

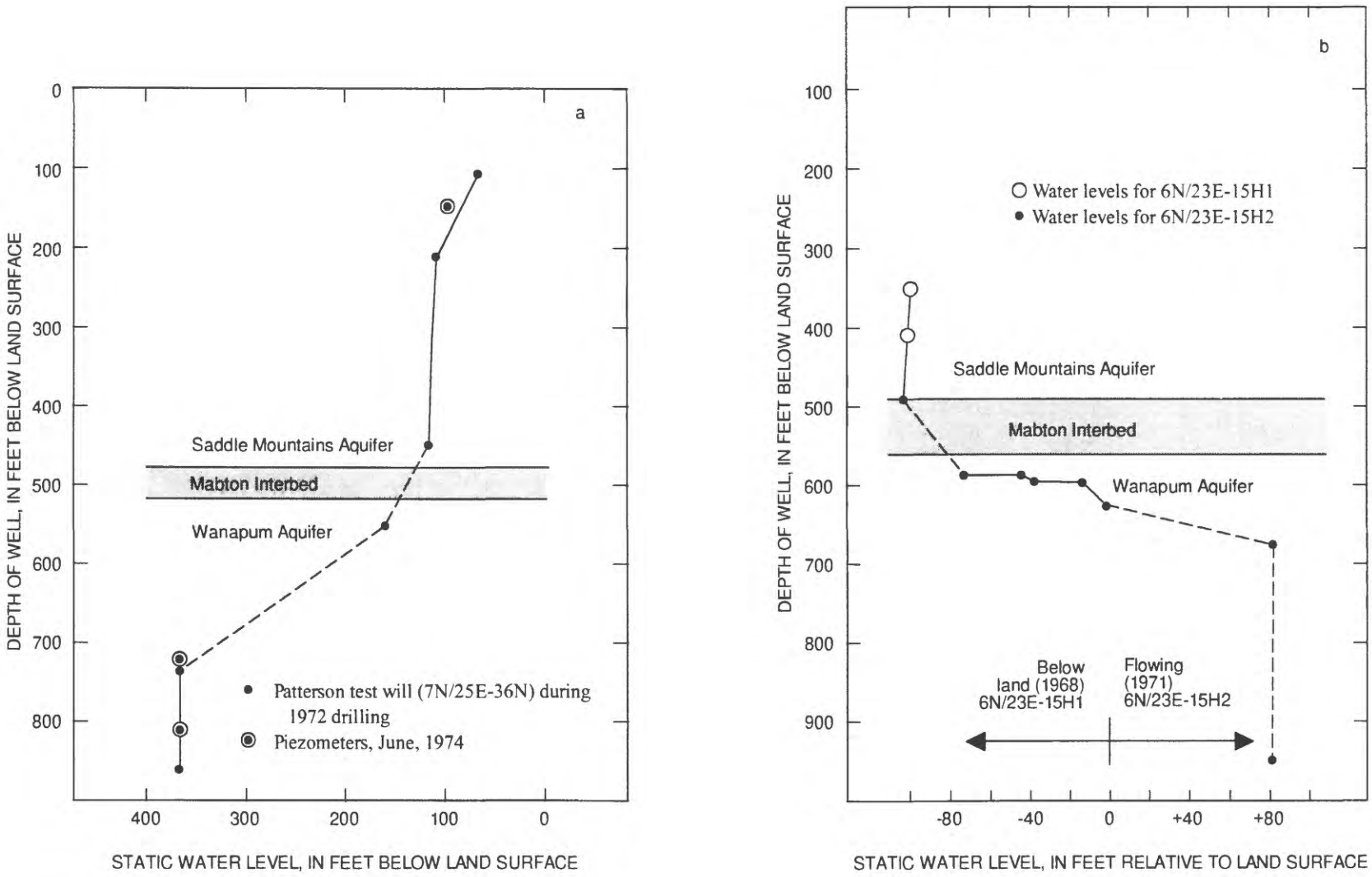

Figure 10. Water-level measurements in (a) the Patterson test well during drilling and in piezometer (b) in wells 6/23-15H1 and 15H2 during drilling.

the synclines. Large fault zones generally are associated with steep hydraulic gradients and, by inference, are zones of low horizontal-hydraulic conductivity, although little test data exist to prove this.

Horizontal-Hydraulic Conductivity

Data for horizontal conductivities were initially derived by calculating transmissivities for those wells with specific capacity data (Brown, 1963). In each case, the total aquifer thickness (interflow and flow center) was divided into calculated test-transmissivity values to obtain an average equivalent hydraulic-conductivity value for the aquifer in question (fig. 11). In a few cases where tests were made across parts of two aquifers and considered valid, the entire calculated-test transmissivity value was divided by the aquifer's open interval and used solely for that aquifer. The best information available indicates that most deep wells in the Horse Heaven Hills were drilled with air or mist, so that few of the tests were affected by formational plugging with bentonite drilling fluid.

The distribution of average equivalent hydraulic-conductivity data in the Saddle Mountains aquifer (fig. 11) suggests that there is a non-random distribution, which is related to the large structural features of the Horse Heaven Hills. Specifically, there are low-calculated hydraulic conductivities along the Horse Heaven Hills anticlinal axis (range from $6x10^{-6}$ to $3x10^{-7}$ ft/s [feet per second]), and higher-calculated hydraulic conductivities along the central and Umatilla synclines (range from $9x10^{-4}$ to $2x10^{-6}$ ft/s). The generalized contours (fig. 11) reflects this apparent relation to large structure. Dashed contours are used to infer low conductivities along the Columbia Hills anticline (Newcomb, 1969).

Hydraulic-conductivity patterns in the Saddle Mountains aquifer show several relations to geometry. The distribution of high conductivity in the central syncline corresponds to an area where the Selah and Mabton interbed lithology is sandier, more permeable, and where basalt flow and interbed thickness is large. In addition, these synclinal areas must have been sites of lower topography during basalt extrusion, thus increasing the likelihood that lava flowed onto water-saturated rock or into impounded water, producing porous and more permeable pillow structures, and spiracles. The reverse would be true of the higher elevations of the Horse Heaven Hills structure; that is, low sand content and a reduced chance of pillow structure.

The small ($1x10^{-7}$ ft/s) hydraulic conductivity measured for well (6/20-36B1), within a zone of steep hydraulic gradient in the Saddle Mountains squifer, is the only test near a hydrologic "barrier" representative of this type feature (Strait, 1978; Newcomb, 1961). Reasons that might explain such phenomena are: (1) a single, vertically oriented fault, offsetting interflows filled with gouge and secondary clay minerals, or a set of clay-filled faults, parallel and closely spaced; (2) stratigraphic pinchout of interflow zones along a linear fault scarp or similar topography; (3) vertical dikes; or (4) a canyon cut in older flows which was refilled with younger basalt, forming a barrier to lateral flow. Any of these features, or a combination, could produce hydraulic boundaries which would affect calculated-conductivity values

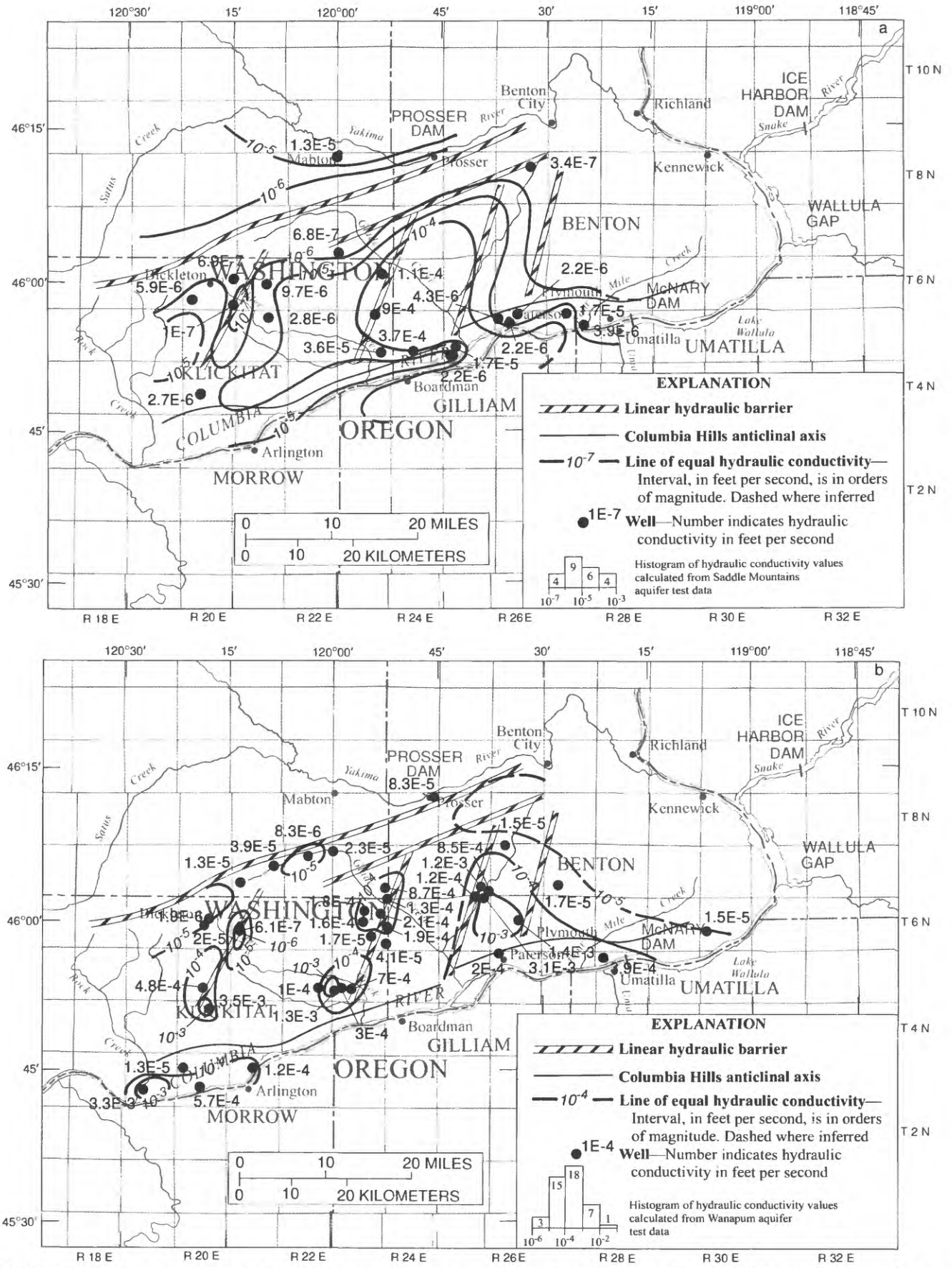

Figure 11. Hydraulic conductivity as determined from specific capacity test data in (a) the Saddle Mountains aquifer and (b) the Wanapum aquifer.

of adjacent wells which penetrated into such a zone. Dikes, or intra-canyon flows, are possible, but none have been mapped in the Saddle Mountains Basalt Formation of this area.

The distribution of test data for the Wanapum aquifer (fig. 11) is less easily associated with large structures than were the data for the Saddle Mountains aquifer. Low hydraulic conductivities along the Horse Heaven Hills axis (range, $2x10^{-6}$ to $4x10^{-5}$ ft/s) have been contoured, and isolated areas of high hydraulic conductivity (range, $1x10^{-4}$ to $3x10^{-3}$ ft/s) have been contoured on the upgradient sides of several shear barriers (shears 1, 2, and 3; fig. 6). One low conductivity value ($6x10^{-7}$ ft/s) lies along the same zone, just southeast of Bickleton (Strait, 1978). Beyond these patterns, the distribution of hydraulic conductivity has been left uncontoured with median values between 10^{-4} and 10^{-5} ft/s assumed for large areas.

The small hydraulic-conductivity values along the Horse Heaven Hills crest within the Wanapum and Saddle Mountains aquifers may be related to closely spaced shear faults of small throw, fractures, and interflow slippage filled with secondary minerals, all of which are associated with tight folding in the axial parts of such large structures. These features would act as barriers to lateral flow producing low hydraulic-conductivity values as calculated from test results. Neutron geophysical log analysis indicates that zones of high porosity (interflow zones) are just as common along the Horse Heaven Hills axis as they are downslope. For this reason, such structural dislocation seems more likely to cause for low-test conductivities than simple basalt stratigraphy. This type of structural deformation also characterizes such features as the tightly folded Columbia Hills anticline.

The large values of hydraulic conductivity associated with the upgradient side of barrier shear zones are not easily explained. Strait (1978) found the same association in his study area in the Saddle Mountains aquifer. The high conductivity values in the Wanapum aquifer in T.5 N., and T.6 N., R.23 E., (above shear 1, fig. 6) occur along zones of thinner basalt flows. One explanation may be that this area was topographically higher during basalt extrusion and that this may have had some effect on the nature of the flow tops over this topography. Detailed mapping of log-derived data yields no clear answer to this question.

Little information is available for hydraulic conductivities of the Grande Ronde aquifer as no tests were carried out in the Horse Heaven Hills area. On the basis of specific-capacity data from Oregon (A. Davis-Smith and others, 1988), the hydraulic conductivities of the upper and middle Grand Ronde aquifer are about one-third to one-fifth of those for the Wanapum aquifer. It was arbitrarily assumed for this study that the pattern of transmissivity for the Grande Ronde aquifer was the same as for the Wanapum aquifer and that the transmissivities of the full Grande Ronde aquifer were one-third of the Wanapum values.

In the Oregon part of the study, hydraulic conductivities for Saddle Mountains and Wanapum aquifers, and transmissivities for the Grande Ronde aquifer, were obtained from contoured maps developed for a similar study of the Umatilla Basin by the Geological Survey (A. Davies-Smith and others, 1988).

Water Budget

Estimation or measurement of the amounts of water recharged to, discharged from and stored within, the ground-water system by natural and man-induced means is crucial to the goal of quantifying a flow system and thereby developing concepts of how it works. The discussion below describes the most important components of the Horse Heaven Hills system.

Surface Water

Large rivers in, and adjacent to, the study area are the Columbia, Snake, and Yakima Rivers, with average flows of 200,000, 70,000, and 5,000 cubic feet per second (ft^3/s), respectively; these rivers are the major drains for the ground-water system in the Columbia Plateau. These rivers are not free-flowing; dams were completed on the Columbia River at McNary in 1957 (pool elevation 340 feet) and at John Day in 1966 (pool elevation 265 feet). Ice Harbor Dam on the Snake River was built in 1962 (pool elevation 440 feet) and Prosser Dam on the Yakima River was built in 1917 (fig. 6; pool elevation 634 feet). Extensive canal systems that divert water from the Yakima River have been in existence since the late 1800's.

Secondary streams in the western one-half of the Horse Heaven Hills, such as Satus, Rock, and Alder Creeks, flow most of the year with average annual discharges of 170, 50, and 8 ft^3/s, respectively (period of record, 1967 to 1971). Secondary streams in the eastern one-half of the area are ephemeral.

Estimates of runoff for much of the Horse Heaven Hills area and baseflow (discharge to the stream from the ground-water system) for the western secondary streams were made for two reasons: runoff values (total runoff minus baseflow) were needed to determine recharge to the ground-water system; and average yearly baseflow for the western streams was needed as a measure of discharge from the ground-water system.

Streamflow information is available for Alder Creek (near Alderdale) and for Rock Creek (near Roosevelt) for 1967 through 1971 (fig. 3). One year of discharge measurements is available for Satus Creek above Wapato drain (1979 to 1980) as measured by the Wapato Water District (Prych, 1983). In addition to these data, monthly measurements were made during 1980 and 1981 at Glade Creek, several hundred yards north of the Paterson highway, and at Fourmile Creek at the Paterson highway. These measurements, and the reactivation of the Alder Creek streamflow gaging station, added to data base of runoff and baseflow for the eastern part of the area. Miscellaneous and peak-discharge measurements, available for a number of small streams in the eastern part of the study area during the 1960's and early 1970's, complimented the monthly discharge measurements and were use as an aide to estimate runoff in this area of ephemeral streamflow.

Hydrographs of Alder Creek and Rock Creek were analyzed to obtain a baseflow separation for the years 1967 through 1972. For this period, estimated average baseflow at the Alder Creek gage was about 2 ft^3/s with about 0.5 ft^3/s coming from Alice Springs, just upstream from the gage. The estimated average baseflow at the Rock Creek gage is 14 ft^3/s for the same period (about 6 ft^3/s of baseflow is from the eastern part of Rock Creek, that is, from the modeled part of this drainage). On the basis of data, the average baseflow for Satus Creek, at a point above the Wapato drain is

estimated to be about 60 ft^3/s, with an estimated 10 ft^3/s coming from the southeastern part of this drainage in the modeled area.

During 1983, several seepage runs were made in Pine Creek, which lies between Alder and Rock Creeks. These seepage runs were used, in conjunction with Alder and Rock Creek baseflow separation estimates to estimate the Pine Creek baseflow as between 2 and 4 ft^3/s. Wood Gulch flow (just west of Pine Creek) was similarly estimated to be between 3 and 5 ft^3/s.

The monthly discharge at Glade Creek averaged 11 ft^3/s during 1981, with a maximum of 14.8 ft^3/s and a minimum of 9.1 ft^3/s. Much of this flow comes from irrigation return a short distance upstream from the measurement site. Seepage-run data along Glade Creek document this, and water-level measurements in nearby basalt wells, which lie below the loess-basalt interface, indicate that most seepage must come from a perched saturated zone located above that interface.

Recharge

Recharge to the shallow ground-water system in the Horse Heaven Hills comes from infiltration of precipitation, water pumped by irrigators from the Columbia River, and water pumped by irrigators from deep aquifers. Calculation of the distribution and rate of recharge involves a determination of the distribution and rates of precipitation and pumpage, a calculation of evaporation and transpiration rates, and a measurement and extrapolation of runoff rates. The water that remains after evapotranspiration (ET) and runoff (SR) are subtracted from a value that includes precipitation plus pumpage or irrigation return flow (PPT) is ground-water recharge (RECH):

$$RECH = PPT - ET - SR. \quad (1)$$

In many previous water-resources investigations, average monthly weather information has been used with the Blaney-Criddle method (U.S. Department of Agriculture, 1967) to determine ET. When applied to the dry climatic conditions of Horse Heaven Hills, however, this type of computation showed that all precipitation is evapotranspired over large parts of the study area and that no recharge takes place. This is in contradiction to the fact that ground-water levels near the surface are maintained by recharge over these same areas. It then became necessary to assume that recharge occurs only during certain sporadic, short-term periods, when rainfall exceeds evapotranspiration plus runoff. Daily, instead of monthly, precipitation and temperature data were used over a period of record of about 20 years to compute recharge on a day-by-day basis. The results of the computations indicated that surplus water is available for recharge nearly everywhere in the study area during short intervals (days), usually in the fall and spring (fig. 12).

Using selected basins in the Horse Heaven Hills where runoff (total runoff minus baseflow) had been measured, daily values of ET and PPT were determined. These values were used to calculate daily amounts of excess moisture (EM) available for recharge.

$$EM = SR + RECH. \quad (2)$$

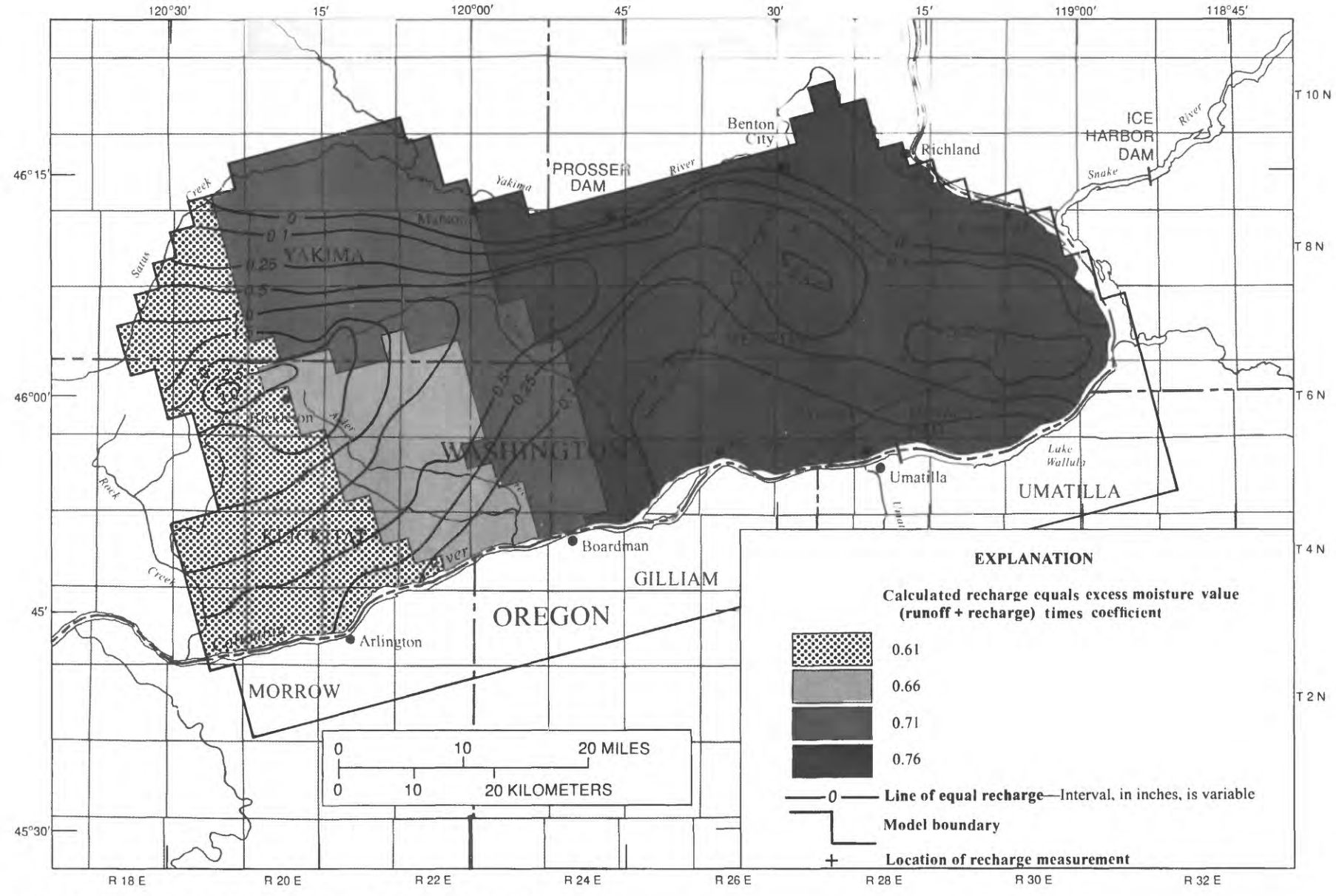

Figure 12. Calculated recharge to the Horse Heaven Hills study area.

The daily EM values were used to arrive at a 20-year, average annual EM content for each test basin. Average-annual runoff was then subtracted from average EM for the basin to calculate recharge and the RECH/EM fraction for that basin. Distribution of these fractions was generalized on a map (fig. 12) and thereafter, EM calculated for part of a basin (each model node) was multiplied by the appropriate fraction to calculate recharge values. The calculation of ET and EM for a given location involved extrapolation of daily temperature and precipitation to that location from the Bickleton and McNary weather stations, and involved use of the Blaney-Criddle equation with daily data rather than monthly data.

Calculation of Evapotranspiration

The rate of evapotranspiration is dependent on many variables such as air temperature, sunshine intensity, vapor pressure, wind speed, soil moisture, soil type, type of vegetation, and stage of plant growth. In addition, experiments have shown that nearby differences in vegetation also affect evapotranspiration at any given location. In order to simplify evapotranspiration analysis, the concept of potential evapotranspiration (PET) is used extensively. It is a measure of the amount of water that will be evaporated and (or) transpired under a given set of physical conditions (for example, temperature) with unlimited availability of water. Once PET is determined, ET, or actual evapotranspiration, is expressed as a function of PET and other variables affecting the availability of water. ET is never greater than PET, but can be significantly less if the supply of water is limited.

Of the many available methods used to determine PET, the numerical method used by Blaney-Criddle was chosen because it requires only temperature and crop type. Although this method was designed for monthly usage, it was assumed to be correct when applied on a daily basis. This was the only modification to the Blaney-Criddle calculation. The Blaney-Criddle equation for calculating daily PET is

$$PET = (0.142ta + 1.095)(ta + 17.8)\, k_c d \qquad (3)$$

where d = hours of daylight obtained from a table as a function of the latitude and time of year,
ta = mean daily temperature (extrapolated from the McNary and Bickleton weather station), and
k_c = empirical factor determined from water consumption data for different crops during the growing season. Values are published as curves of k_c as functions of time for each crop.

In the study area, only two long-term weather stations are available to establish daily distributions, although there are additional stations with shorter-term data sets. In order to establish the daily precipitation distribution, a method was devised that compensated for elevation and orographic position for each point. It was assumed that the annual lines of equal precipitation, as interpreted in this study (fig. 3), are linearly related to daily amounts of precipitation; in other words, that daily precipitation is distributed in the same manner as mean annual precipitation. Thus, for any given location:

$$PPTL = \frac{ISOL}{ISOW} \quad PPTW \qquad (4)$$

where PPTL = daily precipitation at the location,
ISOL = annual precipitation at the location,
ISOW = annual precipitation at a selected nearby weather station, and
PPTW = daily precipitation amount at the weather station.

This method is considered better than simple distance interpolation because the control which elevation exerts on rainfall is taken into consideration. Because many weather stations are at low elevations in the Horse Heaven Hills area and in the anticlinal ridges to the north (Yakima Fold Belt), extrapolation from these weather stations to higher elevations along ridge tops would be inappropriate.

Extrapolation of Daily Temperature--The main independent variable in the Blaney-Criddle equation is temperature, and it was necessary to extrapolate average-daily temperatures from the weather station to all node locations. Because mean-annual- temperature maps were not available, it was assumed that these lines of equal annual temperature are parallel to annual lines of equal precipitation as drawn, and that daily temperatures are distributed in patterns parallel to lines of equal annual temperature. It was further assumed that the difference in mean daily temperature between the two study-area weather stations could be linearly distributed along a line between them. For all other points, the distribution of mean-daily temperature is constant along lines of equal temperatures or precipitation. Thus,

$$Td = \frac{d}{D} (TB - TA) + T1 \qquad (5)$$

where Td = daily temperature to be calculated at a point along lines of equal annual temperature,
T1 = average daily temperature of one of the weather stations,
TA = average annual temperature at the same weather station,
TB = average annual temperature at the second weather station,
D = distance along straight line between the two weather stations,
d = distance along same straight line between the first weather station and the line of equal precipitation on which the location lies.

Potential evapotranspiration (PET) is greater than precipitation plus pumpage transpiration (PPT)--During any one day, at any point in the study area, when calculated PET is greater than PPT (extrapolated), water must be extracted from the soil to meet PET demands. In these cases, certain simplifying assumptions have been made:

1. Soil moisture that is evapotranspired is supplied from depths no greater than the root zone. In this study, soil moisture is considered to be only that moisture which is available for consumptive use by plants; that is, moisture in excess of the wilting-point moisture content.

2. Precipitation (PPT) on any given day is evaporated at up to the potential rate but for that day only.

3. The rate of evapotranspiration of water within the root zone during any given day is proportional to the ratio of average available soil-moisture content (ASM) to available water content at field capacity (FCAP), and to PET minus PPT, that part of PET not used in the evaporation of the day's rainfall.

These assumptions may be expressed more concisely as follows:

$$ET = PPT + ETS, \qquad 0 < PPT < PET \tag{6}$$

$$ETS = \frac{ASM}{FCAP} (PET - PPT), \qquad FCAP > ASM > WP \tag{7}$$

$$ETS = 0, \qquad WP > ASM > 0. \tag{8}$$

The variables are defined as follows:

PPT = total precipitation for the 24-hour period,
ETS = evapotranspiration from the root zone for the 24-hour period,
ET = total evapotranspiration for the 24-hour period,
PET = total-potential evapotranspiration for the 24-hour period,
ASM = average moisture content of the root zone during the 24-hour period,
FCAP = moisture-holding capacity of the root zone, and
WP = wilting point.

Evapotranspiration from the root zone depletes the moisture content. The soil moisture is variable, depending on prior soil-moisture conditions. For any given day, the average soil moisture in equation 7 is approximately

$$ASM = \frac{BSM + (BSM - ETS)}{2} = \frac{2BSM - ETS}{2} = BSM - 0.5ETS. \tag{9}$$

where BSM = soil moisture at the beginning of the day.

Substituting (6) and (7) into (9) and solving for ET:

$$ET = BSM \Big/ \left[\frac{FCAP}{PET-PPT} + 0.5\right] + PPT. \tag{10}$$

Daily precipitation and temperature data for the two weather stations in the study area were obtained from the National Oceanic and Atmospheric Administration Environmental Data and Information Service, Ashville, North Carolina. Moisture-holding characteristics of different soil types prevalent in the Horse Heaven Hills area were obtained from a study by Washington State University (1970). Root depths were determined from field observations and communication with personnel of the Yakima County Agricultural Extension Service.

Potential evapotranspiration (PET) is less than precipitation plus pumpage transpiration (PPT)--On those days when PET is less than PPT, the following occurs:

(a) $$ET = PET, \tag{11}$$

(b) After ET is satisfied, the extra moisture (PPT minus PET) is first used to fill the root-zone soil moisture back to field capacity. If any additional moisture remains after this, that amount goes to excess moisture (SURP). SURP is summed on a daily basis for each year during the 20-year period, and

$$(c)\ \sum_{i=1}^{20} SURP_i / 20 = \text{average annual excess moisture.} \qquad (12)$$

Relation of Surface Runoff to Excess Moisture and Calculated Recharge

Stream discharge was continuously measured in the western, more humid part of the study area at Alder Creek, near its confluence with the Columbia River, during the period of 1967 to 1972. When the baseflow component of the hydrograph was separated from the surface-runoff component, it was determined that for this 6-year period, 34 percent of the computed SURP for the basin went to surface runoff, while the remainder is the amount of ground-water recharge.

Peak-discharge measurements of intermittent streams located in the eastern part of the study area were made during the period 1962-73 (see fig. 4 for locations of discharge measurements). These peak discharges, when correlated with peak flows at continuously gaged sites, enabled estimation of an average surface runoff for this area, which was calculated to be 24 percent of the computed SURP. Ungaged basins were given surface-runoff percentage values between these two values (24 percent and 39 percent) on the basis of climatic, topographic, and soil similarities. Percentages of SURP, estimated to be ground-water recharge, as well as total inches per year of ground-water recharge, are shown in figure 12. A generalized relation between ground-water recharge, precipitation, and the soil and vegetation in the Horse Heaven Hills area is shown in figure 13.

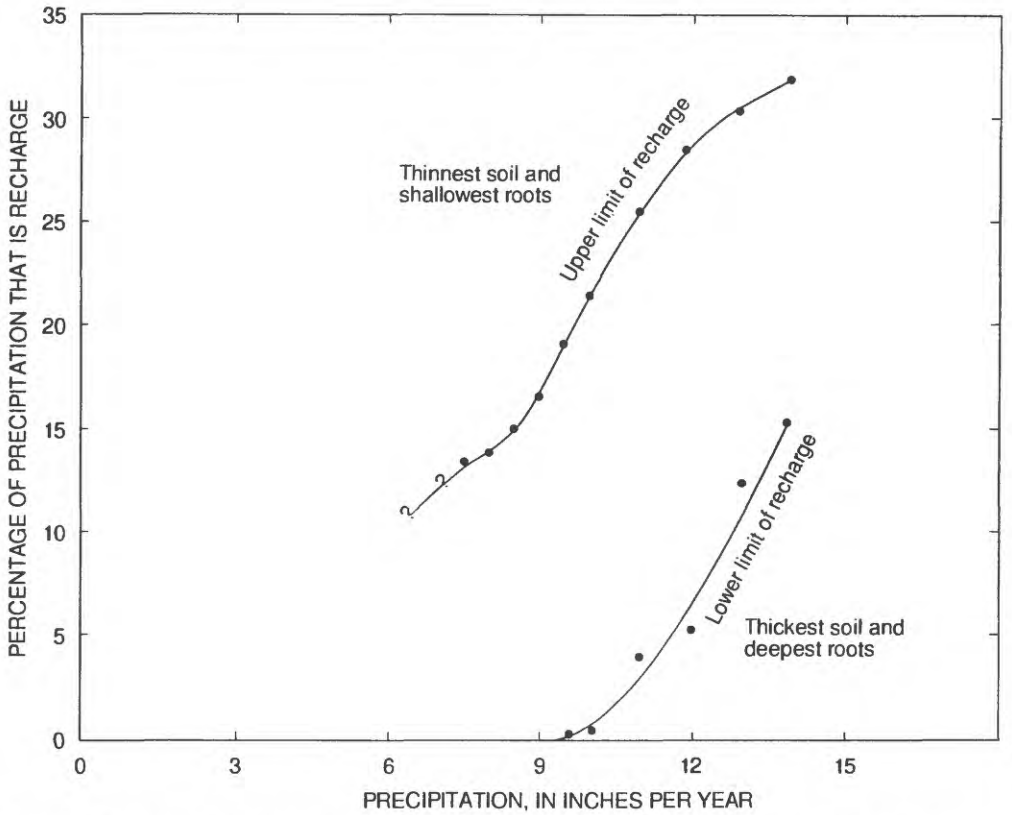

Figure 13. Generalized relation between ground-water recharge, precipitation, soil type, and vegetation in the Horse Heaven Hills study area.

The total calculated recharge from precipitation for the modeled area is 69.7 ft^3/s or 50,470 acre feet per year (acre-ft/yr). Of this, about 12.8 ft^3/s (9,270 acre-ft/yr) is recharged along the north and northeast faces of the Horse Heaven Hills (Satus Creek through Kennewick), 3.1 ft^3/s (2,240 acre-ft/yr) is recharged in Oregon, and 53.8 ft^3/s (38,950 acre-ft/yr) is recharged to the south-facing slope of the Horse Heaven Hills.

Quantities of water that were imported from the Columbia River (as calculated from power use) were processed through the Blaney-Criddle evapotranspiration program described above to arrive at ground-water recharge rates from this moisture source. In the calculation of excess moisture and recharge, runoff was assumed to be small; however, seepage runs along Glade Creek prove that a large part of this irrigation water is seeping back to the surface as return flow. Using the assumption that all of the Glade Creek flow (11 ft^3/s) was return flow, it was estimated that only 20 to 30 percent of the ground-water recharge calculated for imported irrigation water was actually getting into the basalt aquifers; 70 to 80 percent was return flow into Glade and other creeks.

Soil Moisture

A second method was tried for estimating ground-water recharge that would produce an independent evaluation of the calculated recharge. This method was an attempt to estimate rates of downward flux through the unsaturated zone by direct measurement of soil-moisture content.

Vertical movement of water through the unsaturated zone for uniform horizontal conditions is governed by Darcy's law in terms of change of head (H) with change in depth (z):

$$Q = \frac{dH \cdot K}{dz} . \qquad (13)$$

One complicating factor is that K is a unique function of soil-moisture content (ϕ) depending on the particular soil. In addition, the total head, H, is the sum of elevation head, h, and the soil potential or suction, ψ, which is also some unique function of soil-moisture content depending on the particular soil. Thus,

$$Q = \frac{d(h + \psi(\phi)) \cdot K(\phi)}{dz} . \qquad (14)$$

It is apparent from equation 14 that in a zone of ever-changing soil-moisture content (such as in the root zone), computations of downward (or upward) flux become extremely complex and tenuous. With increasing depth, however, seasonal moisture fluctuations tend to damp out. Moreover, if for some depth intervals, the soil properties and moisture content are uniform, it can be seen from equation 14 that the downward flux is simply Q = K. In the eastern part of the Horse Heaven Hills study area, the loess soil properties are very uniform with depth and in some areas it is sufficiently thick that the above conditions were found.

The location of two sets of test core holes, that were drilled where soil- moisture measurements were made by the neutron logging technique, is shown in figure 12. The neutron count distribution with depth for a typical test (hole number 6/25-3B2) for several different times during a 12-month period is shown in figure 14. Few fluctuations are evident in moisture (neutron count) below a depth of 9 feet, and according to the lithologic log, the material is uniform down to a depth of about 18 feet; core samples were collected at 14 and 22 feet. Although the log of drill cuttings does not show any variation between these depths, some caliche was present in the sample at and below 22 feet, but none at 14 feet. The caliche probably is present below about 18 feet. From 9 to 18 feet is a zone of probable steady-state flux to the ground-water system; a zone one where a measurement of the vertical permeability and moisture content was obtained and recharge flux was determined as being equal to the permeability at the measured saturation.

Some consideration was given to measuring the actual vertical permeability by taking split-spoon-drive samples from the holes at depths where moisture content was constant, but it was decided that these cores should not be used because the soil compaction accompanying coring would likely affect saturated hydraulic-conductivity measurements. Instead, the soil-moisture retention curve ($\bar{\phi}$ as related to ψ) and saturated hydraulic conductivity were established through lab analysis of several undisturbed loess samples taken from a nearby road cut. These data were used to determine the hydraulic conductivity as a function of moisture content. The loess was considered lithologically homogeneous which allows use of lab-measured properties from surface samples to be extrapolated to the core holes. In addition, a set of drive cores was obtained at depths where neutron measurements had been made, measured for moisture content, and correlated with neutron count. With this relation, the moisture content of the steady-state flux zone for each core hole (zone of constant moisture content) was determined from the neutron logging. Then, the vertical permeability of the zone with steady-moisture content was determined from the moisture-content permeability curve established in the laboratory, and that value was the steady-state flux to the ground-water system for that hole.

Downward fluxes for all probe holes are listed on table 1, as well as recharge values computed from the weather, crop, and soil data as discussed previously. Except for one site, all "measured" fluxes are close to zero and in agreement with "calculated" recharge for the first three sites. The remainder of the sites have a calculated recharge of about 0.4 inch per year, but only one of the measured fluxes is close to this figure.

These six coreholes were located so that any differences in recharge rate could be measured for ridge crests as compared to adjacent streambeds along first- through third-order (Horton, 1945) ephemeral streams that were cut into the loess cover of the eastern Horse Heaven Hills area. The original concept was that runoff in ephemeral streams would recharge soil at higher rates beneath streambeds because of longer residence times and greater water depths. In addition, it was thought that these small drainages might collect more snow than the ridge crests and that slow snowmelt would additionally increase recharge rates along stream channels and adjacent slopes. In table 1, the flux rates (for the coreholes) have been labeled as to whether they represent

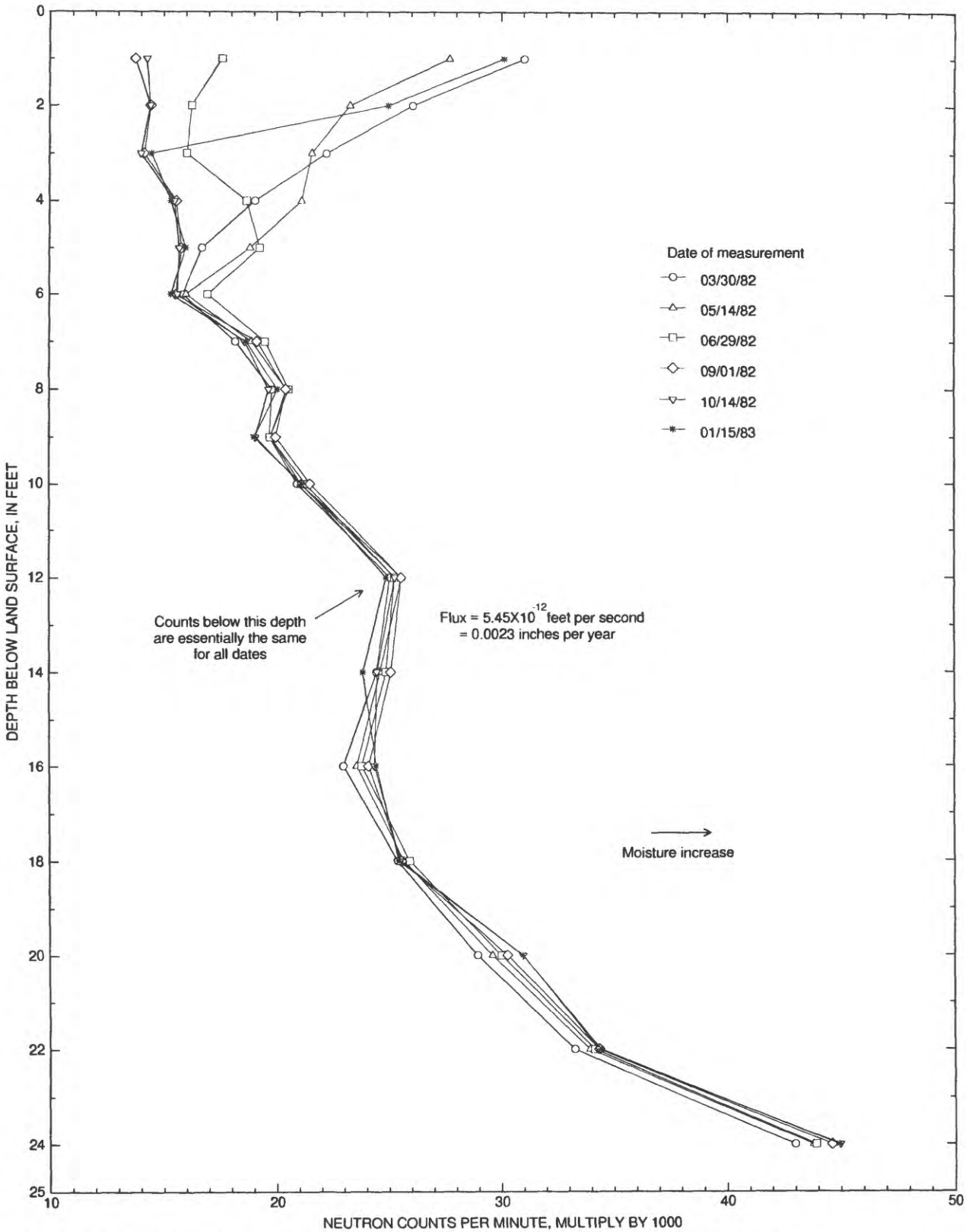

Figure 14. Soil moisture distribution in core hole 6N/25E-3B2 (neutron probe measurement).

Table 1. Calculated recharge versus measured unsaturated fluxes

Location	Physiography	Measured unsaturated steady flux (Inches per year)	Average recharge calculated from weather data (Inches per year)	Percentage of years in which recharge can be calculated
6/25-3B	Ridge	0.00002	0	0
6/25-3B	First-order streambed	.0023	0	0
6/25-3B	Ridge	.000002	0	0
8/26-11Q	Third-order streambed	.1198	.4	42
8/27-8M	Ridge	.003	.4	42
8/27-8N	Ridge	.010	.4	42

streambed or ridge crest positions. In the first three tests listed, the flux along the first-order stream is two to three orders of magnitude larger than along the ridge crests on either side. In the last three tests listed, the streambed flux is one to two orders of magnitude larger than the ridge crests.

Additional work needs to be done to measure the amount and spatial variation of recharge and to integrate these differences across areas the size of a model node (4 mi^2). In addition, some other method should be used to measure the actual unsaturated vertical permeabilities in the steady-state flux zones rather than substitute undisturbed surface samples from adjacent outcrops; there could be an order of magnitude variation in this permeability even within homogenous sediment, such as loess. Such efforts would allow calibration of weather-related recharge calculations like the method used in this report. Last, some method of measurement needs to be attempted to evaluate the amount of recharge taking place along higher-order streams which have incised through the loess and now flow on basalt. Instead of such work, the recharge, as calculated, has been accepted for use in this study, partly because of the closeness to values measured along streambeds.

WATER QUALITY

Ground-water quality in the Saddle Mountains and Wanapum aquifers is not uniform. The areal and vertical variations that exist are mainly determined by physical mixing and chemical interactions between aquifer and soil materials and the ground water as it flows downgradient. Agricultural activities probably influence ground-water quality in some areas.

The nature of water-rock interactions and the evolution of water chemistry along a flow line can be described by a conceptual chemical reaction model (W. Wood, U.S. Geological Survey, written commun., 1982) which was tested by the U.S. Geological Survey (Hearn and others, 1986; Steinkampf and

others, 1985). In general, the model proposes reactions between precipitation-derived recharge and the gases and minerals in the soils, with the basalt aquifers, and with pyroclastics, clays, and other particles of the sedimentary interbeds. In this model, some aquifer minerals and volcanic glasses are partly altered to palagonite, clay minerals, zeolites, and iron hydroxides; calcite is precipitated, and the pH increases. Calcium, sodium, magnesium, and bicarbonate are added to the ground water in the course of this alteration. Calcium and magnesium are exchanged for sodium on the clays and (or) zeolites yielding a water enriched in sodium and bicarbonate. The concentrations of sodium and bicarbonate increase with residence time of the water (with distance down flow lines) as shown by the related distributions of sodium, and by age dates from carbon-14 tests for the formation water (fig. 15 The pH is elevated in the process and conditions then become favorable for increased fluorite dissolution and high sodium absorption ratios (SAR) because sodium is enriched and calcium and magnesium are removed from solution (U.S. Salinity Laboratory Staff, 1954).

The distribution of the more important common ions for the Wanapum aquifer is characterized in figures 15 and 16. Distributions for the Wanapum aquifer better represent the conceptual reaction model than those of the Saddle Mountains aquifer, in part, because the water quality in shallower aquifers can be more readily changed by downward percolation of natural recharge and irrigation water containing dissolved fertilizers. Magnesium and calcium (fig. 15) concentrations for the Wanapum aquifer are largest in the downward flowing region of greatest recharge along the crest of the Horse Heaven Hills, and they are smallest near the discharge points along the Columbia River. Conversely, conductivity, SAR (fig. 16), pH, ground-water age (percentage present-day carbon) and sodium and fluoride concentrations are all larger in discharge areas along the Columbia River and along the central syncline. Potassium and chloride distributions are similar to that of sodium, as larger concentrations are found along line sinks and along the central syncline. The source of chloride is problematic but may be due to upward flux of chloride from sediment beneath the basalts.

Nitrate concentrations larger than the recommended maximum (U.S. Environmental Protection Agency, 1976) occur in places along the Columbia River. The high SAR values (fig. 16) that occur in deeper horizons (Wanapum and Grande Ronde aquifers), and in older waters along the Columbia River, could pose some problems if these waters were used for irrigation. In the study area, most irrigators along the Columbia River use river water on their fields, so the problem is not one of immediate concern. Most of those irrigators that do use ground water are located farther upgradient, where the SAR is more satisfactory for land application. Water from deep wells finished in the lower Wanapum and Grande Ronde aquifers may have high SAR values. Ground water that has high SAR values will necessitate management practices such as dilution with surface water or treatment of soils with gypsum along with providing adequate leaching rates.

SIMULATION OF GROUND-WATER FLOW

The Horse Heaven Hills flow system was simulated by a mathematical, numerical model using the McDonald and Harbaugh (1984) finite-difference code with the strongly implicit procedure (SIP) algorithm to solve the equations that describe ground-water flow in the saturated part of the system. The system was modeled as three-dimensional flow because of the strong vertical

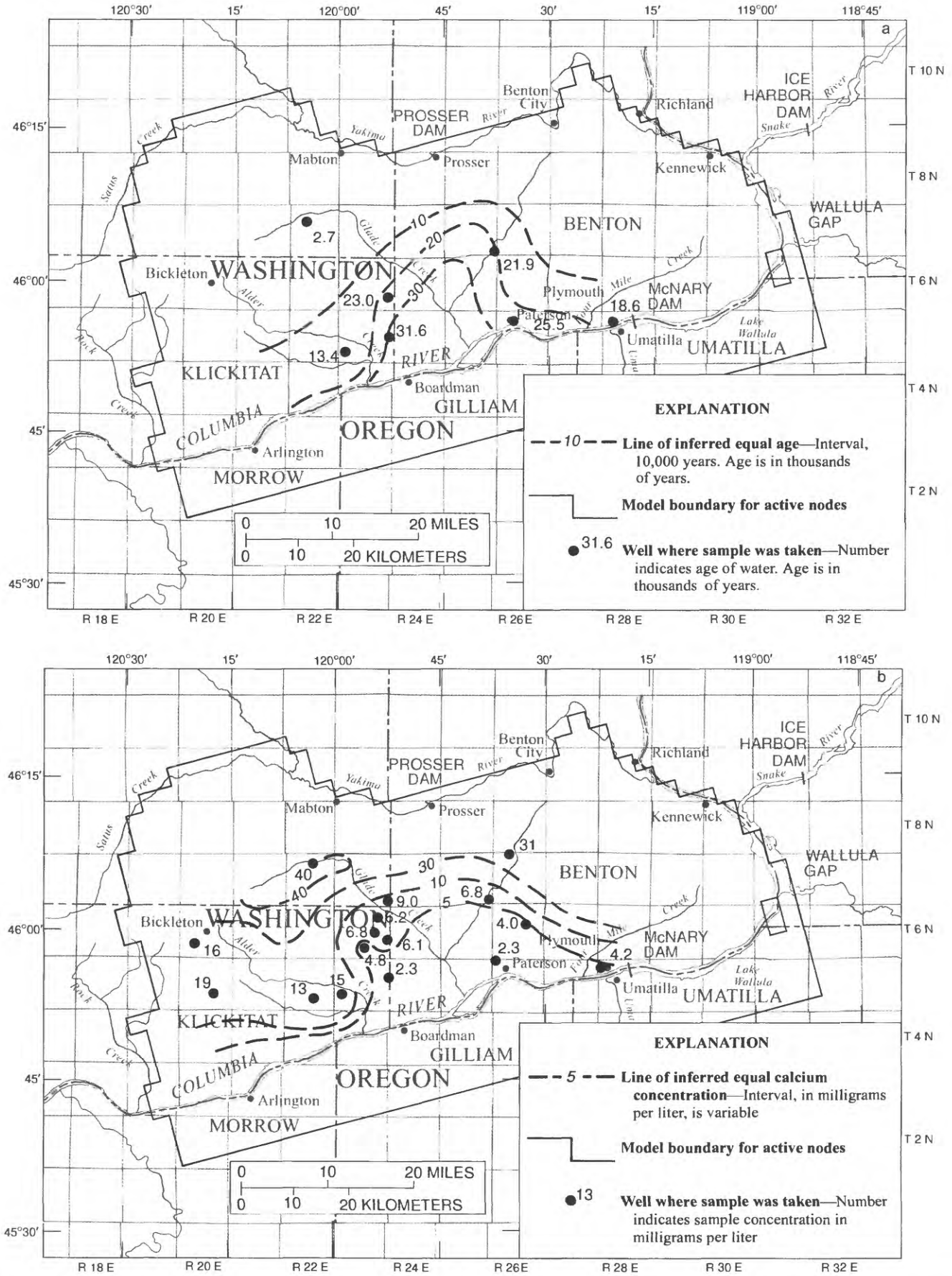

Figure 15. Distribution in the Wanapum aquifer of (a) carbon-14 age dates for water and (b) calcium ion concentrations.

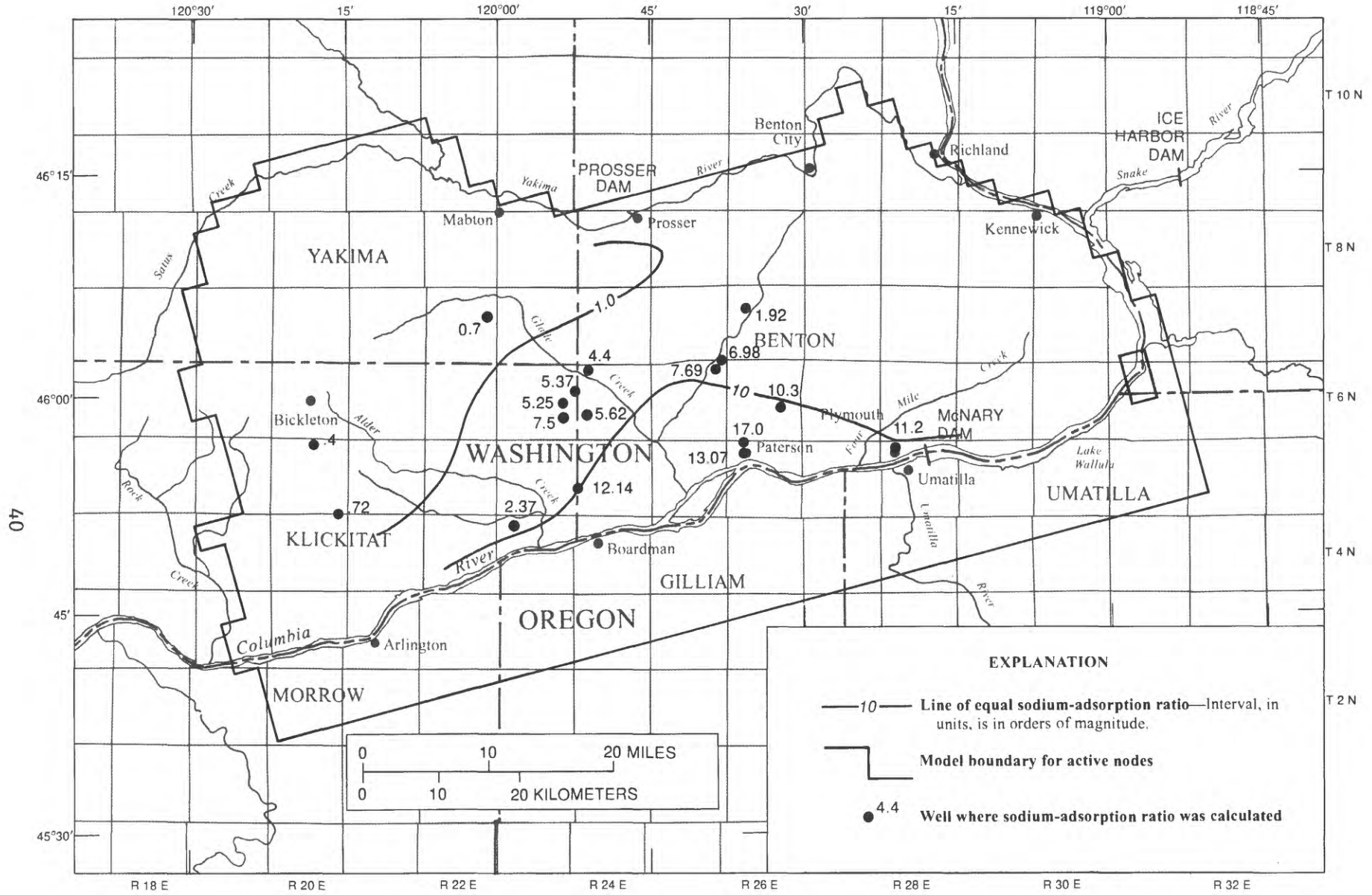

Figure 16. Distribution in the Wanapum aquifer of calculated sodium-adsorption ratios.

gradients encountered in the higher elevations of the area. Outside of several input/output programs, the only additions to the model code were an algorithm used to reduce model instability problems during steady-state simulations (D. Sapik, U.S. Geological Survey, written commun., 1984), and an algorithm to decrease pumpage with reduced saturated thickness (A. Hanson, U.S. Geological Survey, written commun., 1991). Descriptions of each algorithm are given in the Appendix of this report.

Hydrogeologic Units and Discretization

The three major aquifers (Saddle Mountains, Wanapum, and Grande Ronde) are represented in the model as separate layers. Unconsolidated material that overlies the basalt aquifers is saturated at only two locations--in the Satus Basin along the Yakima River and in small discontinuous segments along the Columbia River on either side of Paterson (fig. 1). The saturated thickness of unconsolidated material in the Satus Basin (Prych, 1983) was included within the Saddle Mountains aquifer layer (the net effect was slightly lower-calibrated hydraulic conductivities in the Saddle Mountains aquifer here than probably exist). The small discontinuous segments of saturated, unconsolidated material along the Columbia River were ignored. In Oregon, the thick Quaternary gravels were omitted from the model as a fourth layer because of the generalized treatment of this area.

A horizontal-grid spacing of 2 miles was used for the modeled area. The narrowest hydrologic elements to be simulated were the long, linear fault zones and the tightly folded Columbia Hills anticline near the Columbia River. For these narrow elements, the 2-mile grid was too large, and wells in and near them were the most difficult to calibrate; that is, they caused the largest errors in the final calibration. Outside of these grid elements, the 2-mile spacing was smaller than necessary to accurately simulate average conditions. The 2-mile grid spacing, therefore, was judged appropriate, given the above considerations and the distribution of wells in the area.

Inactive nodes were coded along the crestal parts of the Horse Heaven Hills eastern segment and just to the northeast along parts of the axis of the Rattlesnake anticline where the Saddle Mountains aquifer is thought to be unsaturated (fig. 17). Inactive nodes also are coded within this layer where it pinches out along the western margins of the model and where inliers of Wanapum Basalt occur along deeply entrenched streams or along faults near the crest. Three areas are coded as inactive nodes within the layer representing the Wanapum aquifer (fig. 17). The Wanapum layer is missing where Grande Ronde inliers occur in Upper Satus Creek, lower Rock Creek, and Wallula Gap. Elsewhere, the Wanapum layer is saturated and extends to the boundaries of the model. The layer representing the Grande Ronde aquifer (fig. 17) extends horizontally without break to all external boundaries of the model.

Tops for the Grande Ronde and for the Wanapum layers were coded to the model from structure maps where active nodes for these layers exist. The bottom of the Saddle Mountains layer (same as top of Wanapum) also is coded from structure maps where active Saddle Mountains nodes are present (structure on top of Mabton interbed, fig. 6a, is structure on top of Wanapum layer or aquifer).

Ground-water evapotranspiration is not simulated in the model because the area of the tree growth and transpiration from the water table is limited to a small 20- to 30-mi^2 area in the westernmost parts of the Horse Heaven Hills

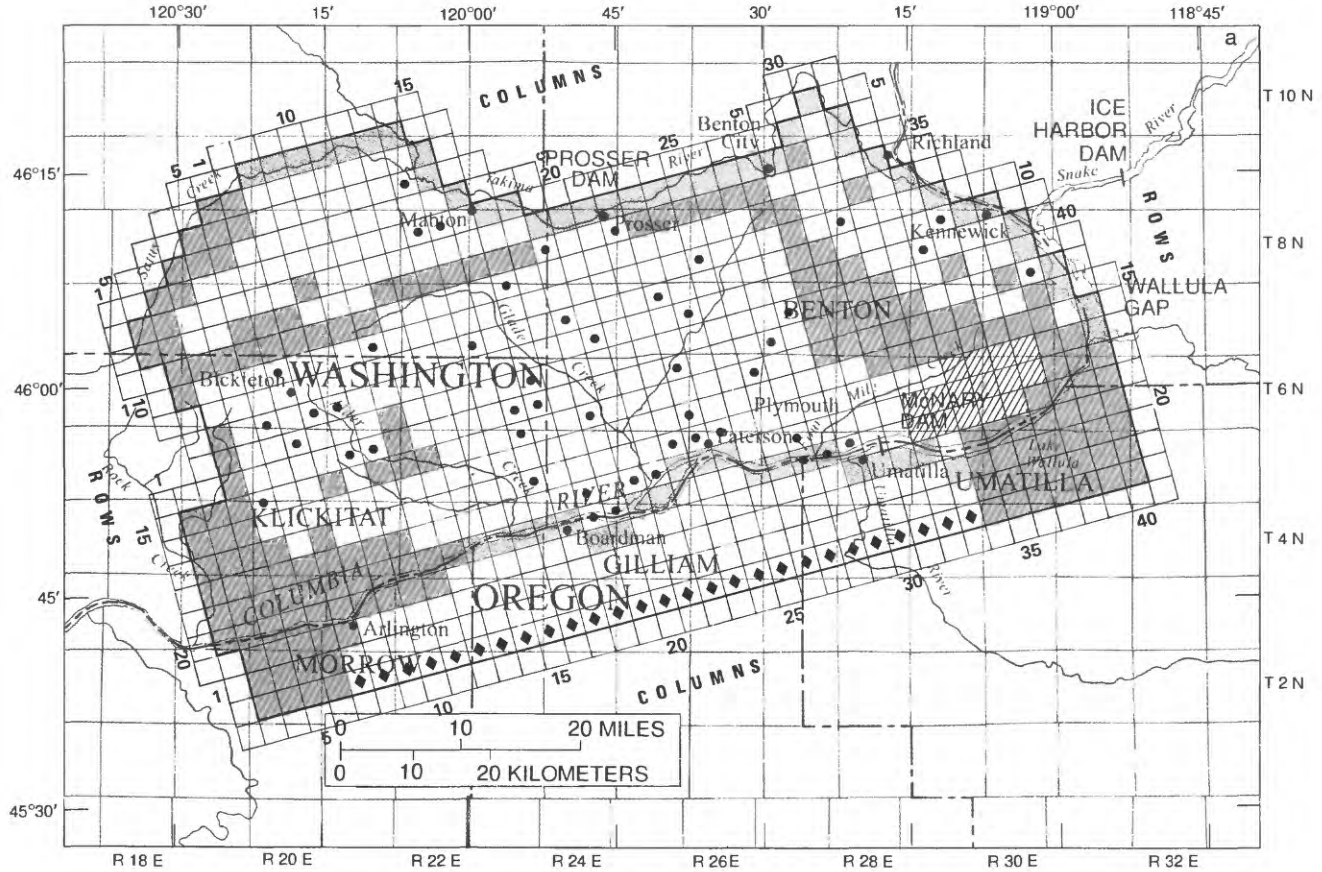
a
120°30′
15′
120°00′
45′
30′
15′
119°00′
118°45′
46°15′
46°00′
45′
45°30′
T 10 N
T 8 N
T 6 N
T 4 N
T 2 N
R 18 E
R 20 E
R 22 E
R 24 E
R 26E
R 28 E
R 30 E
R 32 E
COLUMNS
ROWS
PROSSER DAM
Benton City
Richland
ICE HARBOR DAM
Snake River
Yakima River
Mabton
Prosser
Kennewick
WALLULA GAP
BENTON
WASHINGTON
Bickleton
Gilbert Creek
Plymouth
McNARY DAM
Paterson
Umatilla
Lake Wallula
UMATILLA
KLICKITAT
RIVER
Boardman
GILLIAM
COLUMBIA
OREGON
Arlington
MORROW
Willow Creek
John Day River
0 10 20 MILES
0 10 20 KILOMETERS

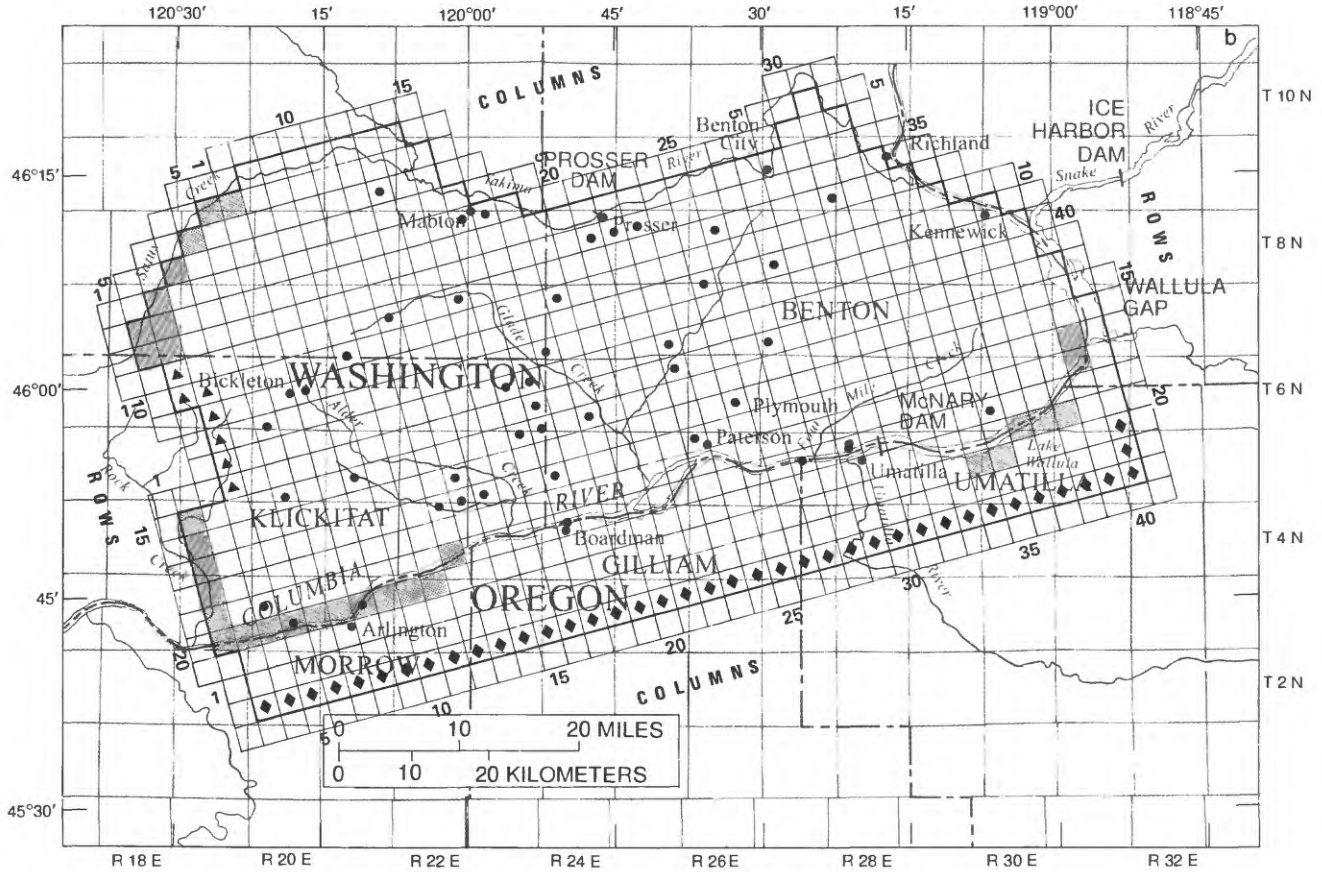
b
120°30′
15′
120°00′
45′
30′
15′
119°00′
118°45′
46°15′
46°00′
45′
45°30′
T 10 N
T 8 N
T 6 N
T 4 N
T 2 N
R 18 E
R 20 E
R 22 E
R 24 E
R 26E
R 28 E
R 30 E
R 32 E
COLUMNS
ROWS
PROSSER DAM
Benton City
Richland
ICE HARBOR DAM
Snake River
Yakima River
Mabton
Prosser
Kennewick
WALLULA GAP
BENTON
WASHINGTON
Bickleton
Gilbert Creek
Plymouth
McNARY DAM
Paterson
Umatilla
Lake Wallula
UMATILLA
KLICKITAT
RIVER
Boardman
GILLIAM
COLUMBIA
OREGON
Arlington
MORROW
Willow Creek
John Day River
0 10 20 MILES
0 10 20 KILOMETERS

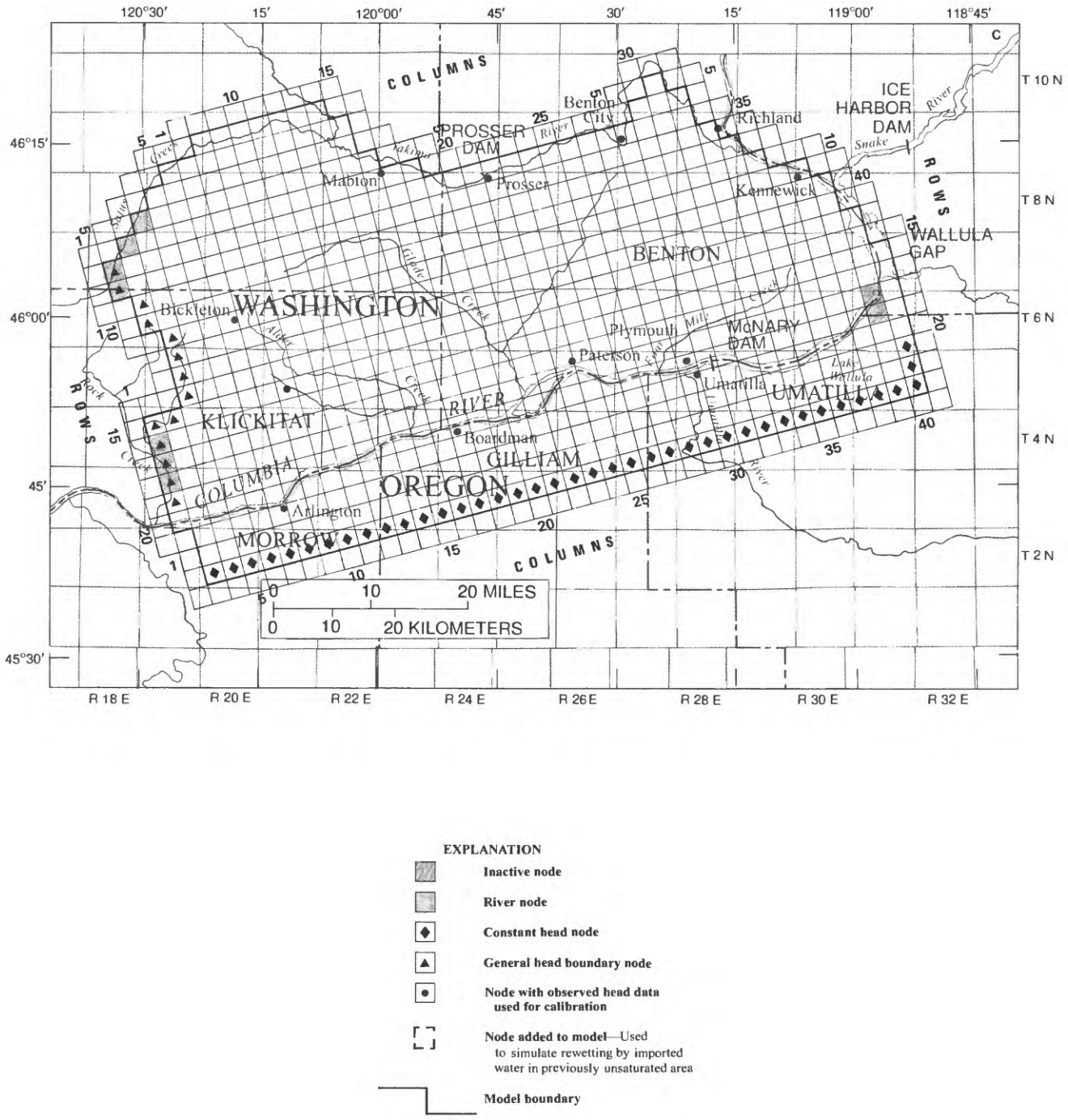

EXPLANATION

- **Inactive node**
- **River node**
- **Constant head node**
- **General head boundary node**
- **Node with observed head data used for calibration**
- **Node added to model**—Used to simulate rewetting by imported water in previously unsaturated area
- **Model boundary**

Figure 17. Major boundaries and calibration points for the numerical model of the (a) Saddle Mountains aquifer, (b) Wanapum aquifer, and (c) Grande Ronde aquifer.

ridge (less than 1 percent of the model area). Recharge is put into the top active layer by the model and in some areas, such as the eastern segment of the Horse Heaven Hills where the Saddle Mountains aquifer is unsaturated, this means that recharge is being placed into the second layer, the underlying Wanapum aquifer. Water imported from the Columbia River or pumped from deep aquifers and recharged to the uppermost aquifer layer is simulated in the model as well recharge.

Hydraulic-conductivity values for Oregon are from a companion Geological Survey study of the Umatilla Basin (A. Davies-Smith and others, 1988). Vertical-conductance values for Oregon are generalized from the calibrated values in Washington.

Model Boundaries

A water table or free-surface boundary exists in the uppermost active layer at each node, and these same nodes function as specified-flux boundaries because of the recharge that passes across the water table to each of them. Along the northern and northeastern edges of the model (fig. 17), river or head-dependent flux nodes comprise the boundary within the uppermost active layer along the lower reaches of Satus Creek, the Yakima River, and the Columbia River near Kennewick. These river nodes were placed within the layer, or aquifer unit, in which the river flows. Along these same boundaries, heads within nodes (layers) immediately beneath the river node layer were allowed to vary, but beyond these nodes to the north, no-flow boundaries were coded.

Water levels in all three layers in the last row or nodes along the southern model boundary in Oregon were set to heads estimated for predevelopment conditions (1952-55) and were held constant with time. In this southern area, river nodes were coded along the Columbia River in the manner described above. Care was taken during calibration to ensure that flow from this area was northward toward the Columbia River to match the conceptual model. Model sensitivity to this boundary treatment was done after calibration was completed. River stage or lake values were taken from 7-1/2 minute quadrangle maps, and river bottom values were assumed to be 10 and 30 feet below pre-dam stage estimates for the Yakima and the Columbia Rivers, respectively.

Along the western part of the model, river nodes were coded to the uppermost active layer for the upper reaches of Satus Creek and for the lowermost reaches of Rock Creek. Upper Rock Creek was coded as a series of drain nodes rather than river nodes to simulate the fact that flow in those upper reaches is at times ephemeral (fig. 18). These drains were used to simulate the aggregate of flow from thick seepage faces along canyon walls as well as direct discharge to adjacent streams themselves. Because the Saddle Mountains aquifer does not extend to the west of Rock or Satus Creeks, this western boundary is appropriately a no-flow boundary for this layer. Because the Wanapum aquifer does extend westward beyond Rock Creek in some places, and the Grande Ronde aquifer extends westward in all places, general head boundary (GHB) nodes were coded along appropriate boundary nodes within these two layers (fig. 17). During transient simulation, these GHB nodes acted as a potential source of water outside of the model to cells within the model when variable heads along the boundary fell below calibrated steady-state levels. Conductance values for these GHB nodes were calculated using average horizontal hydraulic conductivities and projected thicknesses for the aquifer.

The water source was assumed to lie at the western edge of the Rock Creek Basin from 5 to 15 miles west of the model boundaries. Head values for each node were assumed to be the same as the steady-state calculated head for that layer at the border node on which the GHB node was based. These nodes are intended to simulate the base-flow discharge available for capture in Rock Creek to balance the spread of depression cones west of the model.

Over much of the western one-half of the model, the narrow, deeply entrenched stream channels on the dip slope of Horse Heaven Hills and the streams that lie along them have been simulated as drains (fig. 18). Where canyons are entrenched more than 300 feet, these drain nodes have been coded so that drain elevations lie from 50 to 100 feet above the adjacent canyon floors. In this way, a seepage face was simulated in each of these nodes. The conductance values for all nodes were changed until the amount of total discharge obtained for the set of nodes representing each main stream equalled the estimation from gage data in Rock and Alder Creeks.

The base of the Grande Ronde aquifer was treated as a no-flow boundary in the model even though it is likely that a section of sediment and metasediment is present below the aquifer. However, the transmissivity and flow that must exist within the bedrock sediment is considered to be included in the Grande Ronde aquifer transmissivity and flux; that is, the Grande Ronde aquifer layer in the model really represents the entire section below the Wanapum aquifer.

Derivation of Vertical Conductance

Estimates of vertical conductances between aquifers for use in the three-dimensional model were originally derived from a set of five numerical, cross-section models located along flow lines reaching from the ground-water divide at the crest of the Horse Heaven Hills anticline to the Columbia River (fig. 19A). In these flow models, the Saddle Mountains, Wanapum, and Grande Ronde aquifers were represented as single isotropic layers (aquifers) with appropriate thicknesses, and the intervening Mabton and Vantage interbeds, as isotropic layers (confining units) of low-hydraulic conductivity. The Columbia River was modeled as a constant-head boundary; aquifer hydraulic conductivities and recharge were constrained within limits that were considered reasonable at this early stage of the study. Calibration of each of the five models involved changing the hydraulic conductivities of the two confining units in order to match known head separation between aquifers. The calibrated conductivities for the Mabton clay interbed layer were considered the most acceptable measure of the effective or lowest vertical-hydraulic conductivities that exist between the Saddle Mountains and Wanapum aquifers. These conductivities were converted to vertical-conductance values (McDonald and Harbaugh, 1984), mapped, and contoured. A matrix was then coded from this map for use as the initial vertical-conductance matrix for the three-dimensional model.

The general patterns of vertical conductance of the Saddle Mountain-Wanapum interval for the three-dimensional model are essentially identical to those shown for vertical conductivity (Kv) of this interval in figure 18A (the distribution of vertical conductance can be approximated by dividing vertical conductivity (Kv) by 500, an average distance between layer centers). The vertical conductivity (Kv) values are shown rather than those of conductance because vertical conductivity (Kv) relates more directly to rock type. Figure 19A shows 2.5 to 3 order-of-magnitude lower values along the Horse Heaven

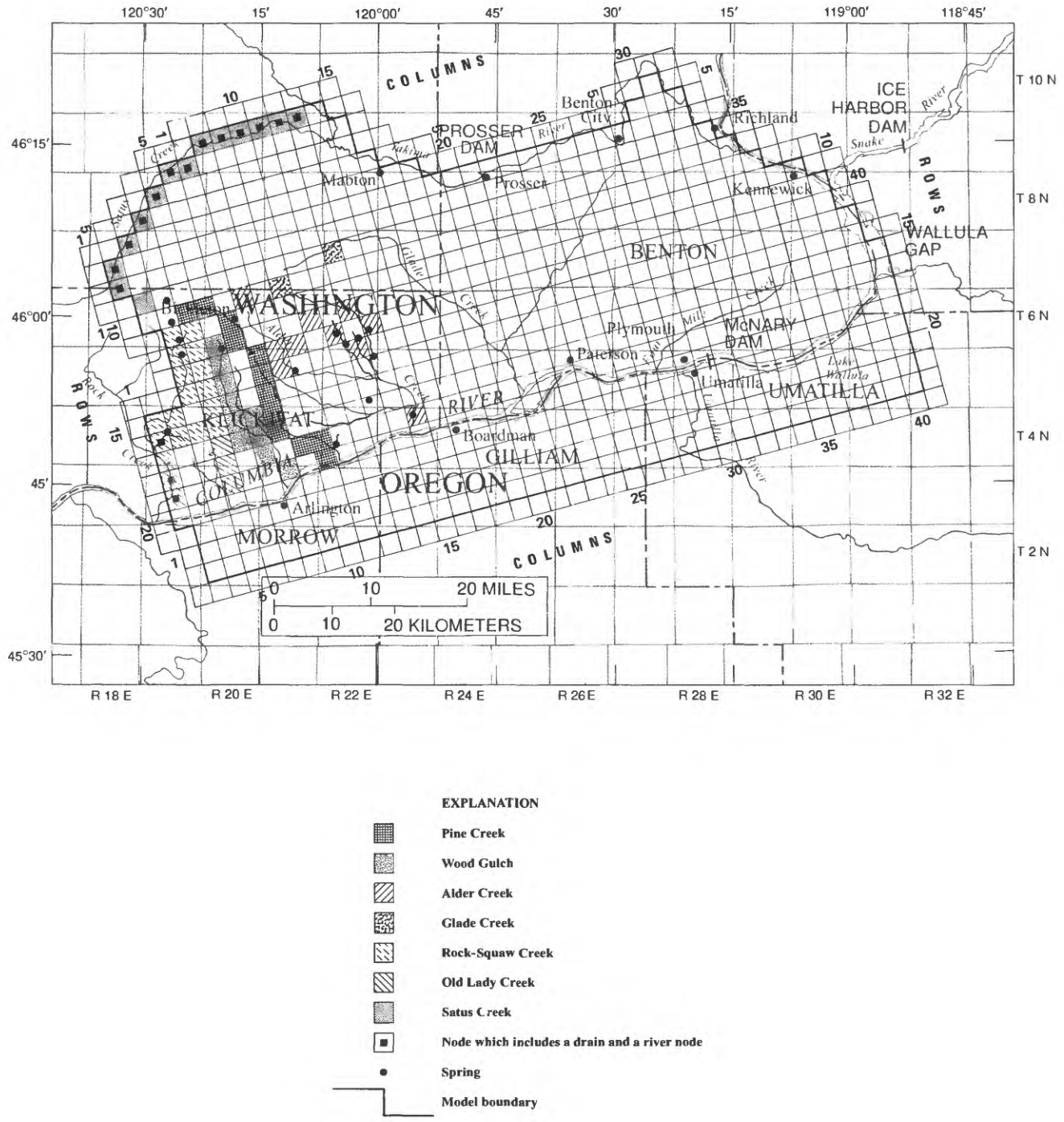

EXPLANATION

- Pine Creek
- Wood Gulch
- Alder Creek
- Glade Creek
- Rock-Squaw Creek
- Old Lady Creek
- Satus Creek
- Node which includes a drain and a river node
- Spring
- Model boundary

Figure 18. Distribution of river and drain nodes numerical model for the narrow canyons of the western Horse Heaven Hills.

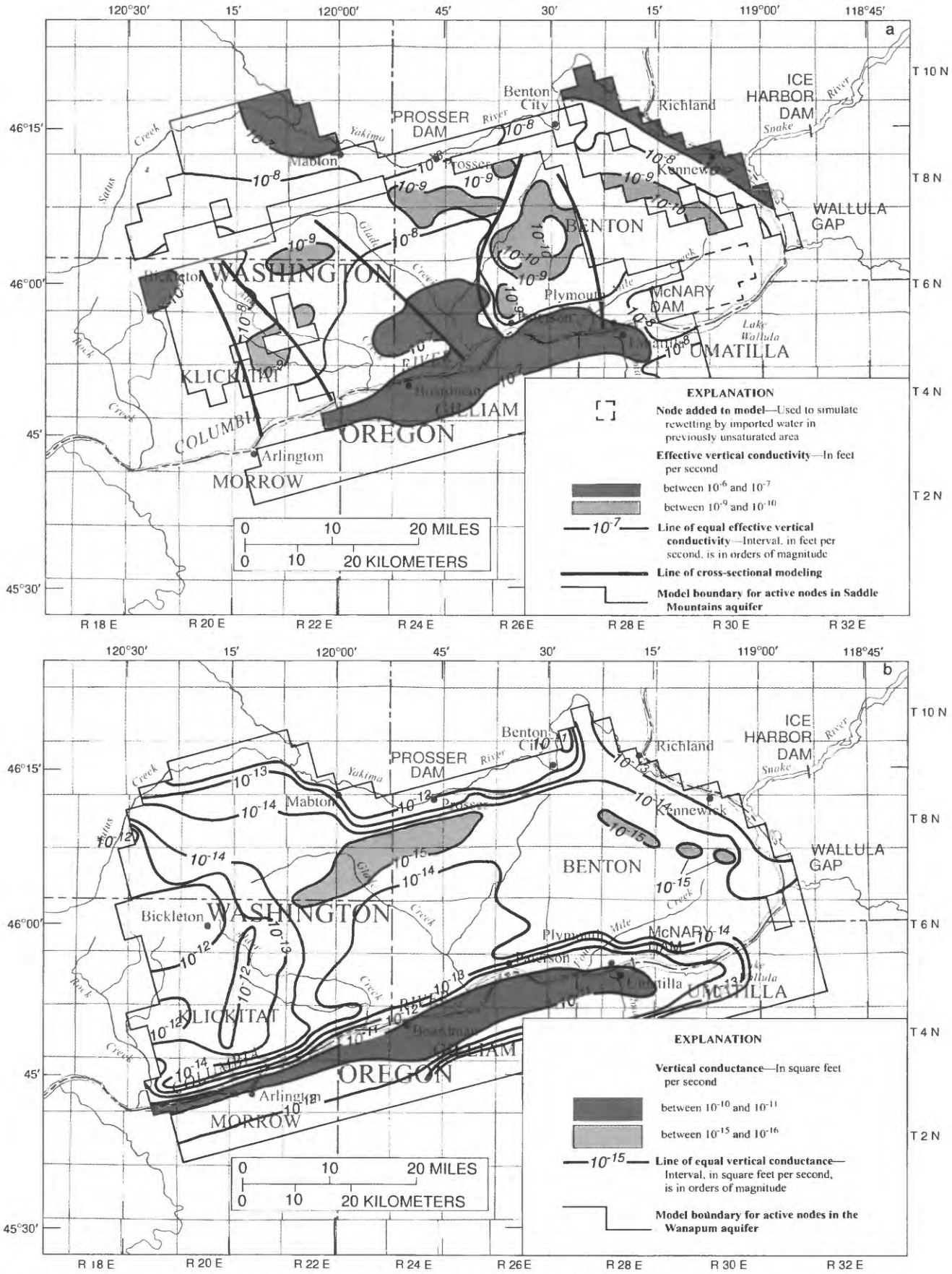

Figure 19. (a) Effective vertical conductivity for the Saddle Mountains-Wanapum interval and (b) vertical conductance for the Wanapum-Grande Ronde interval, from final calibration of the numerical model.

Hills axis than along the Umatilla and central synclines. Along the axis of the Horse Heaven Hills, vertical-hydraulic conductivities (Kv) for the Saddle Mountains-Wanapum aquifers (fig. 18A), averaged 5.7×10^{-9} ft/s, which is in the range of clay. Along the central and Umatilla synclines, these vertical conductivities (Kv) averaged 1.25×10^{-7} ft/s, in the range of silt and fine sand. The pattern of smaller vertical conductivities along the Horse Heaven Hills axis can be explained, in part, by the presence of silt/clay interbeds along most of this axis and along dip slopes to the immediate south. The presence of a sandy fluvial interbed facies along the central and Umatilla synclines may explain the larger vertical conductivity (Kv) here, but the larger values also could be controlled by associated basalt flow-center vertical conductivities (Kv) that were lower than the vertical conductivities (Kv) of the sandy interbeds.

The vertical conductance (Kv/m) of the Saddle Mountains-Wanapum interval, calculated from vertical hydraulic conductivities (Kv), is considered a lumped parameter and is controlled by contained beds with the smallest vertical-hydraulic conductivity (Kv) within the thickness (m) from the center of the Saddle Mountains aquifer to the center of the Wanapum aquifer. Starting with the conductance matrix derived from the cross-section models, the general pattern of larger vertical conductance along the Umatilla syncline was extrapolated during calibration to include smaller structural features, such as the Swale Creek syncline just north of the Columbia Hills anticline. Smaller-scaled changes in vertical conductance of this sort were made during the three-dimensional modeling which were not predicted by the widely spaced cross-section-model control, but the same relation to structure was generally retained until calibration was achieved.

Vertical conductance associated with the Wanapum-Grande Ronde aquifers (fig. 19B) was assumed to have the same general pattern as that of the Saddle Mountains-Wanapum aquifers and was arbitrarily assumed at the start of calibration to be 1/40 (about 1.5 order of magnitude lower than) of the value of Saddle Mountains-Wanapum conductance. Some changes in this matrix were made during calibration, but Wanapum-Grande Ronde vertical conductance is essentially unknown because of the lack of head, thickness, and lithologic data for the Grande Ronde aquifer.

Steady-State Calibration

In the Washington part of the modeled area, south of the Horse Heaven Hills crest, ground-water pumpage and surface-water irrigation began to increase during after 1972-75. During this 4-year period, there was a sudden increase in well-drilling activity and a related increase in the data available to define the ground-water flow system. Because man-induced perturbations to the system began during this time, and because well data previous to this time was inadequate to define the flow system, 1972-75 was chosen as the period for steady-state calibration. There are no long-term hydrographs to effectively document water-level changes over the study area during or previous to this time.

Contour interpretation of 1972-75 water levels for the Saddle Mountains, Wanapum, and Grande Ronde Basalt layers (figs. 20, 21, 22) included 1980 head data for wells not affected by pumping centers or water importation. In addition, water levels were used for those wells in perturbed areas where

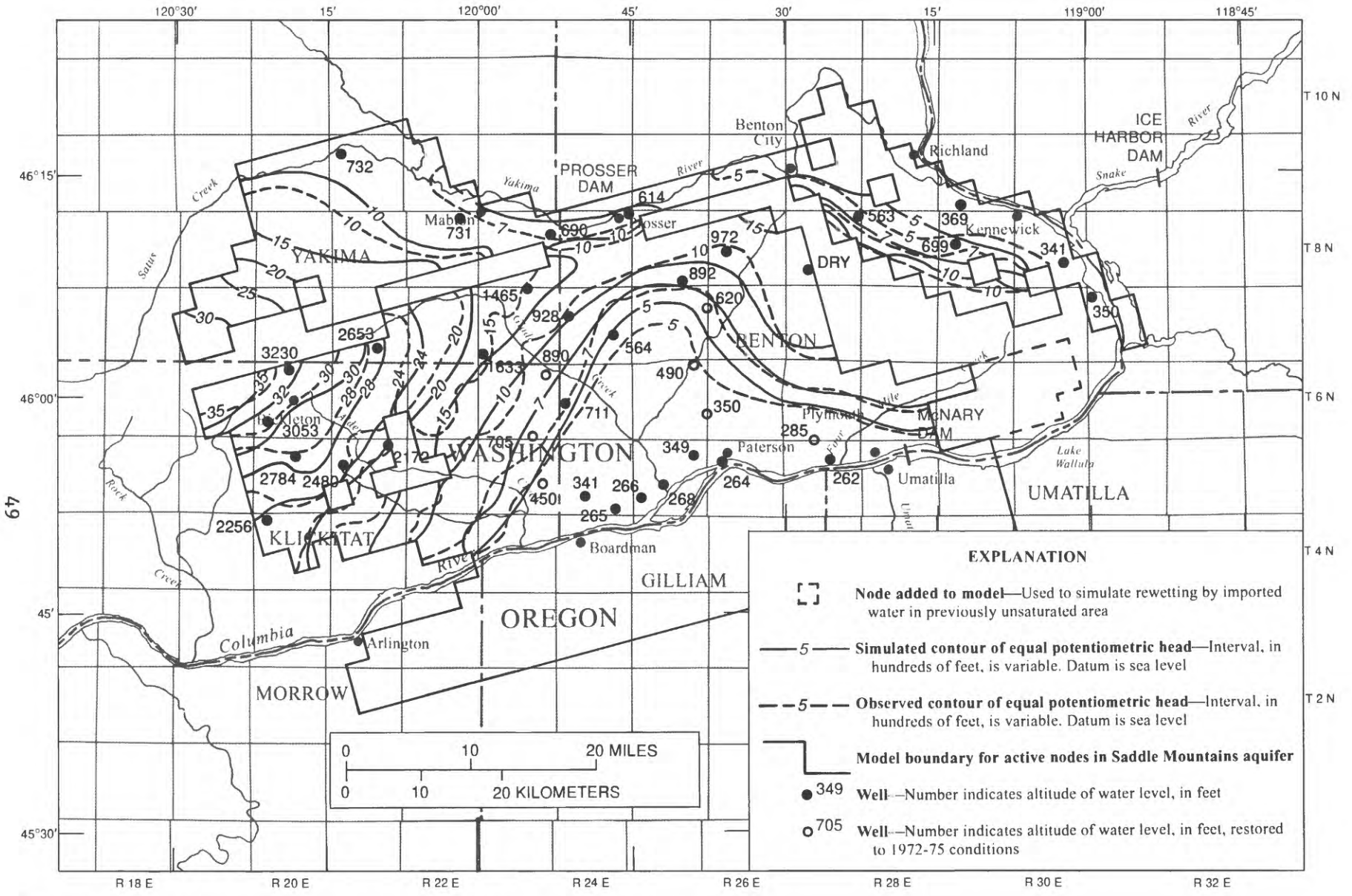

Figure 20. Observed and simulated potentiometric surfaces of the Saddle Mountains aquifer.

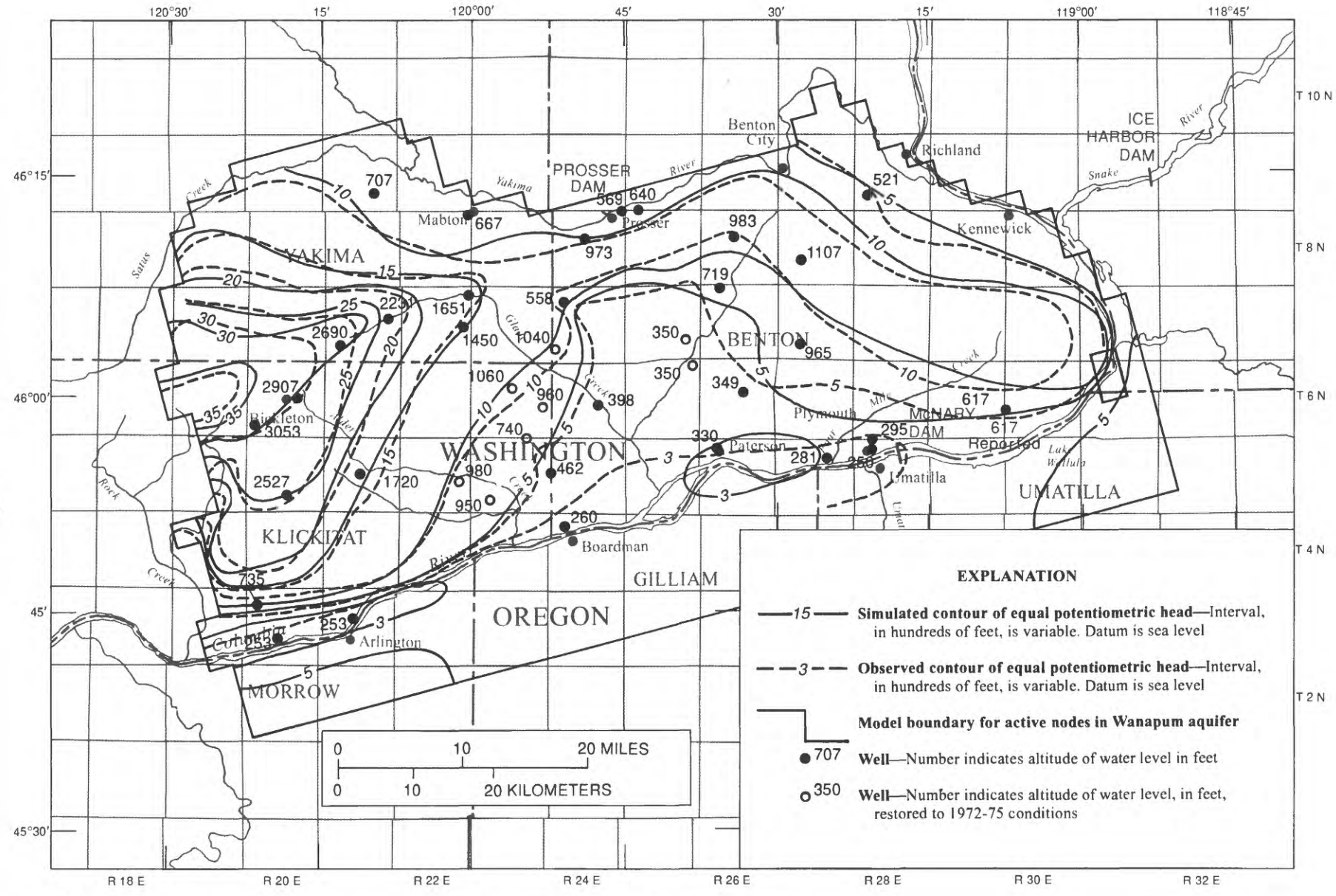

Figure 21. Observed and simulated potentiometric surfaces of the Wanapum Mountains aquifer.

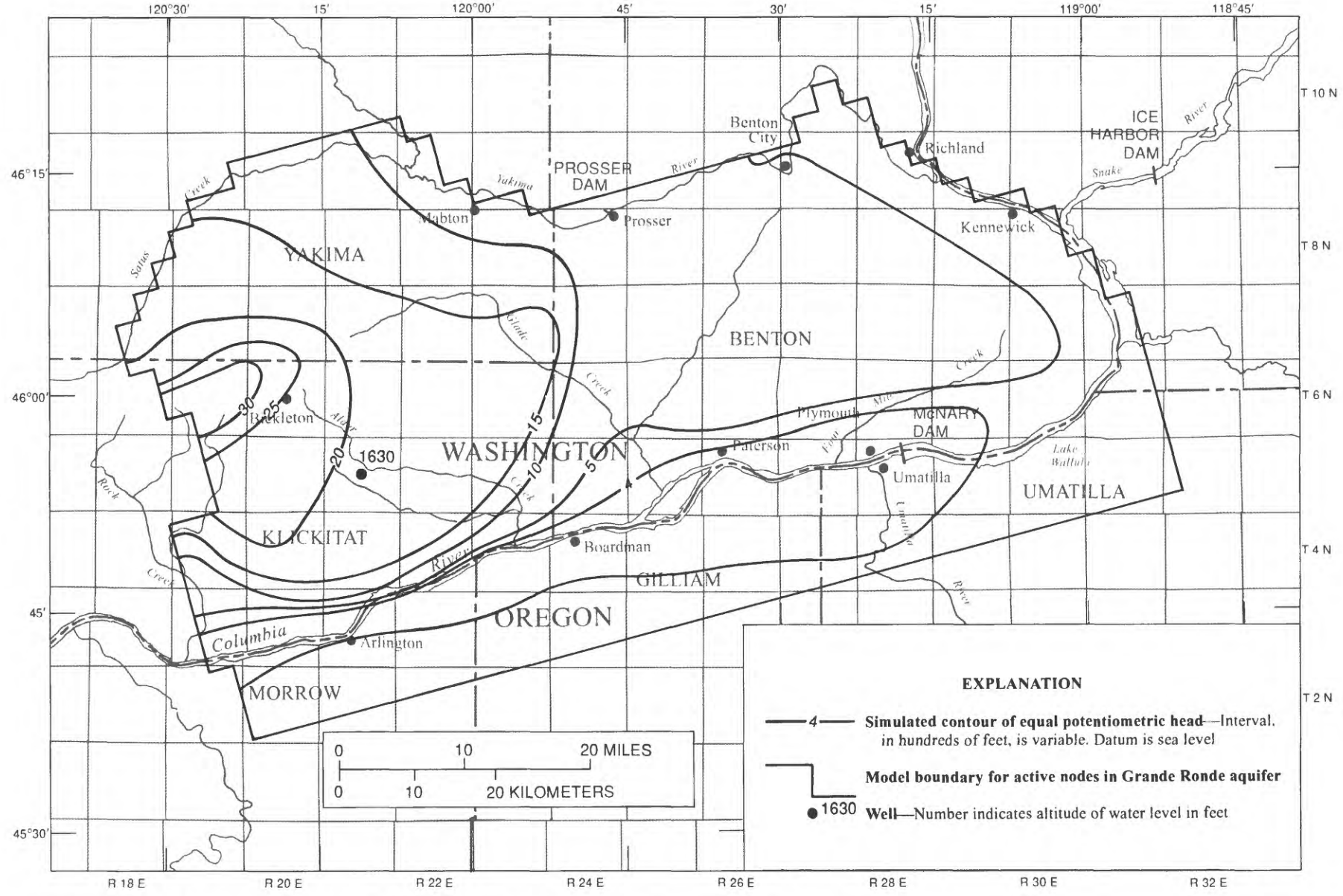

Figure 22. Simulated potentiometric surface of the Grande Ronde aquifer.

reconstruction back to the early 1970 values could be justified. It was assumed in selecting and contouring these data for a steady-state water-level distribution that water-level changes due to emplacement of McNary and John Day Dams in 1953 and 1966, respectively, had stabilized and that water levels were in equilibrium with lake levels along the Columbia River (head levels along the Columbia Lakes were set at 340 feet for reaches above McNary Dam and 265 feet for those downstream). This assumption was later tested. The water levels shown on each aquifer map are mostly from wells completed only in that aquifer. Composite head data were used at some locations, but only where the transmissivity of one aquifer was dominant and the water level was considered valid for that unit.

Geometry and recharge were determined independently, and cross-section modeling was used to derive an estimate of vertical conductances. In the steady-state model, the main calibration technique involved changing values of horizontal-hydraulic conductivities and river-drain conductances. During calibration, water-level data for wells were compared to the total penetration of each well into the aquifer. Because the model predicts heads at the center of the aquifer, it was reasonable to expect that a well with shallow or deep penetration into an aquifer could have a significantly different water level than the model prediction and still offer acceptable calibration. On the basis of vertical gradients calculated by the model, observed water levels were compared with predicted water levels that were adjusted to the appropriate depth within an aquifer.

Calibration of the three-dimensional model began with several experiments. First, a uniform transmissivity was coded for each formation, equivalent to its median-test-transmissivity value. Vertical conductance was coded from the cross-section model results and recharge was coded from the calculations described earlier. Low hydraulic conductivities for faults and tight folds were omitted even though cross-section model results showed them to be necessary for calibration. Different multipliers for the set of transmissivity matrices were used to see if head distributions could be duplicated in this simplistic manner. After a best fit was obtained, results consistently showed that heads along the Horse Heaven Hills anticlinal ridge were too low and heads along the Columbia and Yakima drains were too high. In addition, transmissivity values were reduced (two orders of magnitude) below what was reasonable when compared with of specific capacity test results.

Subsequent to the uniform-transmissivity experiment, a non-uniform model-transmissivity distribution was used that was derived from the mapped hydraulic conductivity distributions and saturated thicknesses, and was coded without the low-transmissivity zones of the major barriers (faults and folds). The same erroneous model-predicted head distributions resulted (high heads along the major drains and low heads along the Horse Heaven Hills axis). Only when the major fault north of the Horse Heaven Hills crest was coded as a low-transmissivity zone, and when other flexures and implied shear faults were similarly modeled, did the head distribution begin to assume the proper configuration with a ground-water ridge along the Horse Heaven Hills axis, with steep gradients along the north face of the Horse Heaven Hills anticline, and along the shear fault zones in T.5 and 6N., R.26E. In large part, the initial gross matching of water levels across the model was accomplished by controlling flow across low-transmissivity barriers along faults and along the Columbia Hills anticline using the rest of the transmissivity values as originally estimated from specific capacity data. Although high, natural

recharge occurs along the crest of the Horse Heaven Hills, along with generally lower transmissivity values in the Saddle Mountains and the Wanapum aquifers, neither of these two characteristics could bring about an accurate simulation of the ground-water ridge found in this area without also using the low-transmissivity barrier zones.

During calibration, subtle gradations of horizontal-hydraulic conductivity were made along the faults or steep monoclines inferred from the Mabton structure map, and the steep hydraulic gradients of the study area. The Columbia Hills anticline in the western part of the model required small hydraulic conductivities to match head gradients. Without coding the small conductivities along this feature, it was not possible to maintain heads in the Wanapum, Saddle Mountains, and Grande Ronde aquifers upgradient in the Bickleton area.

Subsequent calibration of the head distribution within large blocks bounded by low-transmissivity fault and anticlinal barriers was handled by reducing overall (matrix wide) transmissivity values by factors. A reduction factor was derived in a series of hypothetical transient-model simulations in which the interflows and flow centers of eight basalt units were represented as separate layers (16 layers total) in a rectangular model with a pumping well at one corner. The hydraulic conductivities of interflows were 4.5 order of magnitude larger than the flow centers. Results indicate that with the vertical anisotropy used, hydraulic conductivities for the basalt aquifers are 0.6 to 0.7 of the value calculated from specific capacity test data of the partially penetrating wells. Accordingly, arrays of transmissivity and hydraulic conductivity as mapped from specific capacity data for the Saddle Mountains, Wanapum, and Grande Ronde aquifers were multiplied by a factor of 0.7.

Another major change in the model involved the distribution of inactive nodes (unsaturated Saddle Mountains aquifer) along the crestal parts of the Horse Heaven Hills. This distribution was initially inferred with water-level data from sparse well control and with geologic maps locating those places where the Saddle Mountains aquifer is absent along the crest. Subsequently, the distribution of unsaturated Saddle Mountains aquifer was significantly refined in the model; for example, in areas where reasonable hydraulic conductivities and leakance were unable to maintain heads above the base of the Saddle Mountains aquifer during steady-state calibration, nodes were deactivated (the Saddle Mountains aquifer were assumed to be unsaturated).

Local changes in hydraulic conductivity, transmissivity, and vertical conductivity were avoided where data existed substantiating already coded values. Minor changes in small areas were made to bring predicted heads into calibration, and when these changes were made, geologically similar sets of adjacent nodes were changed to bring about the desired head change.

In later stages of the calibration, an important tool was the use of drains in the western part of the model, where recharge was largest and heads were inordinately high after initial calibration. Baseflow separation for Alder and Rock Creeks, and, to a lesser degree, for Satus Creek, provided good measurements for the minimum amount of water being discharged from the ground-water system, which was simulated in the model by flux from sets of drains

used to represent springs, streams, and seepage faces. Location of springs along canyons and other lesser drainages in the area (Pine, Wood, Old Lady, and Glade Creeks) and seepage run data in Pine Creek, provided additional information in locating and calibrating drains. Calibrated conductance values for drains in the western Horse Heaven Hills were used to calculate effective hydraulic conductivities for the sediment and basalt along these streams; these values range from 1.8×10^{-7} ft/s to 2.8×10^{-9} ft/s with a mean value of 3.2×10^{-8} ft/s. River-node conductance values along the Yakima and Columbia Rivers are higher and effective hydraulic conductivities calculated from these values range from 9.8×10^{-6} ft/s to 1.2×10^{-7} ft/s. Conductance values for drains and river nodes are a function of the effective vertical-hydraulic conductivity for the sediment along the streambed, plus the the basalt layer in which the stream is flowing. In addition, they are a measure of the placement of the drain elevation above the flow of the tributary stream. Arbitrarily, it was assumed that a seepage face and drain elevation started one-third the distance up the canyon wall from the bottom of the cliffs. It should be noted that the calibrated model flux from drains in Alder and Rock Creeks, and similar tributaries was matched, as closely as possible, to measured discharge values estimated from streamflow records for these streams. It is possible that a larger flux from the ground-water system takes place along these tributary canyons than is measured at these streamflow-gaging stations. For example, evapotranspiration of seepage high up on canyon walls, before it can reach the canyon floor and be recorded at the gage, is one way that this could occur.

Calibrated drain conductances ranged from 10^{-2} ft²/s to 8×10^{-5} ft²/s and averaged 1.8×10^{-3} ft²/s. Conductances along the upper reaches of the deeply entrenched streams in the western parts of the area ranged between 10^{-3} ft²/s and 10^{-4} ft²/s, whereas in their lower reaches and in the upper parts of Alder Creek, conductances range between 10^{-4} ft²/s and 10^{-5} ft²/s. Calibrated river conductances ranged from 1.3×10^{-4} ft²/s to 8×10^{-1} ft²/s and averaged 4×10^{-1} ft²/s. Conductances for Satus and Lower Rock Creeks ranged between 10^{-3} ft²/s and 10^{-2} ft²/s and between 10^{-2} ft²/s and 10^{-1} ft²/s for the Upper Yakima to Mabton and for the Columbia River from Richland to Wallula Gap. Conductances for the Yakima River below Mabton and for the Columbia River from Wallula Gap downstream to Rock Creek ranged from 10^{-1} ft²/s to 1 ft²/s. General head-boundary conductances averaged 2×10^{-3} ft²/s and had a narrow range between 7×10^{-4} ft²/s and 6×10^{-3} ft²/s.

For the Saddle Mountains Basalt layer (fig. 20) sum-of-squares error for estimated contoured data, as compared with the actual water-level data, shows an average error of $\pm$77 feet. For the Wanapum Basalt layer (fig. 21), the corresponding average error is $\pm$96 feet. Most of the large errors for the Saddle Mountains Basalt layer are associated with the hydrologic effect brought about by deep narrow canyons cutting through this aquifer in the western part of the Horse Heaven Hills. Most of the large errors in the Wanapum Basalt layer are associated with wells in steep-gradient (barrier) areas, or with wells whose depth is much greater than the midpoint of an aquifer, or with the combination of both. In other words, the error is not randomly distributed across the modeled area.

A water budget for the calibrated steady-state model is listed in table 2, along with a comparison of modeled and measured discharges to Rock, Status, Pine, Wood, and Alder Creeks. In the Washington part of the model, the percentage of total flow in the Saddle Mountains, Wanapum, and Grande Ronde aquifers was 44 percent, 46 percent, and 10 percent, respectively.

In comparing the final matrices of hydraulic conductivities and transmissivities (fig. 23) with the original, final hydraulic conductivities (ratio of geometric means) for the Saddle Mountains and Wanapum Basalt layers were 0.45 and 0.22 of the original, respectively. Much of this model-wide reduction is due to the 0.7 reduction made in both matrices noted earlier. Hydraulic conductivities for the Saddle Mountains Basalt layer (fig. 23) were significantly reduced (1 to 1.5 order of magnitude) for large parts of the Oregon area, in the Satus Creek Basin, and in the northern parts of the central syncline. In the Wanapum Basalt layer (fig. 23), the most significant changes were reductions along barriers (1 to 2 orders of magnitude). Additional Wanapum layer reductions (1 to 2 orders of magnitude) also occurred along Rock and Satus Creeks and along the Rattlesnake anticlinal ridge.

The most significant change made to the vertical conductance matrix was to increase values from original coding along the synclinal areas underlying the Yakima and Columbia Rivers. Without such increases along the Yakima River, the ground-water ridge within the Grande Ronde aquifer could not have been maintained along the length of the Horse Heaven Hills axis. Without increase in leakance along the Columbia River, the river could not be maintained as the major drain for water flowing south from the Horse Heaven Hills axis. Specifically, before increases in vertical conductivity along the Columbia River, flux in the western part of the model was directed from the Horse Heaven Hills crest across the Columbia River and out of the model into the constant head nodes in Oregon.

Transient Model and Calibration

The 3-year period 1980-83 was used in calibrating the model to water-level changes. Transient model calibration involved making additional changes in hydraulic- conductivity and vertical-conductance values where needed, such as in areas where reasonable changes in storage could not bring the model into calibration. When this type of change was made, the steady-state model was rerun to see if effects on this model were acceptable. This iterative process from transient to steady-state model was common in the final stages of calibration.

Ground-water pumpage and surface-water importation calculated from electric-power usage were used during this 3-year period. Pumpage was coded as a set of 20, cyclic 6-month pumping or irrigation stress periods alternating with 6-month irrigation periods. Quantities of imported water and city-water use were arbitrarily distributed across the entire year rather than just during the 6-month growing season. Six time steps were used in each stress period with 1.6 as a multiplier for the length of successive time steps. Steady-state heads calibrated for 1972-75 were used as initial heads for the transient simulation (1973-83). For the 1980-83 calibration period, initial heads were those calculated by the model after 8 years of transient simulation (1973-80) had been produced. A portion of the ground water pumped from deep aquifers was returned to the upper aquifer as recharge (irrigation return flow). During transient simulation, 15 nodes were reactivated in the

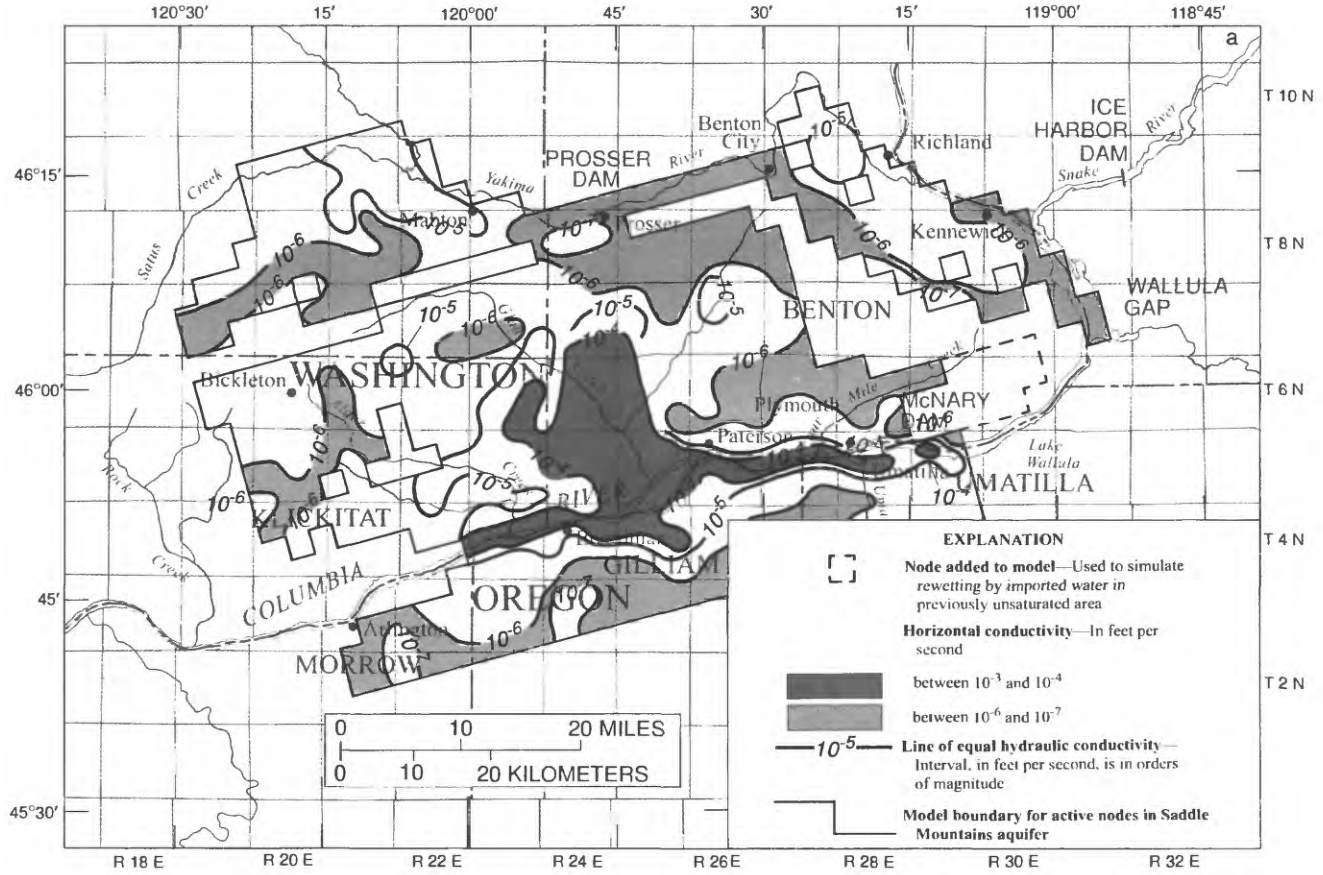
a
120°30′
15′
120°00′
45′
30′
15′
119°00′
118°45′
46°15′
46°00′
45°30′
T 10 N
T 8 N
T 6 N
T 4 N
T 2 N
R 18 E
R 20 E
R 22 E
R 24 E
R 26 E
R 28 E
R 30 E
R 32 E
PROSSER DAM
Benton City
Richland
ICE HARBOR DAM
Kennewick
WALLULA GAP
BENTON
WASHINGTON
Bickleton
Plymouth
McNARY DAM
Paterson
Lake Wallula
UMATILLA
KLICKITAT
GILLIAM
COLUMBIA
OREGON
MORROW
Yakima River
Snake River
Satus Creek
Rock Creek
Mill Creek
Alder Creek
0 10 20 MILES
0 10 20 KILOMETERS
EXPLANATION
Node added to model—Used to simulate rewetting by imported water in previously unsaturated area
Horizontal conductivity—In feet per second
between 10^{-3} and 10^{-4}
between 10^{-6} and 10^{-7}
10^{-5} Line of equal hydraulic conductivity—Interval, in feet per second, is in orders of magnitude
Model boundary for active nodes in Saddle Mountains aquifer

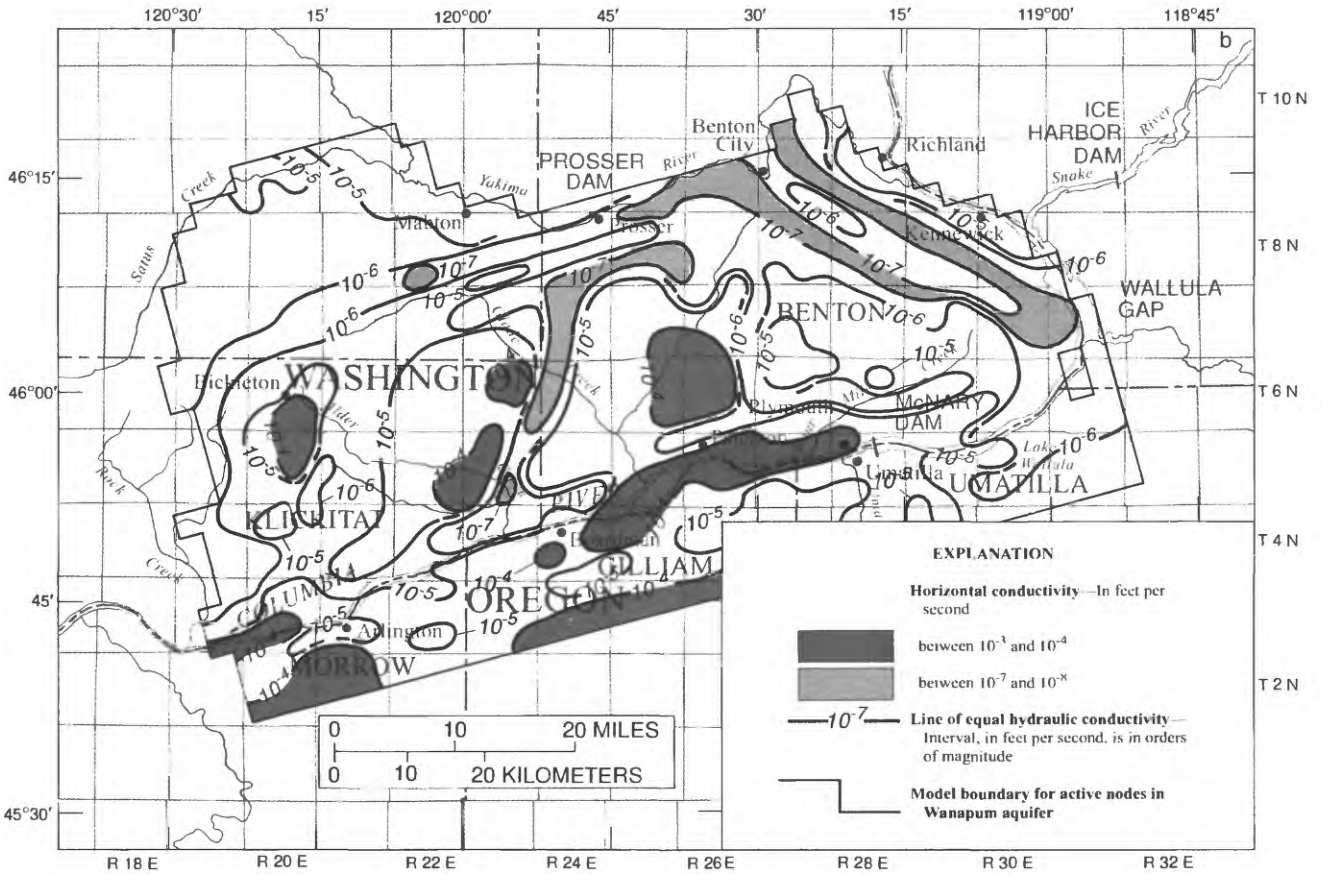
b
120°30′
15′
120°00′
45′
30′
15′
119°00′
118°45′
46°15′
46°00′
45°30′
T 10 N
T 8 N
T 6 N
T 4 N
T 2 N
R 18 E
R 20 E
R 22 E
R 24 E
R 26 E
R 28 E
R 30 E
R 32 E
PROSSER DAM
Benton City
Richland
ICE HARBOR DAM
Kennewick
WALLULA GAP
BENTON
WASHINGTON
Bickleton
Plymouth
McNARY DAM
Lake Wallula
UMATILLA
KLICKITAT
GILLIAM
COLUMBIA
OREGON
MORROW
Yakima River
Snake River
Satus Creek
Rock Creek
Mill Creek
Alder Creek
0 10 20 MILES
0 10 20 KILOMETERS
EXPLANATION
Horizontal conductivity—In feet per second
between 10^{-3} and 10^{-4}
between 10^{-7} and 10^{-8}
10^{-7} Line of equal hydraulic conductivity—Interval, in feet per second, is in orders of magnitude
Model boundary for active nodes in Wanapum aquifer

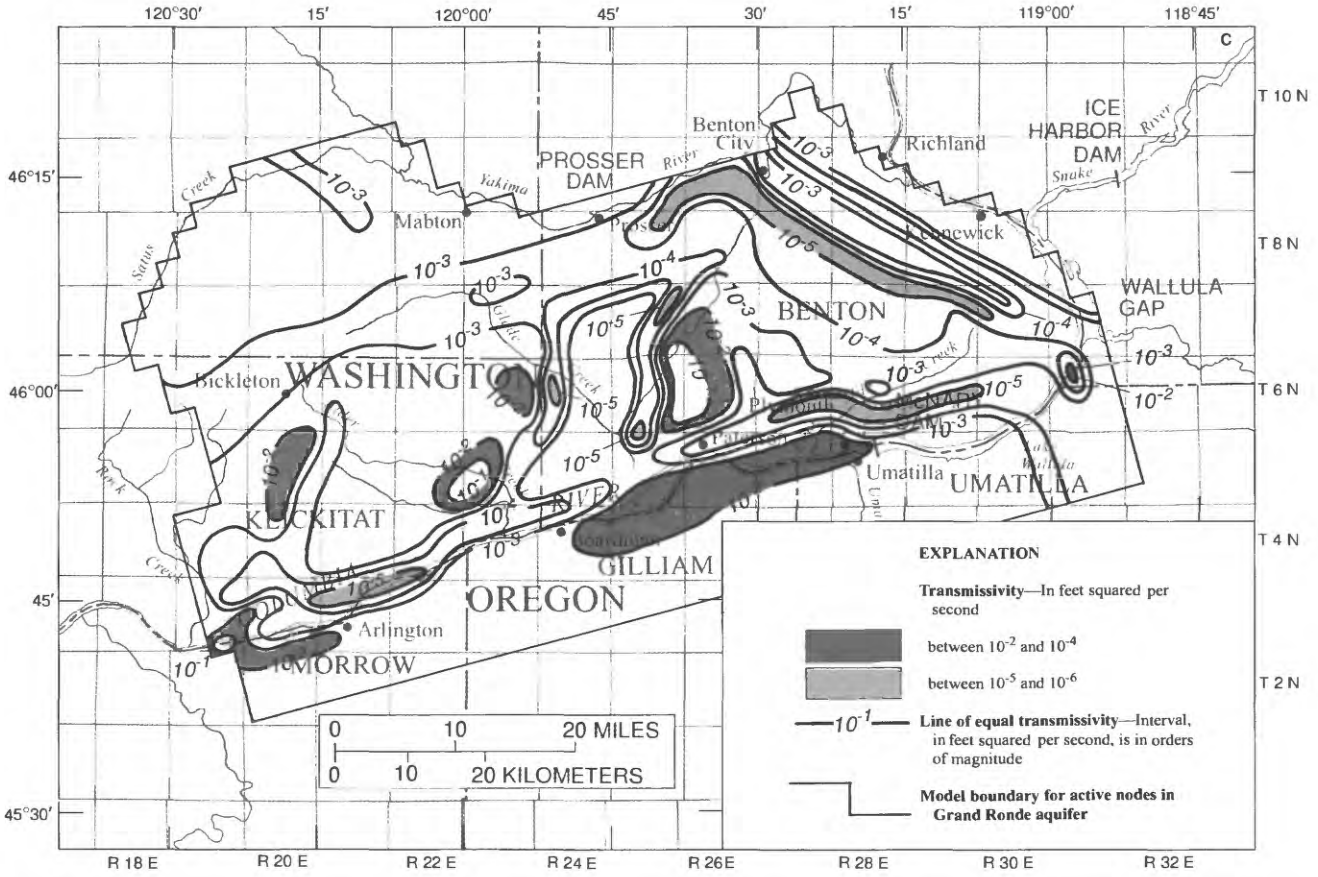

Figure 23. Hydraulic conductivity as determined during model calibration in (a) the Saddle Mountains and (b) Wanapum aquifers; and (c) transmissivity in the Grande Ronde aquifer.

Saddle Mountains aquifer (fig. 17) along the unsaturated crest of the eastern Horse Heaven Hills segment, to allow modeling of the irrigation water imported from the Columbia River and used in this area.

Transient calibration used initial storage values of $1x10^{-3}$ for the Grande Ronde and Wanapum aquifers and $1x10^{-2}$ for the Saddle Mountains aquifer. Calibration was made to cumulative-water-level changes for the 3-year period (1980 to 1983) [fig. 24] rather than for each separate year. Several refinements, such as an increase in the hydraulic conductivities of some barrier elements that ran parallel to steady-state flow were added during this calibration (this was the only way the model could be calibrated in these areas). Vertical-conductance values for the Saddle Mountains-Wanapum interval were changed in several areas where imported water was being added in order to balance Saddle Mountains and Wanapum aquifer changes in the same area. Except for small adjustments in a few small areas, calibration for the 3-year measurement period was acceptable (fig. 24) with these storage values. Storage matrices for the Saddle Mountains and Wanapum aquifers are shown in figure 25 (Grande Ronde storage was a uniform $1x10^{-3}$).

Table 2. Water budget for steady-state model with model flux from drains and river nodes

WATER BUDGET

Rates
(cubic feet per second)

In:

Storage	0.00000
Constant head	26.069
Drains	.00000
Recharge	69.743
River leakage	.77672
Total in	96.589

Out:

Storage	.00000
Constant head	.45053
Drains	11.911
Recharge	.00000
River leakage	84.226
Total out	96.588
In - Out	$.96130 \times 10^{-3}$

Percent discrepancy = 0.0010

Sites	Estimated baseflow (in cubic feet per second)	Total flux from all drains and river nodes used to simulate the stream in question (in cubic feet per second)
Alder Creek	2	1.6
Pine Creek	2 to 4	2.4
Wood Gulch	3 to 5	2.8
Rock Creek	6	6.7
Satus Creek	10	7.8
Upper Glade Creek	unknown	.4

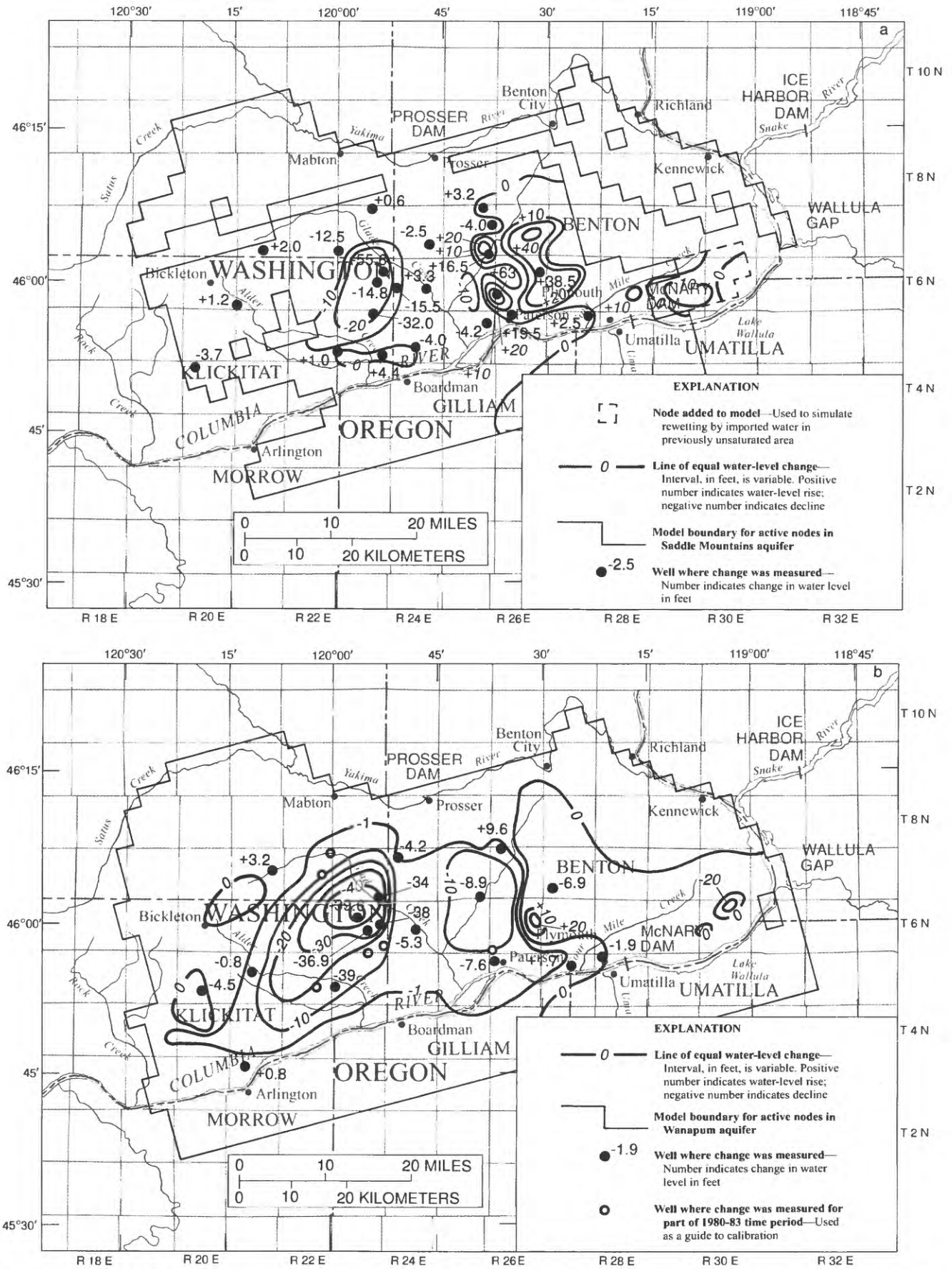

Figure 24. Model-predicted water-level changes in (a) the Saddle Mountains and (b) the Wanapum aquifers, 1980-83.

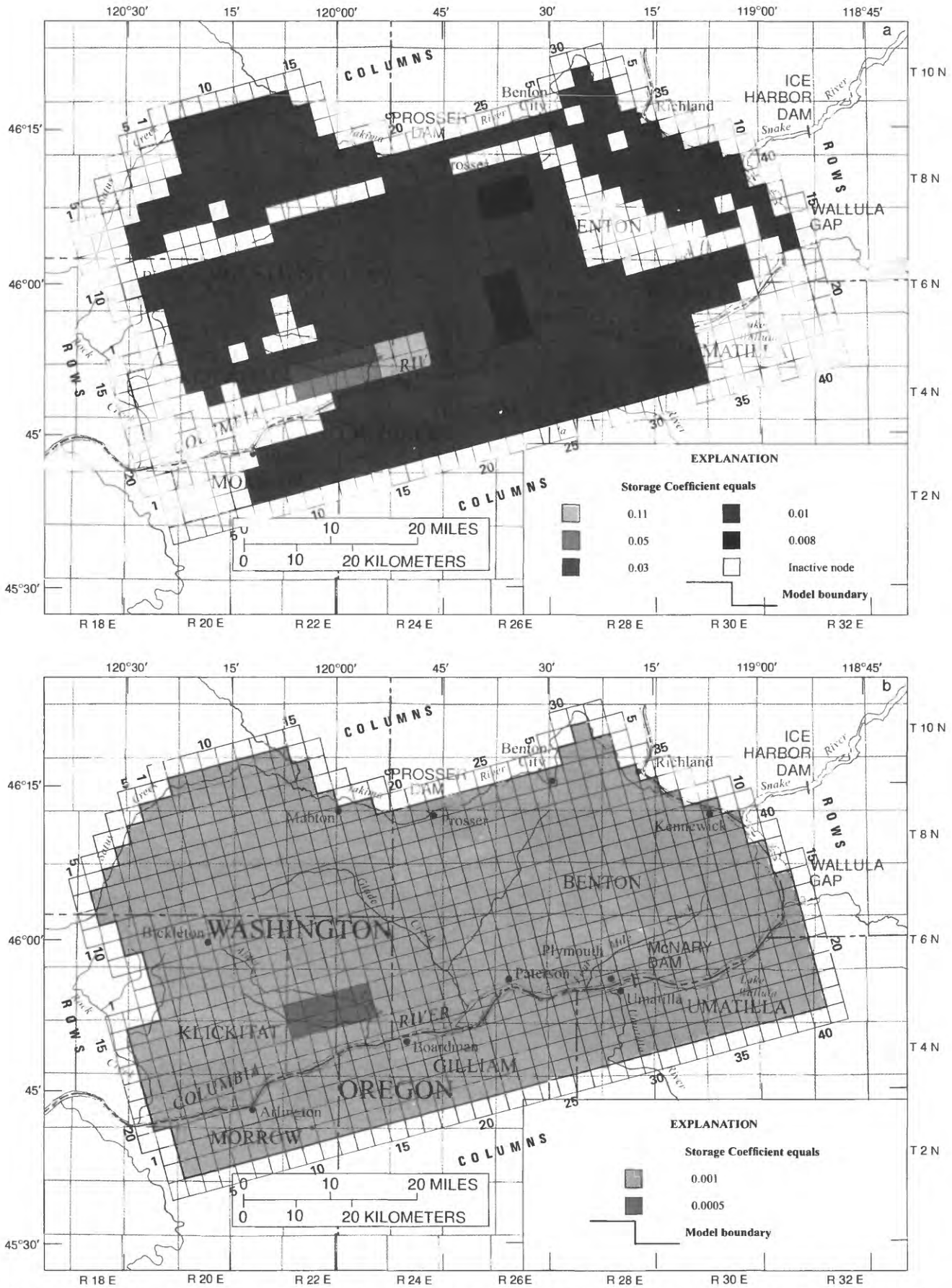

Figure 25. Calibrated storage-coefficient matrices for (a) the Saddle Mountains aquifer and (b) the Wanapum aquifer.

Aggregate ground-water discharge and recharge rates for annual pumpage from 1973 through 1982 are listed in table 3 for several general areas using ground water for irrigation. See figure 25 for locations of these ground-water areas. Recharge rates for four areas irrigated with surface water are listed in table 4 for the same irrigation periods of 1973-82. The locations of surface-water areas are shown in figure 26.

Water-budget results indicate that boundaries have not significantly affected transient results inasmuch as flux from constant head nodes along the southern boundary did not changed appreciably from that of the steady state; general-head boundary flux was minimal on the western boundary, and water-level changes are less than 10 feet (in most cases less than 1 foot) adjacent to all boundaries. In 1983, about 55 percent of the water for pumpage was supplied by storage; most of the remainder was supplied by irrigation leakage to the Wanapum aquifer.

A sum-of-squares error analysis for the Saddle Mountains and the Wanapum aquifers calibration wells, when compared with the estimated contoured values, gives an average error of ± 9 feet for the cumulated 3-year period.

A transient-model run was made to show total drawdown over the 10-year stress period (fig. 27). Although few calibrating points are available, those wells where 1970 and 1971 data exist indicate good agreement with the results of this 10-year run. Hydrographs showing model-predicted and observed-water-level changes for eight wells finished in Saddle Mountains and Wanapum aquifers, and located in the main pumping and water-importation areas, are shown in figure 28. Locations for the wells are shown in figure 4.

Results of Calibration

Model calibration of the north and northeastern slopes of Horse Heaven Hills (in the Satus and Kennewick areas) is more generalized than elsewhere. Inclusion of all well controls was not attempted because these areas were added to the model mainly to observe whether the cones of depression generated on the south-facing dip slope of the Horse Heaven Hills would be propagated over to the Yakima and Columbia Rivers north of the Horse Heaven Hills.

During calibration of the Horse Heaven Hills model, the original conceptualization of the geohydrology was changed in several major ways. One of the most significant of those changes concerned the extent of low-permeability fault and monoclinal barriers present in the area. The number and lengths of these barriers were increased in comparison with those first inferred from structure and thickness maps, but in one instance, an "obvious" barrier was removed. The shear fault barriers were particularly difficult to infer without associated head data and a number of calibration runs. A second change in conceptualization involved the understanding of the relation between vertical hydraulic conductivity, major structure, and interbed facies. Uniform conductance was coded to the preliminary model and only after the initial cross-section flow models were run was additional field data sought to evaluate the concept that higher conductance along the major synclines was a regional pattern. A third significant change involved the amount of Saddle Mountains aquifer that was thought to be unsaturated. The original idea was that much smaller areas were unsaturated than eventually was the case.

Table 3. Ground-water discharge and associated recharge for four major irrigations areas for 1973-82, and for three model scenarios

[D = discharge, R = recharge, -- = not computed]

	Acre-feet per year							
	Glade Creek		Alder Creek		East Glade Creek		Northeast Horse Heaven Hills	
Year	D	R	D	R	D	R*	D	R
				Model Calibration				
1973	1,567	188	76	--	0	--	--	--
1974	1,567	188	76	--	0	--	--	--
1975	1,567	188	76	--	0	--	--	--
1976	2,418	290	76	--	0	--	--	--
1977	3,858	463	3,800	36	0	--	--	--
1978	4,018	481	7,582	688	210	--	--	--
1979	6,276	753	13,715	1,348	2,446	--	--	--
1980	8,455	1,016	10,342	957	2,246	--	--	--
1981	5,723	686	8,304	852	3,077	--	--	--
1982	6,092	730	9,821	825	2,340	--	--	--
				Predictive-Model scenarios				
Developed	9,129	1,071	13,958	1,585	4,619	232	--	--
Undeveloped	11,873	1,310	21,784	2,121	7,594	391	10,295	60
Pending	11,873	1,310	42,359	4,539	11,337	818	--	--

* Recharge for the east Glade Creek area is contained in the surface-water recharge figures for the Bing-Carter Canyons area (table 4).

In light of the calibration procedures discussed above, the hydrologic barriers (in this report, faults and tightly folded anticlines), as named and discussed by Newcomb (1961, 1969), were shown to greatly influence flow in the aquifer system. Little data exist that can be used to measure the hydraulic characteristics of these features. Existing data for the Horse Heaven Hills was obtained from estimates and the results of model calibration. Using data from the calibrated model and from geologic descriptions, these features can be characterized as follows:

(1) The high angle reverse fault on the north and northeast flanks of the Horse Heaven Hills axis produces the steepest topographic and hydraulic gradients and the smallest modeled hydraulic conductivities

Table 4. Recharge for major surface-water irrigation areas for 1973-82, and for three model scenarios

Year	Recharge, in acre-feet per year			
	Dead Canyon	Patterson Ridge	Bing-Carter Canyons	McNary-Wallula
		Mode Calibration		
1973	859	946	723	1,348
1974	2,631	3,164	3,852	1,541
1975	11,038	3,645	6,560	1,293
1976	3,201	1,170	1,986	1,212
1977	3,319	1,113	4,348	1,321
1978	2,180	963	3,414	1,045
1979	3,089	1,176	3,998	1,183
1980	2,470	1,061	3,485	1,018
1981	2,379	1,801	3,939	1,016
1982	2,556	1,064	4,222	825
		Predictive-Model Scenarios		
Developed	2,319	997	4,188	825
Undeveloped	2,319	997	4,188	825
Pending	2,319	997	4,188	825

of the area. The fact that the largest structural disruption in the area occurs along this fault is probably related. Wanapum aquifer conductivities along this feature range from $1x10^{-8}$ to $4x10^{-7}$ ft/s.

(2) The monocline along the south side of the western Horse Heaven Hills segment also is associated with significant hydraulic gradients, and the lateral change in structural relief is related directly to the change in hydraulic gradient and inversely related to the modeled hydraulic conductivities necessary to simulate these gradients. Other monoclinal elements along the north and northeast flank of the Horse Heaven Hills axis were lumped with adjacent and contiguous faults as barrier elements of small hydraulic conductivity in order to inhibit flow from the crest. All of these monoclines undoubtedly change to faults at some depth.

(3) Some shear faults, whose orientation is at angles to regional flow, are associated with steep hydraulic gradients and with upward flow upgradient of the barrier. Many of these shear faults have no surface expression and can only be inferred from detailed structural mapping as abrupt linear changes in strike or as linear zones of change in structural gradient. Where steep hydraulic gradients

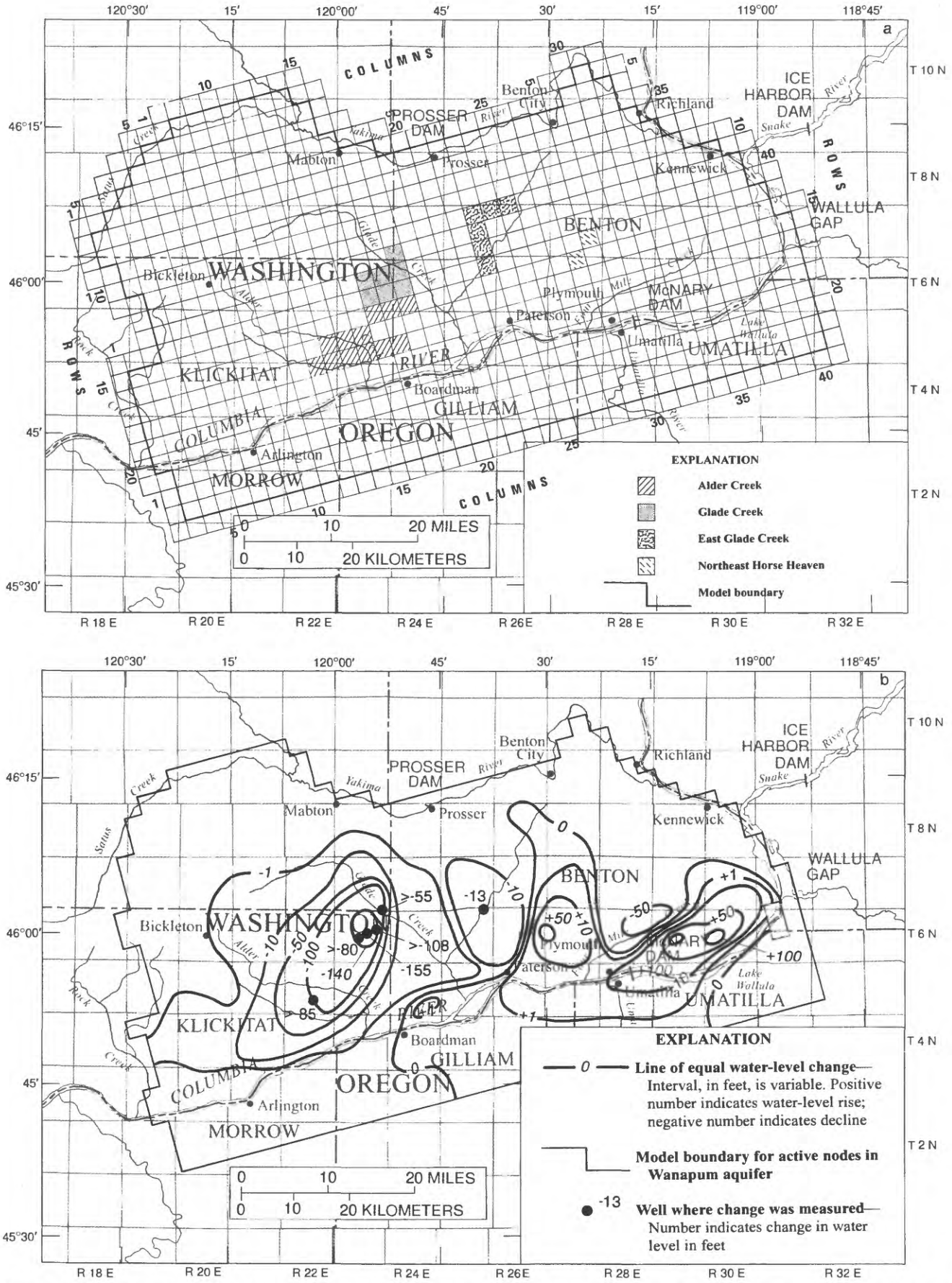

Figure 26. Model grid and location of (a) ground-water pumpage areas and (b) areas of return flow from surface-water irrigation.

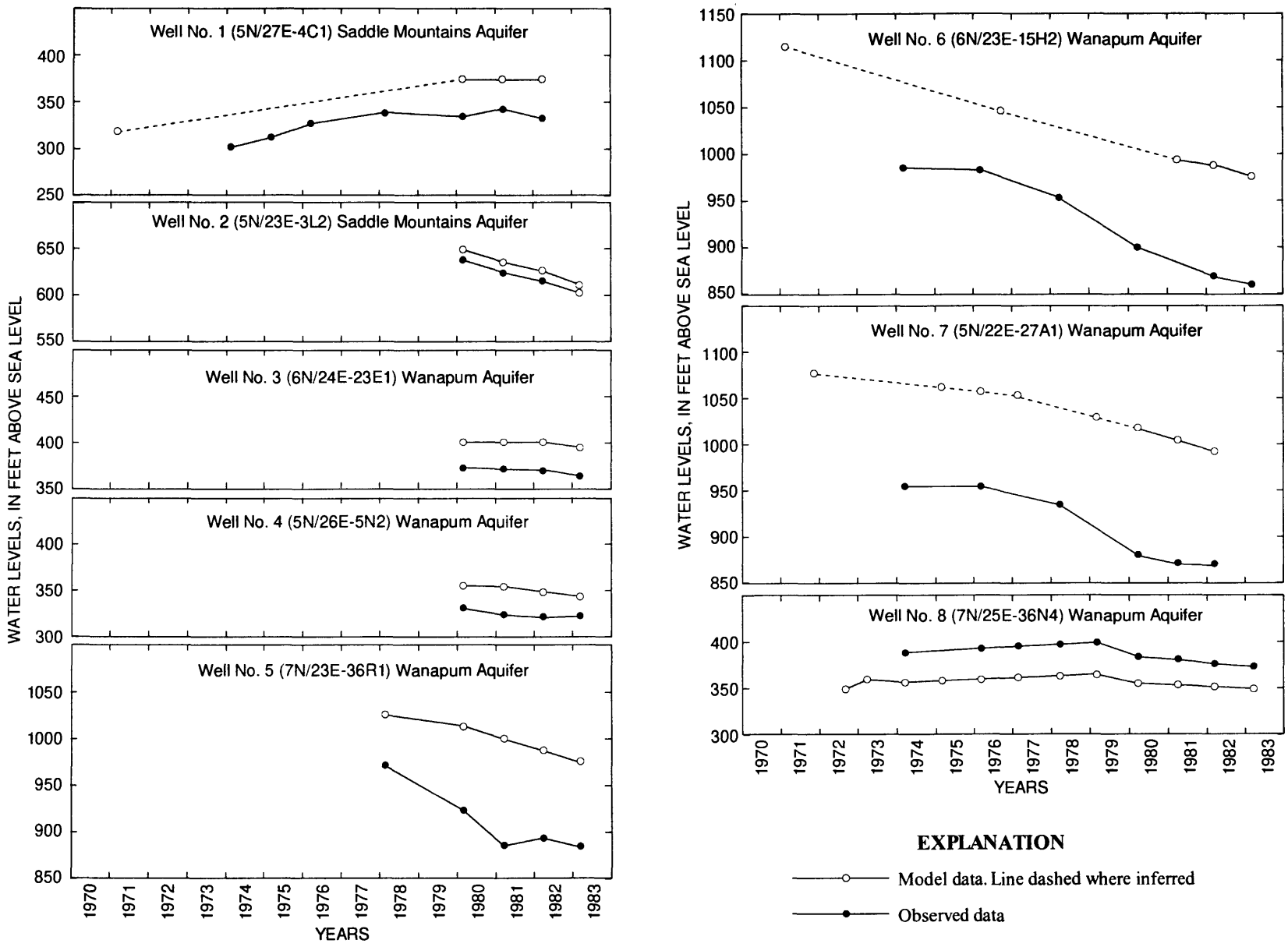

Figure 28. Model-predicted and observed water-level changes in the Saddle Mountains and Wanapum aquifers.

coincide with such features, the hydraulic conductivity of material present is estimated to range from $3x10^{-8}$ to $2x10^{-6}$ ft/s. Undoubtedly, there are many more of these than have been identified in the Horse Heaven Hills model. Swanson and others (1979) mapped a number of northwest-southeast oriented shears in the western part of the study area, but because they parallel regional flow, they do not cause noticeable changes in hydraulic gradients. Unless such fault barriers are located during transient calibration, they will usually go unnoticed.

Hydraulic gradients across shear faults are generally higher in the Wanapum aquifer than for the same barrier immediately above and in the Saddle Mountains aquifer. Calibration of the model resulted in barrier hydraulic conductivities for the Wanapum aquifer that are two orders of magnitude smaller than those for the overlying Saddle Mountains; aquifer hydraulic conductivities vary along the length of each barrier, but this variation cannot be related to identifiable physical features.

(4) A band of higher hydraulic conductivity is found on the upgradient sides of barrier 3 (fig. 6; Strait, 1978). This same phenomenon can be observed in the Wanapum aquifer in three areas; specifically, upgradient of barriers 1, 2, and 3 (fig. 6). However, within the Saddle Mountains aquifer, this rule does not apply to those areas adjacent to the lowest structural parts of the area. Those barriers adjacent to the central and Umatilla synclines have higher hydraulic conductivities in the Saddle Mountains aquifer on the downgradient sides. This condition may be related to the high permeability associated with interbed sands and pillow structures in these synclines.

(5) The Columbia Hills anticline is thought to function as a barrier of low hydraulic conductivity by inference from the steep gradients associated with it in the western parts of the study area, by inference from low to intermediate hydraulic conductivities along the Horse Heaven Hills axis, and by inference from the steep gradients and other data presented by Newcomb (1969) for this same fold in The Dalles, Oregon area to the west.

After model calibration, ratios of horizontal- to vertical-hydraulic conductivity (vertical anisotropy) were calculated for the Saddle Mountains and Wanapum aquifers. The geometric mean ratios for these two aquifers are $5.9x10^{-3}$ and $2.0x10^{-3}$, respectively. A node map of calculated ratios for the Saddle Mountains aquifer generally shows lower values (about $4x10^{-4}$) along the major synclines than along the Horse Heaven Hills axis (about $6.5x10^{-3}$). Both the Wanapum and the Saddle Mountains distributions show highest values ($2.3x10^{-2}$) upgradient from barriers (faults and tight folds). In general, there is a poor correlation between horizontal- and vertical-hydraulic conductivities.

Transmissivity and horizontal-hydraulic-conductivity values used in other basalt-aquifer studies in the Columbia Plateau are compared with Horse Heaven Hills values in table 5. In general, the upper limits to horizontal-hydraulic conductivities are the same in all studies, but the lowest Horse Heaven Hills hydraulic conductivities (along barrier elements) are an order of magnitude lower than in other studies. These lower values may be due to the fact that more severe faulting (throw) and steeper hydraulic gradients exist along the north face of the Horse Heaven Hills than are modeled elsewhere and that lower hydraulic conductivities were needed to simulate them. Vertical-hydraulic-conductivity values (table 6) are not well documented from other studies, but the mean value for the Horse Heaven Hills study area is within a half order of magnitude of the three values cited. The range of Horse Heaven Hills vertical-hydraulic-conductivity values is large with smaller values along the axis of the major anticline. This large range may be more typical of the Yakima Fold Belt than it is of the rest of the Columbia Plateau.

Model Sensitivity

Model sensitivity to change in horizontal conductivity, vertical conductance, river-node conductance, drain-node conductance, and recharge was measured by computing root-mean-square (RMS) changes in calculated head values and vertical head gradients. Several comparisons were made: (1) calculated heads and vertical gradients for all active nodes in the model were compared to calculated heads and gradients from the steady-state model, (2) calculated heads and vertical gradients for each layer in the model were compared to calculated heads and gradients for that layer from the steady-state model, and (3) calculated head values for those nodes in the model containing observation wells were compared to the calculated heads from the steady-state model for those nodes. These RMS differences provide understanding of how the modeled system is affected by change in the input variables, and provides a better understanding of the calibration procedure.

During sensitivity testing, numerical instability caused a large number of dry nodes to develop along the axis of the anticline with Kh (horizontal hydraulic conductivity) multipliers of as little as $\pm$ 10 percent. For this reason, the Double-Do-Loop algorithm (see Appendix) had to be used to obtain stable solutions for most sensitivity analyses performed. Kh multipliers of 1.4 (40 percent increase) and recharge multipliers of 0.7 (30 percent decrease) produced several dry nodes (<10) along the anticlinal axis which could not be eliminated. A stable solution without excessive dry nodes could not be obtained for Kh multipliers greater than 1.4 or for recharge multipliers less than 0.7. Therefore, the range of sensitivity testing was limited to $\pm$ 40 percent for Kh and Kv (vertical-hydraulic conductivities) and +40 percent and -30 percent for recharge. Empirically, when the RMS head changes for all nodes in the model exceeded about 220 feet, stable solutions with <10 dry nodes could not be obtained. The model was not as sensitive to changes in riverbed and drain conductivities so the full range of 0.6 to 1.4 multipliers were used.

Within the range of change tested, results of the sensitivity analyses indicate:

(1) The largest model-wide RMS changes are associated with increased Kh or decreased recharge (fig. 29, table 7);

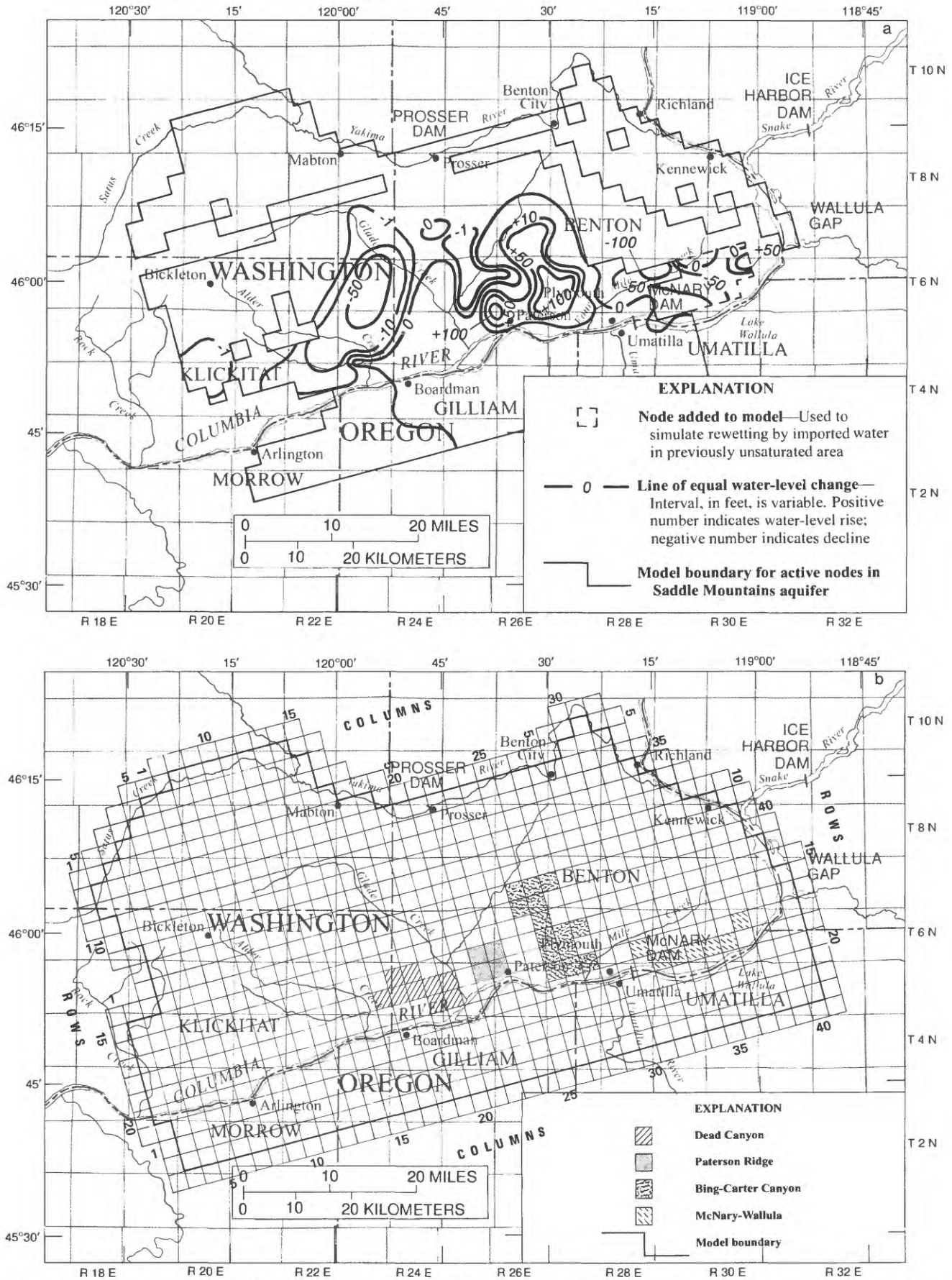

Figure 27. Model-calculated water-level changes in (a) the Saddle Mountains and (b) the Wanapum aquifers, 1973-83.

Table 5. Model horizontal-hydraulic conductivities (K) and transmissivities (T) for basalt aquifers derived in other studies in the Columbia Plateau

[Conductivities in feet per second; transmissivities in feet squared per second]

Study Area	Range	Mean	Remarks
Lower Status Creek Basin (Prych, 1983)	$T=7.x10^{2}$	Same	The hydraulic conductivity has been estimated from reported values of transmissivity by assuming that all T is assigned to a 300-ft thickness of Saddle Mountains aquifer.
	$K=9.x10^{-5}$	Same	
Pullman-Moscow (Barker, 1979)	$1.x10^{-3}<T<3.3x10^{-1}$	?	The hydraulic conductivity range has been estimated from reported values of transmissivity by assuming that all T is assigned to 200-3,000-ft thickness of the Grande Ronde aquifer with thickness patterns discussed in the report.
	$3.x10^{-7}<K<3.x10^{4}$	?	
Odessa-Lind (Luzier and Skrivan, 1973)	$3.x10^{-3}<T<4.6x10^{-1}$	?	The hydraulic conductivity range has been estimated from reported values of T assuming that zone B is a 4,000-ft thick section of Grande Ronde aquifer.
	$7.8x10^{-7}<K<1.2x10^{-4}$	?	
Walla Walla (McNish and Barker, 1976)	$5x10^{-3}<T<4x10^{-1}$	?	The hydraulic conductivity range has been estimated from reported values of T assuming that the primary aquifer was a 400-800-ft thick section of Wanapum aquifer.
	$6x10^{-6}<K<7.5x10^{-4}$		
Horse Heaven Hills (this report)			
Saddle Mountains aquifer	$1.7x10^{-7}<K<8.5x10^{-4}$	$3.1.10^{-6}$	
Wanapum aquifer	$3.3x10^{-8}<K<7.6x10^{-4}$	$3.7x10^{-6}$	
Grande Ronde aquifer	$2x10^{-6}<T<2.2x10^{-1}$	$1.2x10^{-3}$	

Table 6. Vertical conductance (Tk) and vertical-hydraulic conductivities (Kv) for basalt aquifers derived in other studies in the Columbia Plateau

[Hydraulic conductivities in feet per second; conductance in feet squared per second]

Study area	Values	Remarks
Walla Walla (McNish and Barker, 1976)	$Kv=5x10^{-8}$	A minumum value
Pullman-Moscow (Barker, 1979)	$Kv=2x10^{-9}$	
Quincy (Bauer, unpublished)	$Tk=1x10^{-10}$ $Kv=2x10^{-8}$	Kv estimated from TK by assuming a Wanapum and Grande Ronde aquifers combined total thickness thickness of 4,000 feet, a center-to-center of aquifer thickness 1/2 of this;
Horse Heaven Hills Saddle Mountains- Wanapum interval	$3.4x10^{-11}<Kv<2.7x10^{-7}$ average = $1.5x10^{-8}$	Crest of anticline Kv values average $5.7x10^{-9}$; synclinal values average $1.3x10^{-7}$

(2) In general, the model is most sensitive to Kh and is least sensitive to riverbed conductance; variation in Kh caused larger changes in vertical gradients than did variation in the other five parameters;

(3) For increases and decreases in the five parameters, the least change in head was consistently located in the deepest layer, the aquifer with the smallest model-wide relief in its potentiometric surface; in most cases of parameter increase or decrease, the most sensitive layer was the shallowest aquifer, the water-table aquifer which exhibits the largest model-wide potentiometric-surface relief. This layer's sensitivity is indicated not only in the RMS data but in its increased tendency to develop dry nodes relative to the other layers;

(4) For the largest increases or decreases in Kh and recharge, the RMS change at the observation well nodes usually exceeds the model-wide RMS change, indicating that the observation wells as a set were better than average tools for use in evaluating most changes made during calibration. As a

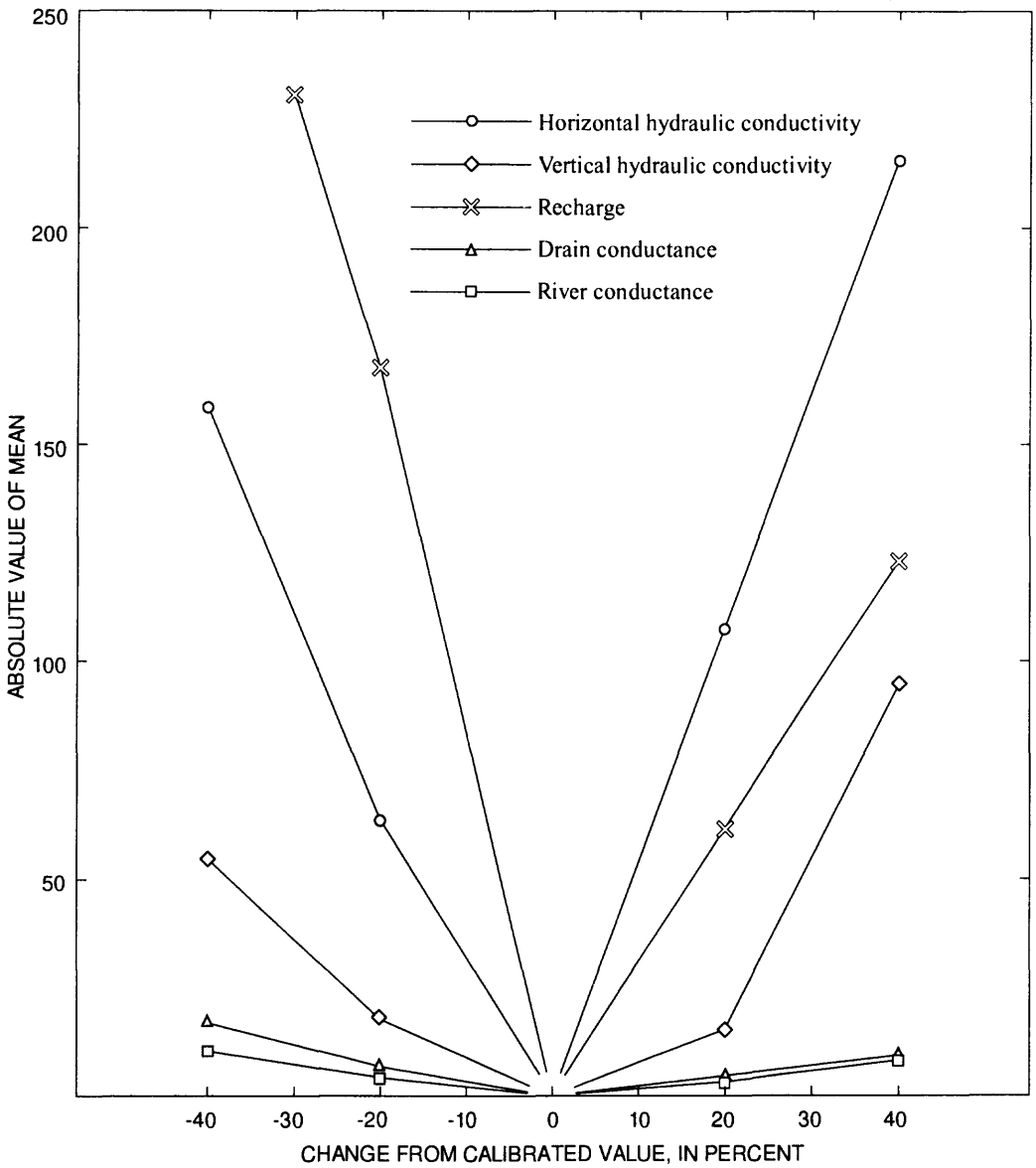

Figure 29. Relation of change in mean residual water level from calibrated model to change in recharge, hydraulic conductivity, and conductance.

matter of interest, the largest increases or decreases cause RMS change at the observation points which exceed the mean absolute residuals (observed as compared to calculated heads) for the steady-state model (±77 feet for the Saddle Mountains aquifer and ±96 feet for the Wanapum aquifer).

Discharge to drains and river nodes is sensitive to changes in recharge and in the four classes of hydraulic conductivity (fig. 30). Drains in the model represent discharge to springs and to the upper parts of drainages tributary to the Columbia and Yakima Rivers. River nodes represent the Columbia and Yakima Rivers and the lowest parts of these same tributaries. Drain discharge is more sensitive to changes in conductivity and recharge than river discharge. Drain and river discharge are most sensitive to recharge and horizontal conductivity and least sensitive to change in riverbed conductivity.

Table 7. Variations in root-mean-square (RMS) error between all-node and selected-node model results for changes in horizontal-hydraulic conductivity, vertical-hydraulic conductance, riverbed conductivity, drain conductance, and recharge

Layer	With 0.6 multiplier		With 1.4 multiplier	
	Number of nodes	RMS	Number of nodes	RMS
Horizontal-hydraulic conductivity				
Head match				
Layer 1 all nodes	456	146	456	396
Layer 1 selected nodes	47	129	47	506
Layer 2 all nodes	624	211	624	103
Layer 2 selected nodes	40	171	40	96
Layer 3 all nodes	636	103	636	62
Layer 3 selected nodes	1	134	1	101
All layers, all nodes	1,716	160	1,716	217
All layers, all nodes	88	150	88	376
Vertical gradient match				
Layer 1, all nodes	439	39	430	45
Layer 1, selected nodes	42	53	46	39
Layer 2, all nodes	592	159	608	71
Layer 2, selected nodes	40	113	40	55
All layers, all nodes	1,031	123	1,038	61
All layers, selected nodes	82	87	86	47
Vertical-hydraulic conductivity				
Head gradient match				
Layer 1 all nodes	456	87	456	179
Layer 1 selected nodes	47	51	47	28
Layer 2 all nodes	624	21	624	14
Layer 2 selected nodes	40	27	40	17
Layer 3 all nodes	636	45	636	25
Layer 3 selected nodes	1	50	1	19
All layers, all nodes	1,716	54	1,716	94
All layers, selected nodes	88	42	88	23
Vertical gradient match				
Layer 1, all nodes	444	54	448	29
Layer 1, selected nodes	46	57	44	31
Layer 2, all nodes	613	53	618	31
Layer 2, selected nodes	40	57	40	32
All layers, all nodes	1,057	54	1,066	30
All layers, selected nodes	86	57	84	31

Table 7. Variations in root-mean-square (RMS) error between all-node and selected-node model results for changes in horizontal-hydraulic conductivity, vertical-hydraulic conductance, riverbed conductivity, drain conductance, and recharge--Continued

Layer	With 0.6 multiplier		With 1.4 multiplier	
	Number of nodes	RMS	Number of nodes	RMS
	Riverbed conductance			
Head match				
Layer 1 all nodes	456	9.2	456	4.4
Layer 1 selected nodes	47	4.9	47	2.2
Layer 2 all nodes	624	9.3	624	4.5
Layer 2 selected nodes	40	4.6	40	1.9
Layer 3 all nodes	636	13	636	7.4
Layer 3 selected nodes	1	3.1	1	1.5
All layers, all nodes	1,716	11	1,716	5.8
All layers, all nodes	88	4.8	88	2.1
Vertical gradient match				
Layer 1, all nodes	455	1.3	456	.7
Layer 1, selected nodes	47	.5	47	.2
Layer 2, all nodes	624	5.5	624	3.6
Layer 2, selected nodes	40	2.5	40	1.2
All layers, all nodes	1,079	4.2	1,080	2.8
All layers, selected nodes	87	1.8	87	.8
	Drain conductance			
Head match				
Layer 1 all nodes	456	18	456	10
Layer 1 selected nodes	47	23	47	12
Layer 2 all nodes	624	19	624	11
Layer 2 selected nodes	40	19	40	11
Layer 3 all nodes	636	10	636	5.5
Layer 3 selected nodes	1	19	1	10
All layers, all nodes	1,716	16	1,716	9.2
All layers, selected nodes	88	21	88	12
Vertical gradient match				
Layer 1, all nodes	456	3.8	456	2.8
Layer 1, selected nodes	47	4.6	47	3.0
Layer 2, all nodes	624	9.9	624	6.1
Layer 2, selected nodes	40	8.6	40	5.0
All layers, all nodes	1,080	7.9	1,080	4.9
All layers, selected nodes	87	6.7	87	4.0

Table 7. Variations in root-mean-square (RMS) error between all-node and selected-node model results for changes in horizontal-hydraulic conductivity, vertical-hydraulic conductance, riverbed conductivity, drain conductance, and recharge--Continued

Layer	With 0.7 multiplier		With 1.4 multiplier	
	Number of nodes	RMS	Number of nodes	RMS
	Recharge			
Head match				
Layer 1 all nodes	456	407	456	135
Layer 1 selected nodes	47	511	47	123
Layer 2 all nodes	624	123	624	149
Layer 2 selected nodes	40	113	40	130
Layer 3 all nodes	636	57	636	68
Layer 3 selected nodes	1	98	1	113
All layers, all nodes	1,716	225	1,716	121
All layers, selected nodes	88	381	88	126
Vertical gradient match				
Layer 1, all nodes	429	36	448	24
Layer 1, selected nodes	45	29	47	26
Layer 2, all nodes	611	79	606	101
Layer 2, selected nodes	40	58	40	69
All layers, all nodes	1,040	65	1,054	78
All layers, selected nodes	85	46	87	51

Additional model runs were made to test the sensitivity of the steady-state and transient calibrations to boundary conditions along the southern edge of the model in Oregon. Pre-development heads (1952-55) were used in constant-head nodes along this boundary as contrasted with the 1972-75 heads used in the Washington part of the model. Assuming linear water-level change from 1965-80, heads for 1973 were estimated for each layer at the boundary (water-level declines in Oregon from 1965-80 [Oberlander, 1981] were used to reconstruct alternative heads along this boundary), and the steady-state model was rerun using these to see if significantly different heads were propagated in the Washington part of the model. Model-estimated differences from the original calibration were less than 1 foot just north of the Columbia River and 0 within 5 miles. After measuring sensitivity of the steady-state model, 1980 heads along this boundary were estimated with the same data to test the sensitivity of the transient calibration. Using these heads along the boundary, the transient model was rerun and the 3-year (1980-83) change obtained was compared to that generated with the pre-development heads originally used for the boundary. There was less than 0.1 feet difference for all nodes for the 3-year change. Based on these two sets of runs, the steady-state and transient calibrations were judged insensitive to the boundary conditions along the southern edge of the model and were accepted. It should

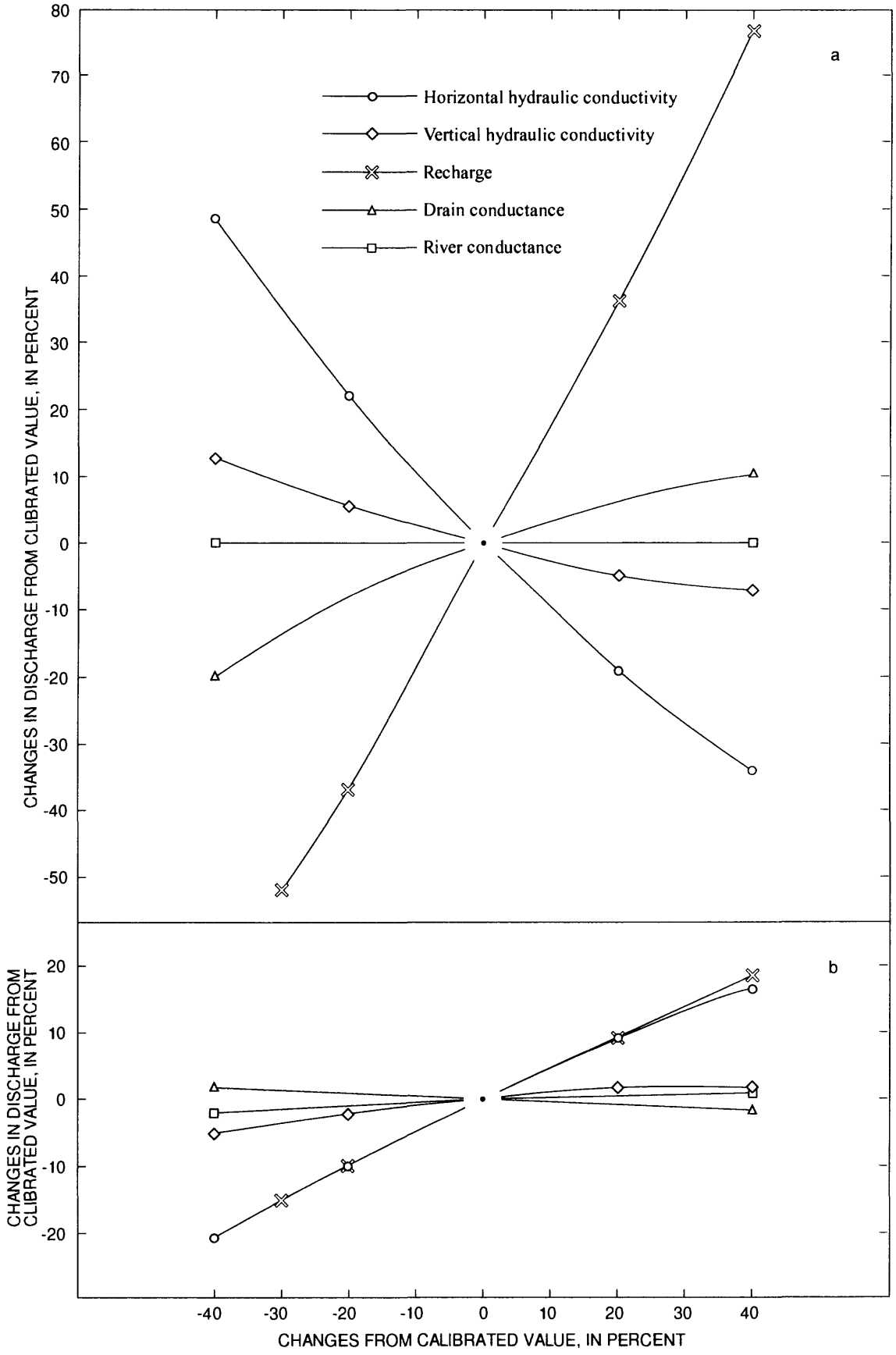

Figure 30. Relation of change in (a) drain and (b) river discharge to change in recharge, hydraulic conductivity, and conductance.

be reiterated that the part of the model in Oregon was included in the model to move the boundaries far enough away from the pumping centers in Washington to minimize the effect of boundary conditions during the predictive runs.

Transient-model runs also were made to evaluate the assumption during steady-state calibration that the amounts and distribution of water-level change brought about in the Horse Heaven Hills by McNary and John Day Dams had reached equilibrium by the 1972-75 time frame. These runs supported the concept that: (1) water levels 1 to 2 miles on either side of the river had essentially reached equilibrium by 1980, (2) most water levels in the central syncline had reached 40 to 70 percent of the total predicted change, and (3) the remaining changes in water levels in the upper central syncline and in the rest of the Horse Heaven Hills area were negligible compared with the average difference between measured and model-calibrated output heads.

PREDICTIVE-MODEL SCENARIOS

Before proceeding to a discussion of predictive runs on the model, a consideration of the possible sources of water to scenario wells is in order. The four ground-water pumpage centers (fig. 25), in T.7 N., R.25 E. and in T.5 N., and 6 N., R.23 E., and T.5 N., R.22 E., largely extract water from the Wanapum aquifer and return part of it to the Saddle Mountains aquifer as additional recharge. Over time, the cones of depression from these centers must spread outward through loss of stored water and induce additional recharge or leakage to the system and divert or reduce discharge from the system. Along the south dip slope of the Horse Heaven Hills, and even in the high recharge areas along the Horse Heaven Hills axis, there are no obvious areas of rejected natural recharge (marsh areas), so it is reasonable to assume that little or no additional recharge from precipitation can be induced. To the west of the pumping centers, these cones could intercept and reduce or eliminate seepage into the deep canyons of Pine, Wood, Alder, and Old Lady Creeks, and eventually Rock Creek (a total of about 22 ft^3/s or 15,900 acre-ft/yr within the modeled area; an additional 8 ft^3/s or 5,900 acre-ft/yr can be captured in the Rock Creek basin to the immediate west of the modeled area). This would virtually eliminate streamflow in late summer and early fall.

To the north, Yakima River discharge could be captured if these cones could lower the ground-water ridge along the Horse Heaven Hills axis and move it to the north, but linear zones of low transmissivity (barriers) on both sides of the ridge axis would strongly buffer this tendency.

To the south and east of these pumping centers are the artificial ground-water mounds within the Saddle Mountains aquifer brought about by infiltration of irrigation water imported from the Columbia River. Through leakage, these sources of water could reduce the spread of cones of depression in the Wanapum aquifer depending on the distribution and amounts of this man-induced recharge as compared with pumpage, and on the distribution of vertical- and horizontal-hydraulic conductivities in the system. Last, capture of water flowing to the Columbia River could balance pumpages, providing that wells are drilled deep enough to induce appropriate gradients into the pumping centers. This capture could be accompanied by a reduction of water levels and baseflow discharge on the Oregon side of the Columbia River. In order to extract water directly from the Columbia River, aquifer water levels near or beneath the river would have to be lowered to elevations below the Columbia River (lake) levels. Such

head reduction beneath the river and flow induction would depend, in part, on the vertical conductivities connecting the Columbia River to the ground-water system. In a like manner, water-level rises beneath areas being irrigated with Columbia River water could, in places where unbalanced by nearby pumpage, cause exactly opposite effects to pumpage, including increased discharge to the surface in the form of local soil water logging and seepage, and increased baseflow to the Columbia. In some areas, these water-level rises could cause pressure changes which would pass beneath the Columbia River into Oregon and cause water-level rises there.

Three different development alternatives were simulated, using specified distribution and rates of ground-water pumpage and surface-water applications as follows:

(1) Pumpage for already developed, certificated, and permitted acreage (presently active wells) projected at rates for each water-right parcel equal to the maximum reached during the previous 10 years (fig. 28; usually this meant 1979 rates). All imported surface water also was applied at maximum rates for that time period (table 4; fig. 26). This simulation is discussed under the heading, "Developed-Pumpage".

(2) All pumpage and imported water included in the "Developed-Pumpage" simulation plus all undeveloped permits in existence (water rights for which a permit has been issued but no well drilled). These wells are to be pumped at a rate of 4 acre-feet per year per acre of undeveloped land (table 3; fig. 26). This simulation is discussed under the heading "Undeveloped-Pumpage Alternative".

(3) All pumpage and applied water in the two simulation above, plus all pending applications for water rights (water rights applied for but not yet granted or permitted). These wells are to be pumped at the rate of 4 acre-feet per year per acre of undeveloped land (fig. 26). This simulation is discussed under the heading "Pending-Pumpage Alternative".

The total imported water for each scenario was 64 ft^3/s, but this water was reduced by 75 percent to match the quantity determined by calibration to recharge the basalt aquifers (the rest is assumed to be evaporatranspired or to run off). For the developed acreage alternative, pumpage totaled 41.2 ft^3/s (29,800 acre-ft/yr); for the undeveloped alternative, 62.2 ft^3/s (45,000 acre-ft/yr); for the pending alternative, 104.3 ft^3/s (75,500 acre-ft/yr, about two and one-half times the developed pumpage). Initial heads for each of the three scenarios were final 1983 heads taken from the calibrated transient model. Fifteen time steps were used with a 1.6 multiplier for each of the 25-year stress periods.

Developed-Pumpage Alternative

Successive maps showing the spread of the cones of depression at the 10th, 50th, and 100th years after 1983 are shown on plate 1. The water budgets for the 5th, 10th, 30th, 50th, 75th, and 100th years are listed in table 8, and a graph showing the source of water for this pumpage is shown on plate 1.

Table 8. Developed acreage water budgets (in cubic feet per second)

	Steady-state	10-year transient	5-year	10-year	30-year	50-year	75-year	100-year
In								
Storage	0	11.47	29.29	25.57	16.44	11.94	9.06	2.17
Constant head	26.07	25.88	25.98	26.07	26.30	26.74	26.57	26.63
Irrigation return	0	15.01	15.98	16.00	15.98	15.60	14.80	14.39
Drains	0	0	0	0	0	0	0	0
Recharge	69.74	69.74	69.74	69.74	69.74	69.74	69.74	69.74
River leakage	.78	.65	.66	.66	.67	.72	.72	.72
Head dependent boundaries	0	.002	.005	.008	.02	.02	.04	.05
Out								
Storage	0	23.06	3.69	2.64	1.32	.85	.74	8.02
Constant head	.45	.45	.45	.44	.43	.42	.42	.41
Wells	0	20.9	41.21	41.21	41.21	41.21	41.21	28.6
Drains	11.9	11.75	12.62	12.92	12.83	12.59	12.36	12.21
Recharge	0	0	0	0	0	0	0	0
River leakage	84.24	87.44	83.68	80.83	73.41	69.43	66.20	64.45
Head dependent boundaries	0	.004	.004	.003	.002	.002	.001	.001

The graphs and successive maps show the cones spreading from the two pumping centers toward the water-import areas and toward the Columbia River. The water supplied by storage rapidly decreases during the first 30 years and that supplied by capture of water flowing to the Columbia River increases. After 30 years, the aquifer storage supplies a steadily decreasing quantity until at the 100th year it is almost zero. Between the 75th and 100th years, several Wanapum aquifer wells in T.6 N., R.23 E., are pumped dry and overlying Saddle Mountains aquifer nodes also are desaturated. The quantity of water supplied from captured Columbia River discharge climbs to 80 percent in the 100th year. Leakage during the early years rises rapidly to 25 percent and stabilizes as the water imported to the Saddle Mountains aquifer leaks downward in the central syncline to help stabilize the Wanapum aquifer cones of depression. In the last 25 years,leakage gradually decreases as capture of Columbia River discharge dominates. At the 100th year, the cone of depression in the Wanapum and Saddle Mountains aquifers has crossed under the Columbia into Oregon in the vicinity of Paterson. Water declines of 10 to 20 feet are predicted in Oregon in the Wanapum aquifer.

Water levels in the western parts of the Horse Heaven Hills study area are lowered from 10 to 20 feet but baseflows in the streams (drains) of this area are only slightly affected. The ground-water ridge along the Horse

Heaven Hills crest has been lowered a small amount and moved a short distance to the north; however, capture of Yakima River discharge is not a major source of water to the pumpage.

Little change in the constant head flux in Oregon has taken place during this 100-year simulation, and the general head boundary nodes in the west are similarly unaffected. In addition, water-level changes adjacent to the eastern and western boundaries of the model are 10 feet or less, implying that the boundaries have not significantly affected drawdowns in the model area.

Undeveloped-Pumpage Alternative

Drawdown maps (pl. 2) for the 50th and 100th year after 1983 show the cones of depression of the undeveloped-pumpage alternative spreading more rapidly than those of the developed-pumpage alternative. At the 50th year, predicted water-level declines of 40 to 60 feet occur adjacent to the river in the vicinity of Paterson and the cone has spread beneath the river into Oregon. In addition, some Wanapum and Saddle Mountains aquifer nodes have been pumped dry in T.6 N., R.23 E., at this date. At the 100th year, additional Saddle Mountains and Wanapum aquifer nodes have been pumped dry in the same area, but this dewatering is more severe than in the developed-pumpage alternative. Greater drawdowns have occurred in T.5, 6, and 7 N., R.25 E., the ground-water mound in R.27 E., has been reduced in size, and the cone has spread a greater distance into Oregon than in the developed-pumpage alternative.

The water-budget graph (pl. 2) shows a pattern similar to the one presented for the developed-pumpage alternative. Water supplied by aquifer storage decreases from 100 to 4 percent during the 100 years, while Columbia River discharge supplies an increasing quantity (from 0 to 75 percent) during the same time period. Water supplied by leakage quickly rises in the early years and stabilizes at a point where it supplies about 20 percent of the water for the rest of the simulation.

The undeveloped-pumpage alternative does not realistically delineate the last 25 years of drawdowns. So many nodes in the Wanapum and the Saddle Mountains aquifers in T.6 N., R.26 E., have been dewatered near the middle of the simulation period that some unrealistic flow paths were caused by the deactivation of those nodes. The deactivation brought about small areas of unrealistic predicted water-level rises upgradient. The effects, a more severe drawdown and dewatering than in the developed-pumpage simulation, are shown on plate 2. In this simulation, the model predicts that the high altitude western areas around Bickleton will not be severely affected in the first 100 years of pumpage. Predicted water-level declines are 10 to 20 feet in the Saddle Mountains aquifer and 10 to 50 feet in the Wanapum aquifer. Baseflow from streams in this area will not be reduced significantly. The ground-water ridge along the Horse Heaven Hills crest to the north of pumping centers will be lowered moderately from 10 to 50 feet, but will not move much to the north, and captured Yakima River discharge will not be large.

Just as in the developed-pumpage simulation, model boundaries do not affect the simulation to any appreciable extent. Discharge from the constant head nodes in Oregon remains almost constant throughout the simulation and the general head boundary fluxes do likewise. Near the edge of the model, water-level changes of 10 feet or less indicate little effect.

Pending-Pumpage Alternative

Maps of drawdowns of the 50th and 100th years of this simulation (pl. 2) show increased effect over the undeveloped-pumpage simulation. By the 50th year, an increased number of dry nodes appears within the Saddle Mountains and Wanapum aquifers, in T.6 N., R.23 E., and increased drawdowns occur in T.5 N., R.22 E. The cone has spread a large distance into Oregon and has eliminated the water-level rises in R.26 E., in the Wanapum aquifer. In the 100th year, additional Saddle Mountains aquifer nodes have gone dry in the T.6 N., R.23 E., area and for the first time in T.6 N., R.25 E., where drawdowns are more severe. In the Wanapum aquifer, the 100-year map shows that fewer nodes have gone dry in the T.6 N., R.23 E., but several more have in T.5 N., R.22 E.

In the water-budget graph (pl. 2), the water supplied from storage dropped faster than in the undeveloped pumpage simulation and that supplied by captured Columbia River discharge increased more rapidly. This simulation in the 50th to 100th year shows the same problems discussed in the undeveloped-pumpage alternative; that is, a number of nodes go dry starting before the 25th year and these dry nodes then constitute blockage for upgradient flow. The result is an area of water-level rise just north of the pumping centers that is unrealistic. Even so, the 100th-year maps are worth presenting because of the contrast and effect they show with the other two alternatives. Boundary effects remain small in this simulation, as in the others.

Although the developed-, undeveloped-, and pending-pumpage simulations are correctly modeled to show that Wanapum aquifer nodes are eventually pumped dry, these dry nodes are never rewet in subsequently modeled years after the wells are turned off. When several contiguous Wanapum aquifer nodes are pumped dry, they act as barriers to flow from upgradient parts of the model and cause head buildup that is unrealistic. Changes in time-stepping did not alter this dry-node condition but an alternative reduced-pumpage scheme of modeling the Pending-Pumpage Alternative was constructed to change some of these unrealistic effects. In this scheme, it is assumed that when pumpage has caused water levels to decline below the top of the Wanapum aquifer in a node, the Wanapum pumpage in that node is reduced in each iteration in proportion to the reduction of Wanapum transmissivity. Although reduction in actual well yield for Wanapum pumping wells may not be linearly related to reduction in initial transmissivity, this is one method which may more realisitically simulate the flow system as water levels decline through time. In the reduced-pumpage simulation, at the end of 100 years, the Saddle Mountains aquifer has several dry nodes (pl. 2) just as in the original simulation but the Wanapum aquifer has none. The distribution of Wanapum aquifer water-level decline in this simulation has the same general character and shape as the original but the damming effect of contiguous Wanapum aquifer dry nodes is absent. Water budgets for the original and reduced-pumpage simulations show that at the end of 100 years, pumpage is reduced 69 ft^3/s or 57 percent for the original and by 58 ft^3/s or 48 percent for the reduced-pumpage scheme. A map of pumpage reduction for the Saddle Mountains and Wanapum aquifers at the end of 100 years using the alternative scheme is shown on plate 2.

SUMMARY AND CONCLUSIONS

The Horse Heaven Hills area lies in the Yakima foldbelt and comprises a large anticlinal ridge with 1,600 to 2,500 feet of structural relief and 1,400 to 3,500 feet of topographic relief; it is bounded on the north by the Satus-Yakima syncline and on the south by the Umatilla syncline. On the south-facing dip slope of this structure, there are large areas of dryland wheat farming, two significant centers of irrigation from pumped ground water, and along the Columbia River, several large irrigation centers using surface water pumped from that river. Three basalt aquifers--the Saddle Mountains, Wanapum, and Grande Ronde--comprise the aquifer system in the Horse Heaven Hills with most recharge and irrigation return flow going into the Saddle Mountains aquifer and most irrigation pumpage coming from the Wanapum aquifer.

The steady-state ground-water flow system, as modeled, includes a natural recharge concentrated along the anticlinal ridge axis, a ground-water divide along this axis with downward flow along its length, lateral flow along the mid-slopes, and upward flow into the Yakima and Columbia Rivers, major drains in the area. The three aquifers in the area have been segmented by structural deformation into large blocks with intermediate to high permeabilities bordered by narrow linear zones or barriers of low permeability. These barriers lie along major faults and monoclinal flexures which border the Horse Heaven Hills anticlinal ridge, along shear faults which occur along dip slopes, and along the narrow Columbia Hills anticline adjacent to the Columbia River. This segmented configuration forces ground-water flow into a step-like pattern as it flows from the ridge axis to the rivers with narrow zones of steep gradient and broad zones of gentle gradient. In places, there is upward flow along the upgradient sides of barriers. Additional control of the flow system is brought about by low vertical permeabilities along the anticlinal ridge as compared with the major synclines. In general, there seems to be a low correlation between vertical and horizontal permeabilities in the basalts. In the Saddle Mountains aquifer, there is an indistinct relation of anisotropy to the major structures with smaller ratios associated with the synclines than with the anticlines.

Estimates of recharge, using a modified Blaney-Criddle method, yielded results which were larger than core and moisture-content measurements of steady-state recharge flux along gentle topographic ridge axes. However, these calculated recharge values may be in line with steady-state flux along small adjacent ephemeral streams which flow on loess or on the basalt. Model calibration indicates that these calculated recharge quantities are realistic and for this reason they were accepted.

Model calibration and sensitivity show that the low permeability barriers exercise a large amount of control on flow in the system. In addition, it supports the existence of high vertical permeabilities along the major synclines in the area. The calibrated models show that of the 67 ft^3/s of recharge in the Washington part of the study, approximately 22 ft^3/s is discharged as baseflow to streams in the western half of the area and 45 ft^3/s is discharged to the Yakima and Columbia Rivers.

Three development alternatives were run in which 16 ft^3/s of imported surface water was recharged in the Saddle Mountains aquifer and ground-water irrigation withdrew 41 ft^3/s (developed pumpage), 62 ft^3/s (undeveloped pumpage), and 104 ft^3/s (pending), respectively, from the Wanapum aquifer.

Simulation showed, in all cases within 50 to 100 years, a number of Wanapum aquifer pumping centers went dry and the overlying Saddle Mountains aquifer was dewatered. At the 100th year, the system was close to equilibrium with remaining pumpage; capture of discharge to the Columbia River ultimately supplied about 80 percent of the water to pumpage with most of the rest coming by way of leakage from areas of imported water in the Saddle Mountains aquifer. Effects on stream baseflow in the western part of the area and on domestic aquifers in the Bickleton area were small. Lowering of the ground-water ridge along the anticlinal axis and capturing Yakima River discharge also were small, and there was virtually no effect on the Kennewick area due to pumping in the Horse Heaven Hills.

Modifications to the standard, modular-finite-difference, flow-model code, as used in this study, are discussed in the Appendix of this report. Procedures used to archive the model source code, model input data, and model output files also are discussed in the Appendix.

On the basis of the work done to date, the following additional work would improve understanding andallow more accurate simultation of alternative development schemes.

(1) The computation schemes using daily weather data for calculating ground-water recharge need to be improved. Better methods for measuring steady-state flux need to be used beneath low-order ephemeral streams and adjacent ridge crests so that integrated measurements across the plateau can be used to calibrate the values calculated from weather data.

(2) More detailed stratigraphic analysis of interbeds needs to be made to better define the relation to vertical permeabilities in the area. Some effort is needed to determine whether paleosoils developed on interbed material might have produced higher clay content along the higher structural parts of the area; places where higher rainfall due to higher topography may have generated higher clay content in these soils and may have produced soil horizons on the basalts themselves that were not as well developed farther downslope.

(3) Additional evaluation is needed of the possibility that high heads predicted by the model for the Grande Ronde aquifer in areas north of the Columbia Hills anticline barrier and west of the shear 1 (fig. 6) barrier may present an economic source of water for irrigation. Another possible barrier of economic importance may be present in the Satus Basin on the upgradient side of the east southeast oriented fault in T.8 N. and 9 N., and R.21 E.

(4) The origin of low hydraulic conductivities in fault barriers and the possible association with secondary clay minerals deposited during or after fault movement could be studied in several parts of the Horse Heaven Hills. Further evaluation of the less well-defined "barriers" and of model sensitivity to this type of feature is needed.

(5) Additional development simulations that would more closely mimic the interaction between water-right laws and the pattern of water-level declines predicted by the model could be made. Evaluation of junior

water-right pumpage and their projected contribution to water-level declines in areas of senior water right could be evaluated in more detail. In addition, scenarios that evaluate effects of current ground-water wells pumped at the lower rates of 1982 could be tested.

(6) As deeper well control is added in the area, horizontal and vertical-hydraulic conductivities of the Grande Ronde aquifer need to be better defined by testing and modeling. These conductivities are some of the least known variables in the model.

SELECTED REFERENCES

Barker, R.A., 1979, Computer simulation and geohydrology of a basalt aquifer system in the Pullman-Moscow Basin, Washington and Idaho: Washington Department of Ecology Water-Supply Bulletin 48, 119 p.

Blaney, H.F., and Criddle, W.D., 1950, Determining water requirements in irrigated areas from climatological and irrigation data: U.S. Soil Conservation Service, Technical Publication 96.

Brown, J.C., 1978, Discussion of geology and ground-water hydrology of the Columbia Plateau with specific analysis of the Horse Heaven Hills, Sagebrush flat, and Odessa-Lind areas, Washington: Washington State University, College of Engineering Research Report 78/15-23, 51 p.

_____1980, Stratigraphy and ground-water hydrology of selected areas, Columbia Plateau, Washington: Washington State University, College of Engineering Research Report 80-/15-39, 20 p.

Brown, R.H., 1963, Estimating the transmissibility of an artesian aquifer from the specific capacity of a well, in, Benthal, Ray, Methods of determining permeability, transmissibility, and drawdown: U.S. Geological Survey Water-Supply Paper 1536-I, p. 336-338.

Campbell, N.P., 1985, Stratigraphy and hydrocarbon potential of the northwest Columbia Basin based on recent drilling activity: Rockwell Hanford Report SD-BWI-TI 265, 5 p.

Cline, D.R., 1984, Ground-water levels and pumpage in east-central Washington, including the Odessa-Lind area, 1967-1981: Washington Department of Ecology Water-Supply Bulletin 55, 34 p.

Davis-Smith, A., Bolke, E.L., and Collins, C.A., 1988, Geohydrology and digital simulation of the ground-water flow system in the Umatilla Plateau and Horse Heaven Hills area, Oregon and Washington: U.S. Geological Survey Water-Resources Investigations Report 87-4268, 72 p.

Drost, B.W., and Whiteman, J.J., 1986, Surficial geology, structural features, and thicknesses and tops of selected geohydrologic units in the Columbia Plateau: U.S. Geological Survey Water-Resources Investigations Report 84-4326.

Hearn, P.P., Steinkampf, W.C., Bortleson, G.C., and Drost, B.W., 1986, Geochemical controls on dissolved sodium in ground water in Columbia Plateau basalts, Washington: U.S. Geological Survey Water-Resources Investigations Report 84-4304.

Horton, R.E., 1945, Erosional developments of streams and their drainage basins; hydrophysical approach to quantitative morphology: Geological Survey of America Bulletin, v. 56, p. 275-370

Luzier, J.E., and Skrivan, J.A., 1973, Digital simulation and projection of water-level declines in basalt aquifers of the Odessa-Lind area, east-central Washington: U.S. Geological Survey Open-File Report, 56 p.

McDonald, M.G., and Harbaugh, A.W., 1984, A modular three-dimensional finite-difference ground-water flow model: U.S. Geological Survey Open-File Report 83-875, 528 p.

McNish, R.D., and Barker, R.A., 1976, Digital simulation of a basalt aquifer system, Walla Walla River basin, Washington and Oregon: Washington Department of Ecology Water-Supply Bulletin 44, 51 p.

Molenaar, Dee, 1982, Water in the Horse Heaven Hills, south-central Washington: Washington Department of Ecology Water-Supply Bulletin 51, 122 p.

Newcomb, R.C., 1961, Storage of ground water behind subsurface dams in the Columbia River basalt, Washington, Oregon and Idaho: U.S. Geological Survey Professional Paper 383-A, 15 p.

____ 1969, Effect of tectonic structure on the occurrence of ground water in the basalt of the Columbia River Group of the Dalles area, Oregon and Washington: U.S. Geological Survey Professional Paper 383-C, 33 p.

____ 1971, Geologic map of the proposed Paterson Ridge pumped-storage reservoir south-central Washington: U.S. Geological Survey Miscellaneous Geologic Investigations Map I-653.

Oberlander, P.L., and Miller, D.W., 1981, Hydrologic studies in the Umatilla Basin: Oregon Water Resources Department, Open-File Report.

Prych, E.A., 1983, Numerical simulation of ground-water flow in Lower Satus Creek basin, Yakima Indian Reservation, Washington: U.S. Geological Survey Water-Resources Investigations Report 82-4065, 78 p.

Steinkampf, W.C., Bortleson, G.C., and Packard, F.A., 1985, Controls on ground-water chemistry in the Horse Heaven Hills, south-central Washington: U.S. Geological Survey Water-Resources Investigations Report 85-4048, 26 p.

Strait, S.R., 1978, Theoretical analysis of local ground-water flow in the Bickleton area, Washington: Washington State University, College of Engineering M.S. thesis, 79 p.

Swanson, D.A., Wright, T.L., and Helz, R.T., 1975, Linear vent systems and estimated rates of magma production and eruption for the Yakima basalt on the Columbia Plateau: American Journal of Science, v. 275, p. 877-905.

Swanson, D.A., Wright, T.L., and Hooper, P.R., 1977, Revision in stratigraphic nomenclature of the Columbia River Basalt Group: U.S. Geological Survey Bulletin 1457-G, 59 p.

Swanson, D.A., Bentley, R.D., Byerly, G.R., Gardner, J.N., and Wright, T.L., 1979, Preliminary reconnaissance geologic maps of the Columbia River Basalt Group in parts of eastern Washington and northern Idaho: U.S. Geological Survey Open-File Report 79-534, 25 p.

U.S. Department of Agriculture, April 1967, Irrigation water Requirements: Soil Conservation Service Engineering Division, Technical Release No. 21, (rev.2), Sept. 1970.

U.S. Environmental Protection Agency, 1976, National interim primary drinking water regulations: EPA-570/9-76-003, 159 p.

U.S. Salinity Laboratory Staff, 1954, Diagnosis and improvement of saline and alkali soils: U.S. Department of Agriculture Handbook 60, 160 p.

Washington State University, 1970, Horse Heaven Hills irrigation and development potential: College of Agriculture, Pullman, Washington, 132 p. (mimeographed report to Horse Heaven Irrigation, Inc.).

APPENDIX: Model Archiving

This appendix describes the process used to archive computer files containing the source code for the finite-difference flow model plus input and output files for the Horse Heaven Hills model. These 33 files are stored on optical disk at the U.S. Geological Survey's Pacific Northwest Area Oregon District office of the Water Resources Division, Portland, Oregon. For a nominal fee, floppy disk or tape copies of these files can be obtained from the District Chief, Water Resources Division, U.S. Geological Survey, 10615 S.E. Cherry Blossom Drive, Portland, Oregon 97216.

SOURCE CODE FILES

The FORTRAN 66 source code for the modified modular finite-difference flow model is stored on optical disk as file 1 (MDL.F77). FORTRAN 66 is a subset of FORTRAN 77 and as such, can be run on most machines with present compiling software (McDonald and Harbaugh, 1984). The main code has been altered in the following ways:

(1) "Double-do-loop" -- During calibration, water-table and convertible-layer nodes in the steep-sloped areas adjacent to the Horse Heaven Hills crest were subjected to large changes in calculated head during the first iterations, and this local numerical disturbance spread so that a large number of adjacent nodes went dry during the first 20-30 iterations and were eliminated from the simulation. In order to decrease this model instability, coding was changed to keep values of transmissivity constant for a selected number of iterations while allowing water levels to vary. At the end of this iteration set, transmissivity was allowed to change and then was again kept constant for the same number of iterations as the initial set. Successive sets of these constant transmissivity iterations were processed within a model run in order to dampen model instability and allow it to converge to a reasonable solution. Usually after a significant change in model hydraulic conductivity was made, an initial model run was carried out using the double-do-loop coding during which several nodes went dry. Output heads were then used as input heads, nodes were rewetted and several additional double-do-loop model runs were made to arrive at a stable solution.

    These iterative loops are controlled in two places, in one by the first two records placed in the Basic Package file before the heading cards, and in a second by the MXITER variable in the Strongly Implicit package file (the MXITER variable defines the number of iterations to be processed within each iteration set). In the first of the two records, there are two variables written in I3 format. The first of these, MXTWO, is the maximum number of iteration sets to be processed. The second variable, MTSAT, is an output control which directs the mapping of saturated thicknesses for each layer at the end of each iteration set. Code a 1 to print thickness maps and a 0 or blank to turn off the mapping option (mapping saturated thicknesses allows the hydrologist to identify problem areas/nodes and to understand the evolution of these problems with each iteration set). In the second of these two records, a single variable, TWOK, coded in F13.0 format defines the head-closure criteria desired for termination of the model run. That is, if the head change in all nodes from iteration to iteration is less than this amount, the model run is

terminated and the rest of the double-do-loops are not processed. When these functions are not needed for a steady-state run or when the analysis is a transient simulation, code 1 and 0 on the first record and a 1 on the second record. Remove these two records when using the original (unaltered) MOD-FLOW code. The most successful combination of total loops and transmissivity-constant iterations for the Horse Heaven Hills model calibration was 50 iteration sets with 3 iterations in each constant-transmissivity loop.

(2) WELDEL -- In the Pending-pumpage scenario, two types of transient simulations were carried out, one like the Developed and Undeveloped scenarios in which irrigation wells in the Wanapum aquifer were allowed to pump until the node was dried and the node and pumpage were turned off for the rest of the simulation. An alternative simulation also was run in which pumpage of wells in the Wanapum aquifer was altered so that when water-level declines caused heads to drop below the top of the Wanapum aquifer in a node, pumpage was thereafter reduced in proportion to the reduction in transmissivity as water levels continued to drop. In addition to reducing pumping rates from wells in the Wanapum aquifer, the companion well that simulated return flow (recharge) to the Saddle Mountains aquifer also was reduced by the same fraction. Both reductions were carried out at each iteration during each time step.

These simulations were controlled in the well package coding within the first record. In addition to the maximum number of wells (MXWELL) and the record/print flag, IWELCB, a third flag variable WLDL is entered in the 30th column in I10 format. A 1 signals the model to use the WELDEL routine in which pumpage is reduced. A 0 or a blank bypasses this option. Output from the WELDEL package includes a listing for each well of the pump period, the time step, node location (K,I,J,), pumping rate at the end of the noted time step, and the fraction by which the original pumpage has been reduced.

(3) Post processing routines were inserted into the model code for selecting pumping-periods for mapping heads and drawdowns, for reloading heads from the preceding pumping period, for listing output heads, and for printing budgets. Control records for these four options are placed in the Basic package after record 3 (NLAY,NROW,MCOL,NPER,ITMUNI) as follows:

(a) MAPHED - code up to 24 pumping periods for which mapped heads and drawdowns are desired in 24I3 format. In steady-state, code a 1 in column 3 to get maps.

(b) LODHED - code those pumping periods for which output heads should be reloaded as input heads for the following pumping-period calculations. Code in 24I3 format. In steady state, code a 0 in column 3.

(c) LISTHED - Code the pumping periods for which calculated heads should be listed for capture and reloading as initial heads for the next steady-state run. Code in 24I3 format. Code a 1 in column 3 for steady-state runs in which listed heads are needed and a 0 when they are not.

(d) LISTBUD - Code the pumping periods for which budgets are to be printed. Code in 24I3 format. For steady-state, code a 1 in column 3 to get a list of budget items and a 0 if you do not want these printed.

(4) A mapping routine has been inserted into the model code which maps input array data or calculated output data into a 23 by 40 grid with 1/2 inch spacing. An entire model layer can be printed onto two regulation sized line-printer pages in this way.

If this routine is used, the output control in record 4 of the Basic package (IUNIT 12) must be left blank.

(5) A hydrograph output post-processing routine was inserted into the model to print drawdown values for selected nodes after each pumping period calculations were completed. The nodes selected for such hydrographs are listed by row and column and placed in the Basic Package file between starting heads and the record with PERLEN, NSTP, AND TSMULT. As written, the model requires that 14 nodes be selected and listed for each of layers one and two (a total of 28 nodes with layer 1, the water-table layer, listed first) even if the output is not needed. Specifically, a total of four records are required, two for each layer. The 14 node locations for each layer are coded in 24I3 format--12 on the first and third records and 2 on the second and fourth records.

FLOW MODEL INPUT FILES

Input for seven different model runs is stored in 18 files grouped into seven sets described below. The seven different model sets are (a) steady state (1974), (b) transient 3-year (1980-83), (c) transient 10-year (1974-83), (d) transient developed-pumpage scenario (100 years, 1983-2082), (e) transient undeveloped-pumpage scenario (100 years, 1983-2082), (f) transient pending-pumpage scenario (100 years, 1983-2082), and (g) an Oregon-drawdown-cone projection run to equilibrium.

(a) Steady state--The seven files used in this run, Numbers 2-8, are SSBAS, SSBCF, SSDRA, HHRIV, HHGHB, HHRCH, and HHSIP corresponding to the Basic, Block Centered Flow, Drain, River, General Head Boundary, Recharge, and Strongly Implicit packages required in this run.

(b) Transient 3-year and 10-year--The eight files used in these two runs are TRBAS, TRBCF, TRWEL, TRDRA, HHRIV, HHGHB, HHRCH, and HHSIP. These correspond to the same sequence of packages listed in the steady-state description above. Files 9, 10, 11, and 12 are the transient Basic, Block Centered Flow, Well and Drain packages used in the two transient runs. The remaining packages used in these runs are the same as in the steady-state runs. In the 10-year run, steady-state heads were those from which final calculated heads were subtracted to derive drawdowns. In the 3-year transient run, 1980 heads (pumping period 14) were reloaded as starting heads and drawdowns were calculated from these. In the first case (10-year), the LODHED function was coded as a 0, and in the second (3-year), the LODHED function was coded with a 14 (that is, the end of the 7th year out of 10 because a pumping period is 1/2 year long).

(c) 100-year Developed-Pumpage scenario--The eight files used in this run are SNARBAS, SNARBCF, DEVWEL, SNARDRA, HHRIV, HHGHB, HHRCH, and HHSIP. The first four of these eight files comprise file numbers 13-16. The other files were used in the steady-state run. 1983 heads output from the 10-year transient run were used as starting heads. Hydraulic characteristics (storage, hydraulic conductivity, transmissivity), drains, rivers, general head boundary, and recharge node values and SIP values are the same as those used in the transient runs.

(e) 100-year Undeveloped-Pumpage scenario--The eight files used in this run are SNARBAS, SNARBCF, UNDEVWEL, SNARDRA, HHRIV, HHGHB, HHRCH, and HHSIP. The third of these files, the well package, is file number 17. The rest have been described above.

(f) 100-year Pending-Pumpage scenario--The eight files used in this run are SNARBAS, SNARBCF, PENDWEL, SNARDRA, HHRIV, HHRCH, and HHSIP. The third of these files, the well package, is file number 18.

(g) 100-year Pending-Pumpage WELDEL scenario--Wanapum pumpage is reduced as transmissivity decreases with water-level decline. The eight files used in this run are are SNARBAS, SNARBCF, PENWLDL, SNARDRA, HHRIV, HHRCH, and HHSIP. The third of these files, the well package, is file number 19.

FLOW MODEL OUTPUT FILES

Files 20-26 are output files from the seven model runs, respectively noted above:

(a) file 20 (steady state)--Most input data files are mapped in this output including the three boundary arrays, hydraulic conductivity, bottom elevation, and vertical conductance of the upper two units, and the top elevation of layer 2, plus the transmissivity of the bottom layer. Drains, recharge, river reaches, and general boundary node values are listed as are the fluxes from or to these nodes. Last, calculated heads for each layer are mapped and the budget is listed.

(b) file 21 (transient 3 year)--Boundary arrays are mapped as are primary storage arrays but basic input data for hydraulic conductivity and conductance, structure and recharge are not mapped. Wells plus drain, recharge, river-reach, and general head boundary nodes and fluxes are listed and calculated heads and drawdowns are mapped. Finally, the budget is listed.

(c) file 22 (transient 10 year)--Calculated heads and drawdowns are mapped and the budget is listed.

(d) file 23 (100-year developed-pumpage scenario)--Calculated heads and drawdowns and budgets are mapped/listed for 25, 50, 75, and 100 year intervals of time as well as flux rates to head dependent boundary nodes and wells.

(e) file 24 (100-year undeveloped-pumpage scenario)--Same as (d) above.

(f) file 25 (100-year pending-pumpage scenario)--Same as (d) above.

(g) file 25 (100-year pending-pumpage scenario)--Same as (d) above.

COMMAND INPUT FILES

The command input files for compiling the model and for the seven runs discussed above comprise files 27-33. File 29 is setup for either the transient 3 year or 10 year runs and only the LODHED coding is different in the two. The steady-state file is file 28, and 30-33 are, respectively, the 100-Year Developed, 100-Year Undeveloped, 100-Year Pending, and Oregon-Cone files. Files 28-33 require the segmented code runfile created by the MDLSEG.COMI (file 27).

Table A1. File descriptions

File	Filename	Description of file
1	MDL.F77	Source code for the modular flow model version used in the study
2	SSBAS	Basic package input file for steady-state run
3	SSBCF	Block centered flow package input file for steady-state run
4	SSDRA	Drain package input file for steady-state run
5	HHRIV	River package input file for all runs
6	HHGHB	General head boundary input file for all runs
7	HHRCH	Recharge package input file for all runs
8	HHSIP	Strongly implicit procedure input file for all runs
9	TRBAS	Basic package input file for transient 3-year and 10-year runs
10	TRBCF	Block centered flow package input file for 3-year and 10-year transient runs
11	TRWEL	Well package input file for 3- and 10-year transient runs
12	TRDRA	Drain package input file for 3-year and 10-year transient runs
13	SNARBAS	Basic package input file for 100-year scenario runs
14	SNARBCF	Block centered flow package input file for the 100-year scenario runs
15	DEVWEL	Well package input file for the developed-pumpage scenario run
16	SNARDRA	Drain package input file for the 100-year scenario runs
17	UNDEVWEL	Well package input file for the undeveloped-pumpage scenario runs
18	PENDWEL	Well package input file for the pending-pumpage scenario run
19	PENWLDL	Well package input file for the pending-pumpage WELDEL scenario
20	STEDST	Output file for steady-state model run

Table A1. File descriptions

File	Filename	Description of file
21	TRAN3YR	Output file for 3-year transient run
22	TRAN10YR	Output file for 10-year transient run
23	DEVWEL100	Output file for 100-year developed-pumpage scenario run
24	UNDEVWEL100	Output file for 100-year undeveloped-pumpage scenario run
25	PENDWEL100	Output file for 100-year pending-pumpage scenario run
26	PENDWLDL100	Output file for 100-year pending-pumpage WELDEL scenario run
27	MDLSEG.COMI	Command input file that compiles and loads the flow model source code as a segmented code runfile
28	STED.COMI	Command input file for steady-state run
29	TRAN.COMI	Command input file for 3-year and 10-year transient runs
30	SNRDEV.COMI	Command input file for 100-year developed-pumpage scenario run
31	SNRUND.COMI	Command input file for 100-year undeveloped-pumpage scenario run
32	SNRPEN.COMI	Command input file for 100-year pending-pumpage scenario run
33	SNRPENWLDL.COMI	Command input file for 100-year pending-pumpage WELDEL scenario run

☆ U.S. GOVERNMENT PRINTING OFFICE: 1996 - 790-123 / 41709 REGION NO. 10